2016

A discrete population of ciliated cells express the piRNA binding protein MIWI2 to regulate lung inflammation

BOSTON UNIVERSITY

SCHOOL OF MEDICINE

Dissertation

A DISCRETE POPULATION OF CILIATED CELLS EXPRESS THE PIRNA BINDING PROTEIN MIWI2 TO REGULATE LUNG INFLAMMATION

by

GREGORY ALEXANDER WASSERMAN

B.S., University of Vermont, 2009
M.S., Long Island University, 2011

Submitted in partial fulfillment of the

requirements for the degree of

Doctor of Philosophy

2016

Approved by

First Reader _____

Matthew R. Jones, Ph.D.
Assistant Professor of Medicine

Second Reader _____

Gregory A. Viglianti, Ph.D.
Associate Professor of Microbiology
Director of Graduate Studies

“The important thing in life is not the triumph but the struggle, the essential thing is not to have conquered but to have fought well.”

- Pierre de Frédy, Baron de Coubertin

DEDICATION

for Sally

my wife, my best friend, and the love of my life

ACKNOWLEDGMENTS

As the proverb goes, “It takes a village to raise a child”, I think the same is true for a scientist. This dissertation would not have been possible without the generous help of many people, to whom I am forever indebted.

I would like to start by thanking Dr. Matt Jones for his mentorship over the the last five years. His constant encouragement and incredible support has been a major driving force in my development as a scientist. Matt expertly navigated the dilemma of allowing me to run with my ideas, while keeping me focused enough to actually get something done. I think together we made a great scientific team, and beyond that a great friendship.

I would also like to thank my “surrogate” mentors, Drs. Jay Mizgerd and Lee Quinton for their advice, guidance and encouragement. Thank you for always making time to talk about my science and share your insights. In addition to being great scientists, Jay’s infectious enthusiasm for science and Lee’s determination for perfection are qualities that I hope to carry with me throughout my career.

Together, Matt, Jay and Lee have created a great environment for doing science, and training as a scientist, and I am grateful that I had the opportunity to work with all of the members of the Pneumonia Biology group. To all of you, past and present – this work would not have been possible without all of your help. Thank you for all of the laughs and the fun distractions. They made coming to

work everyday, even in the harshest of temperatures something to look forward to.

I wish to thank my dissertation committee, Drs. Rachel Fearns, David Center, John Connor, Evan Johnson, and Greg Viglianti for their constant support, and comments. Throughout this process they challenged me to be a better scientist, and helped make this project stronger then we could have imagined.

I have been fortunate to have two departmental “homes” throughout my time here at BU. Thank you to the Department of Microbiology, especially Dr. Ron Corley for his support, and to Linda Parlee, Kathy Marinelli, and Becky Washburn for all of their help. I would also like to thank the Pulmonary Center, particularly Dr. Alan Fine, for his scientific insight and valued mentorship, Dr. Christine Campbell-Reardon for her incredible support and encouragement of my career goals, and Anne Hinds for her patience, and teaching me everything I know about immunohistochemistry.

I want to take an opportunity to thank all of my friends, both old and new who helped me make it through graduate school, and ensured that I had a great time doing it. I have made incredible, life-long friendships that I wouldn’t trade for the world, and I can’t wait to see what the future has in store for us.

Thank you to my Dad, Dr. Herbert Wasserman, for more than I could ever express. His dedication to his family and his work are a constant source of inspiration in my life. I also want to thank my incredible and amazing family for

their unconditional love and support, I would not be where I am without it. Thank you for always being there for me.

Finally, I want to say thank you, in the most emphatic terms, to my wife Sally. She is the source of inspiration for everything I do in life, my best friend, my biggest fan, and my most trusted advisor. She has helped me in too many ways to describe, however if I can just name one, it is that she always believed in me.

A DISCRETE POPULATION OF CILIATED CELLS EXPRESS THE PIRNA BINDING PROTEIN MIWI2 TO REGULATE LUNG INFLAMMATION

GREGORY ALEXANDER WASSERMAN

Boston University School of Medicine, 2016

Major Professor: Matthew R. Jones, Ph.D. Assistant Professor of Medicine

ABSTRACT

Control of retrotransposon expression in the mammalian germline is regulated by Argonaute family PIWI proteins and their associated small non-coding RNAs known as PIWI-interacting RNAs (piRNAs). To date, no study has demonstrated clear PIWI protein expression nor identified a cellular function(s) for PIWI proteins in the mammalian soma. In contrast to the germline-restricted expression of piRNA associated proteins, we observed that *Miwi2* mRNA was induced specifically in epithelial cells during pneumococcal pneumonia. Further investigation showed that similar to its mRNA, MIWI2 protein was indeed expressed outside of the mammalian germline, and was localized to the cytoplasm of a discrete population of multiciliated lung epithelial cells. Immunoprecipitation of MIWI2 from whole lung lysates indicated that it was bound to a small RNA that was longer than a traditional piRNA. Microarray analysis revealed that depletion of MIWI2 in a murine epithelial cell line or in a whole animal model had no effect on retrotransposon expression, further suggesting that lung MIWI2 is independent of nuclear piRNA silencing pathways. Under basal conditions, MIWI2 was required for the normal maintenance of

airway epithelial cell fate. In fact, *Miwi2* deficiency resulted in an increase in club cells and decrease in ciliated cells indicating that MIWI2 could play a primary role in mucociliary homeostasis or clearance. Similarly, as MIWI2 is induced during lung infection we sought to determine if it participated in host innate immune responses to bacterial infection. Using a clinically relevant model of community acquired pneumonia, *Miwi2* deficient mice exhibited an increased expression of inflammatory mediators and immune cell recruitment thus leading to enhanced bacterial clearance. Taken together, these data support the notion that MIWI2 exerts piRNA-independent functions outside of the germline in the ciliated lung epithelium to regulate innate immunity during pneumonia. More broadly, these studies shed light on new areas in PIWI protein and lung ciliated cell biology, and may have implications for multiple diseases including cancer, inflammatory disorders, and infectious diseases.

TABLE OF CONTENTS

LIST OF TABLES

LIST OF FIGURES

LIST OF ABBREVIATIONS

7-AAD ..... Live/Dead Stain (7-Aminoactinomycin D)

AAT ..... acetylated alpha tubulin

ALI ..... acute lung injury

AM ..... alveolar macrophage

ANOVA ..... Analysis of Variance

APC ..... allophycocyanin

ARDS ..... Acute Respiratory Distress Syndrome

BAL ..... bronchoalveolar lavage

BALF ..... BAL fluid

BSA ..... bovine serum albumin

CD ..... Cluster of Differentiation

CMRL ..... Connaught Medical Research Laboratories

Cy ..... cyanine dye

CRISPR ..... Clustered regularly-interspaced short palindromic repeats

DAB ..... 3,3′-diaminobenzidine

DALY ..... Disability-Adjusted Life Years Lost

DNA ..... deoxyribonucleic acid

DPBS ..... Dulbecco's modification of Phosphate-buffered saline

ECL ..... enhanced chemiluminescence

EDTA ..... ethylenediaminetetraacetic acid

ELISA ..... Enzyme-Linked Immunosorbent Assay

FBS ..... fetal bovine serum

FITC ..... fluorescein isothiocyanate

g .....relative centrifugal force

GFP ..... green fluorescent protein

h .....hours

H & E ..... Hematoxylin and Eosin

HBSS ..... Hank's balanced salt solution

HEPES.....2-[4-(2-hydroxyethyl)piperazin-1-yl]ethanesulfonic Acid

HRP ..... horseradish peroxidase

i.t. ..... intratracheal

i.v. ..... intravenous

ICU..... Intensive Care Unit

Ig .....immunoglobulin

kg ..... kilogram

LDS..... lithium dodecyl sulfate

LIF..... Leukemia Inhibitory Factor

LINE.....Long Interspersed Nucleotide Element

LPS ..... lipopolysaccharide

mg..... milligram

MID ..... middle

min ..... minutes

mL.....milliliter

mM.....millimolar

MOPS .....3-propansulfonic acid

mRNA ..... messenger RNA

NET..... Neutrophil Extracellular Trap

NF-κB ..... Nuclear Factor Kappa-Light-Chain-Enhancer of Activated B Cells

NP-40.....Nonylphenyl-polyethylenglycol, Octylphenoxy poly(ethyleneoxy)ethanol

nt..... nucelotide

OSM..... Oncostatin-M

P-value.....probability value

PAMP.....pathogen-associated molecular pattern

PAZ..... PIWI Argonaute Zwille

PBS..... phosphate buffered saline

PCR ..... Polymerase Chain Reaction

PCV .....Pneumococcal Conjugate Vaccine

PE ..... phycoerythrin

Pen-Strep..... penicillin-streptomycin

PFA.....paraformaldehyde

pg.....pictogram

PIWI ..... P element induced wimpy testis

PPSV .....Pneumococcal Polysaccharide Vaccine

PVDF ..... polyvinylidene fluoride

qRT-PCR .....Quantitative Reverse Transcriptase PCR

RBC ..... red blood cell

RCF .....relative centrifugal force

RFP..... red fluorescent protein

RNA ..... ribonucleic acid

ROS ..... reactive oxygen species

RPM..... revolutions per minute

RPMI..... Roswell Park Memorial Institute

RSV .....Respiratory Syncytial Virus

RT ..... reverse transcriptase

SBA..... trypticase soy agar plate supplemented with 5% sheep's blood

SDS-PAGE .....Sodium Dodecyl Sulfate Polyacrylamide Gel Electrophoresis

SINE ..... Short Interspersed Nucleotide Element

STAT.....Signal Transducer and Activator of Transcription

TE ..... transposable element

TBS-T .....Tris- buffered saline plus Tween

TLR..... Toll-like receptor

TNFα .....Tumor Necrosis Factor-α

TSA.....trypticase soy agar

TSB.....trypticase soy broth

TWEEN..... Polyethylene glycol sorbitan monolaurate

U ..... units

V ..... volts

WHO.....World Health Organization

WT.....Wildtype

μg.....microgram

μL..... microliter

CHAPTER ONE: INTRODUCTION

The Lung

Preface

The respiratory system is indispensable for mammalian physiology as its primary function is to facilitate organismal gas exchange and oxygenation. The lungs represent the largest surface area exposed to the outside world, even more so than the epidermis. In addition to barrier functions, the lungs also play a physiologic role in circulatory acid base equilibrium, in the creation of sound and oral communication. Fascination with the function of the lung has persisted throughout time, a frequent subject in the work of Aristotle where he declared that life is dependent on breathing (Aristotle, 2014). Centuries later, in an account of his comprehensive work originally compiled in 1653, *Lectures on the Whole of Anatomy: An Annotated Translation of Prelectiones anatomiae universalis*, William Harvey, the preeminent English physician and researcher proclaimed *"Life and respiration are complementary. There is nothing living which does not breathe nor anything which breathing which does not live."* His conclusions, based on numerous years of experiments, and logical reasoning declared the lungs were the most important organs in the body. Despite centuries of research and determination, we still search for an understanding of the awesome power of the lung to facilitate life, while exhibiting exquisite homeostatic mechanisms. These mechanisms are tremendously complex given the massive amount of lung

surface area that is constantly exposed and thus susceptible to an ever-changing, inhaled environment. The broad goal of this dissertation is to delve conceptually and experimentally into these mechanisms and provide some insight into how such a large and vulnerable surface is capable of protecting itself.

Embryology

Gastrulation of the developing embryo results in the formation of three germ layers— ectoderm, mesoderm, and endoderm, which serve as precursor cell populations for organ development (Rock and Hogan, 2011a; Burri, 1984; Pinkerton and Plopper, 2004). The mature lung, capable of normal physiologic function, is comprised of cells derived from all three germ layers. Lung development can be separated into five phases, which were originally defined by structural morphology of the developing organ (Hogan et al., 2014). During the embryonic stage (approximately week 3 in humans and embryonic day 9 in mice), the primordial lung marked by the transcription factor *Nkx2-1* is bud from the anterior foregut endoderm (Herriges and Morrisey, 2014). During the pseudoglandular stage, the bronchial tree is generated through a series of budding and elongation events in a process known as branching morphogenesis (Plopper and Fanucchi, 2004). The generation of airways is highly dependent on the interaction between the endoderm and the mesoderm where both secreted and cell bound signaling molecules instruct critical cell fate decisions (Cardoso,

2004). At the completion of the pseudoglandular stage (approximately week 17 in humans and embryonic day 15 in mice) nearly all the bronchial airways are formed, and the emergence of specialized airways cell types, such as ciliated cells marked by the transcription factor *Foxj1*, and early club cells, marked by expression of the secretoglobin *Scgb1a1*, arise in a proximal to distal fashion (Cardoso, 2004; Rock and Hogan, 2011a; Hogan et al., 2014). The canalicular and alveolar stage begin the process of building the alveoli, or terminal units of the airway where gas exchange takes place. The emergence and differentiation of type I pneumocytes, the major structural cells of the alveoli and type II pneumocytes, the major producers of surfactant can be seen by week 26 in humans and embryonic day 17 in mice. Surfactant, a mixture of phospholipids and specialized hydrophobic proteins is stored in type II pneumocytes and is secreted to coat the alveolar surface and functions to reduce surface tension, and prevent alveolar collapse on exhalation (Nogee et al., 1993). The critical role of surfactant in facilitating lung function is illustrated in patients who carry mutations in surfactant genes, and suffer fatal respiratory failure in infancy(Nogee et al., 1993). The final stage of lung development, the alveolar stage, extends into the post natal period. Primitive alveoli continue to undergo septation, and there is continued innervation of pulmonary capillaries. When the process is complete, nearly 480 million alveoli are generated with over 70 m^2 of surface area available for gas exchange (Green et al., 1977; Levitzky, 2013).

Homeostasis and Host Defense

An average adult human inhales approximately 11,000 liters of air per day which may contain numerous particulates such as pollen, dust, bacteria, viruses and fungi (Levitzky, 2013). Given the high rate of exposure to potentially toxic material, and the need to preserve physiologic function, the lung must possess exquisite mechanisms for maintaining homeostasis (Mizgerd, 2012; 2008). Pulmonary host defense is a multi-tiered protection system that employs anatomical, mechanical and immune cell mechanisms that prevent, identify and respond to pathogens and particulates (Holt et al., 2008; Mizgerd, 2008; Levitzky, 2013). Each of these mechanisms cooperate to ultimately preserve the integrity of the alveoli-capillary barrier to facilitate gas exchange.

The anatomy of the airways represents the initial layer of host defense in the adult lung. Progressively branched airways function to reduce air velocity, prolonging contact of air with the epithelium, and allowing gravity to sediment particulates (Tellier, 2006; Levitzky, 2013; Rackley and Stripp, 2012). By humidifying air on inspiration, hygroscopic particles will increase in size and will be cleared by expectoration or coughing. Sedimented particles are forced onto, and captured by the mucus layer, which coats the airways. Lung ciliated cells drive mucus from the lower airways toward the pharynx where it is eliminated by swallowing in a process known as mucociliary escalator. Generally, particles larger than 2 μM are affected by gravity and cleared via the mucus layer, whereas particles less than 0.5 μM will remain aerosols and be removed by

exhalation (Rackley and Stripp, 2012). Defects in mucociliary escalator either through genetic mutations such as in cystic fibrosis (CF) and primary cilia dyskinesia (PCD), or acquired defects such as cigarette smoking, predispose patients to acute lower respiratory tract infections (Tilley et al., 2015; Leopold et al., 2009).

In healthy individuals the lower airways are considered to be sterile, however the upper airways are colonized with a multitude of microorganisms (Beck et al., 2012). Despite the mechanical and anatomical layers of defense, bacteria are within the size range where these mechanisms are insufficient. Additional layers of antimicrobial defense are produced to limit microbes, from accessing the lower airways. Conducting airway epithelial cells express small molecules with direct or indirect microbial killing activity such as defensins, sufactants, and cathelicidins (Prince, 2013; Parker and Prince, 2011; Whitsett and Alenghat, 2014; Green et al., 1977). B cells secrete Immunoglobulin A (IgA) into the bronchial lining fluid to neutralize bacteria, viruses and immunogenic material. Additionally, immunoglobulin G (IgG) is also found in in the lower respiratory tract, and likely participates in resistance to microbes for which the host has been previously exposed (Green et al., 1977). When bacteria fail to be eliminated by alternative methods, they are encountered by sentinel cells, the alveolar macrophages. Derived from yolk sac progenitors, alveolar macrophages (AMs) represent the first line of cellular defense to microbial insult in the distal lungs**.** Alveolar macrophages patrol the surface area of the airway, and were

previously known as dust cells, for their ability to remove particles, inert materials and low virulence microbes from the airspaces. AMs play an important role in airway homeostasis, responsible for clearing apoptotic, or necroptotic cells, cellular debris, and inactivated surfactant from the airways (Mizgerd, 2008; Dockrell et al., 2013; Hussell and Bell, 2014). The coordinated mechanisms of pulmonary host defense are numerous, and comprehensive, however, are susceptible to failure. While alveolar macrophages are capable of clearing a relatively minor dose of bacteria in the lower airways, deposition of a high inoculum, or high virulence organism requires a more substantial immune response. The recruitment of additional immune cells into the airways and the ensuing inflammation is known clinically as pneumonia.

Pneumonia

Clinical significance, Incidence and Epidemiology

Traceable throughout history to ancient Roman, Greek, and Arabic texts, pneumonia is one of the oldest recognized diseases of mankind and remains centuries later as a major public health burden (Blasi et al., 2007). In 2013, the Global Burden of Disease study reported that pneumonia is the second leading cause of death overall, and the leading infectious cause of death among adults in the United States (GBD 2013 Mortality and Causes of Death Collaborators, 2015; Mizgerd, 2006; Armstrong et al., 1999). The incidence is reported to be between 1.5 and 14 cases per 1000 person years, and disproportionally effects children

under 5 years of age and adults older than 65 years of age (File and Marrie, 2010; Griffin et al., 2013; Jain et al., 2015). During the early part of the 20th century substantial progress was achieved in reducing the death rate due to pneumonia. The implementation of basic sanitation practices, improved nutrition, and numerous other public health interventions reduced the death rate from approximately 200 deaths per 100,000 people in 1900 to 100 deaths per 100,000 in 1930. Indeed, this progress was temporarily halted during the 1918 influenza outbreak where the death rate increased to nearly 600 deaths per 100,000 people per year, many the result of bacterial superinfection (Mizgerd, 2012). The sharpest decline, from approximately 100 deaths per 100,000 to 40 deaths per 100,000 people, occurred in the 1950's and was a direct effect of the development and implementation of antibiotics as routine treatment of pneumonia. Surprisingly, despite the colossal advances in medicine during the later part of the 20th century, mortality due to pneumonia has remained constant (Blasi et al., 2007). The severity of pneumonia can range from mild disease that is self limiting, to more severe presentation requiring hospitalization. Hence the case mortality due to pneumonia is also varied. In patients who do not require hospitalization the mortality rate is less than one percent, however in hospitalized patients, mortality may be as high as 50% (Jain et al., 2015; Griffin et al., 2013).

Clinical Presentation and Microbiology

Pneumonia is clinically defined as an infection involving the alveoli and airways. Patients who present with pneumonia exhibit a number of symptoms

including cough, fever, chills and pleuritic chest pain, which often arise quickly (Metlay et al., 1997). Auscultation of the lung usually reveals crackles or rales in distinct locations, as fluid accumulation presents in a consolidated fashion. The diagnosis of pneumonia is often confirmed with a chest radiograph, in combination with supportive microbiological and hematological assays (Baron et al., 2013; Mandell et al., 2007).

Pneumonia is caused by a large cadre of microbes including, bacteria, viruses and to a lesser degree, fungi (Prina et al., 2015). Several factors influence pneumonia etiology including, age, co-morbidities, geographic location, genetic susceptibilities and vaccine trends. Overall, the predominant pathogen worldwide is the Gram-positive bacteria, *Streptococcus pneumoniae* (Welte et al., 2012; Jain et al., 2015; Howard et al., 2005; Drijkoningen and Rohde, 2014; File and Marrie, 2010). Prior to the routine use of antibiotics, pneumococcus caused greater than 95% of all cases of pneumonia (Austrian, 1981). More recently it has been reported to cause between 5-15% of cases in the U.S. and up to 35% of cases in Europe (Welte et al., 2012; Jain et al., 2015; Howard et al., 2005; Drijkoningen and Rohde, 2014; File and Marrie, 2010). Various factors increase the risk of pneumococcal infection. Antecedent influenza infection (McCullers, 2006), current or former alcohol abuse (de Roux et al., 2006), COPD and asthma (Lee et al., 2007), previous splenectomy (Wara, 1981), genetic mutations, and environmental factors all greatly predispose patients to pneumococcal pneumonia. Strikingly, there is a 50 to 100-fold increase in

pneumococcal disease in patients infected with HIV (Schuchat et al., 1991). The clinical setting of the patient, namely immunocompetency and previous or current hospitalization correlates with different causative pathogens. Other bacterial pathogens including *Mycoplasma pneumoniae, Legionella spp., Staphylococcus aureus,* Enterobacteriaceae species including *Klebsiella and Escherichia*, and *Pseudomonas aeruginosa* are common in particular cohorts of patients (Peleg and Hooper, 2010; Jain et al., 2015; Prina et al., 2015). Recent advances in molecular diagnostics have also increased the identification of respiratory viruses as major causes of community and hospital acquired pneumonia. In fact, a recent study surveyed the likely causative pathogen in radiographic confirmed cases of community acquired pneumonia requiring hospitalization, and found the predominant pathogen recovered were rhinovirus, followed by influenza (Jain et al., 2015). Other viruses identified in the study included human metapneumovirus, and respiratory syncytial virus, however, it should be noted that a pathogen was not identified in 62% of cases of patients with confirmed pneumonia. For these cases, it has been proposed that the etiology is likely the result of *S. pneumoniae.* Even in patients with confirmed *S. pneumoniae* bacteremia, only approximately 50 percent of patients had positive sputum cultures indicating that standard sampling techniques may not be sufficiently sensitive to detect pneumococcus in all cases (Barrett-Connor, 1971; Bartlett and Mundy, 1995). The high prevalence, and sustained mortality in patients with

pneumococcal pneumonia underscores the importance of continued investigation and the development of alternative treatment modalities.

Pathology and Immune Response

Many bacterial species which cause pneumonia are carried, at least transiently in the nasopharynx (Kadioglu et al., 2008; Musher and Thorner, 2014; Bartlett, 2011). When the inoculum size or virulence of the microbe evade or escape the host defenses of the lungs, they are deposited in the alveoli where they are detected by alveolar macrophages. Given their limited direct microbial killing activity, the primary role of AMs is pathogen surveillance and recruitment of neutrophils through chemokine production and epithelial cell communication (Hussell and Bell, 2014). Pattern recognition receptors, particularly Toll-like receptors on the macrophage surface facilitate the detection of bacterial products upon microbial entry to the alveoli, and stimulate the production cytokines and chemokine (Mizgerd, 2008). In the case of pneumococcus, the bacterial cell wall component, lipotechoic acid signals through TLR2 to initiate macrophage production of cytokines and chemokines, many through the activation of NF-kB signaling (Xu et al., 2008). Our group has demonstrated that production of TNF-α and IL-1β by macrophages is critical for defense against pneumococcus (Pittet et al., 2011; Quinton et al., 2007). These cytokines signal in both an autocrine and paracrine fashion, affecting inflammatory gene expression in epithelial cells which cooperate in the recruitment of neutrophils to the airspaces (Yamamoto et al., 2013; 2012; Whitsett and Alenghat, 2014; Bals and Hiemstra, 2004). Once in

the airspace, neutrophils clear bacteria by phagocytosis, produce anti-bacterial reactive oxygen species, express pro-inflammatory cytokines which instruct lymphocytes, and release neutrophil extracellular traps (NETS) to control bacterial spread and proliferation (Mizgerd, 2008; Brinkmann et al., 2004).

While this inflammation is necessary for the control of bacterial growth and dissemination, it can result in extensive damage to the lung tissue and the formation of the often fatal Acute Respiratory Distress Syndrome (ARDS) (Ware and Matthay, 2000). Some of the products of neutrophils that kill microbes, such as proteases and reactive oxygen species also cause lung cell death (Fink, 2002; Ricciardolo et al., 2006). Over exuberant immune responses cause disruption of the epithelial barrier and result in an increased vascular permeability (Matthay and Zimmerman, 2005; Matthay et al., 2012; Ware and Matthay, 2000). The influx of plasma components and proteinaceous edema fluid in the alveolar space is visible on chest radiograph and a defining feature of acute lung injury. Fluid accumulation in the airspace has a number of consequences including inactivation of surfactant causing collapse of the airspace, impaired gas exchange, decreased lung compliance, and increased pulmonary arterial pressure. Patients with ARDS have a mortality rate between 26 and 58% (Wang et al., 2014; MacCallum and Evans, 2005) and survivors of ARDS suffer long term sequelae including increased incidence of cognitive dysfunction, psychiatric illness, and enduring physical limitations (Mikkelsen et al., 2012; Orme et al., 2003).

Given the high rate of mortality in patients with pneumonia and acute lung injury it is clear that further insight is needed into the pathways that regulate both the immune response and the resolution of acute infection. Our laboratory has focused on broad post-transcriptional gene regulation mechanisms, such as small RNA silencing pathways to gain insight into the control of inflammation in the inflamed lung.

Small RNA silencing

The central dogma of biology posits that RNA serves as the intermediate template for which protein polypeptides are built. Over the last several decades however, the expanded role and importance of RNA in the cell has been revealed. In their Nobel Prize winning work in 1998, Fire and Mello discovered that dsRNA was capable of ablating the expression of particular mRNAs through their degradation(Fire et al., 1998). This process, which they termed RNAi or RNA interference was then identified in diverse and distant forms of life from prokaryotes, to plants to humans. Numerous classes of small RNAs have been identified, and they participate in numerous processes and pathways in the cell (Ghildiyal and Zamore, 2009). Given the genome encodes for thousands of genes which must be expressed with great fidelity, their regulation must be precisely controlled to maintain homeostasis. Indeed, protein transcription factors are the main drivers of gene production, however small RNAs are a major constituent of post- transcriptional gene regulation (Bartel, 2004; 2009; Ghildiyal

and Zamore, 2009). Three predominant small RNA classes exist in metazoan including small interfering RNAs (siRNA), micro RNAs (miRNA), and piwi-interacting RNAs (piRNA) (Siomi et al., 2011). Each of these classes differ in their length, biogenesis, tissue expression pattern, and molecular targets, however common to each of these pathways is their association and formation of an RNA Induced Silencing Complex (RISC)(Hutvagner and Simard, 2008). Central to this complex is a highly specialized family of proteins known as Argonaute proteins that coordinate, in association with additional factors, the execution of gene silencing activity.

Argonaute proteins

Originally discovered in 1998, Argonaute (ago1) was identified as a gene necessary for proper leaf development in the plant species *Arabidopsis thaliana* (Bohmert et al., 1998). The authors chose the name “Argonaute” as the mutant leafs closely resemble the tentacle structure of the octopus *Argonauta argo* (Bohmert et al., 1998; Swarts et al., 2014). Subsequent studies have revealed that in addition to eukaryotes, Argonaute proteins exist in prokaryotes and archaea, strongly emphasizing their important biological function (Hutvagner and Simard, 2008). Interestingly, Argonautes have undergone substantial gene duplication and sequence diversification, particularly in metazoan. Several high resolution crystal structures from both prokaryotes and eukaryotes reveal a conserved domain structure including a disordered N terminal domain, PAZ, MID and PIWI domains (Nakanishi et al., 2012; Schirle and MacRae, 2012; Elkayam

et al., 2012). The PAZ domain is found in other RNA binding proteins, and is capable of binding single stranded RNAs with low affinity, whereas the PIWI domain contains an RNAse H fold, which is capable in some species of RNA cleavage (Hutvagner and Simard, 2008). Phylogenetic analysis separates the Argonaute family into two clades, the AGO clade which is most homologous to Arabidopsis AGO and the PIWI clade proteins most homologous to the Drosophila PIWI proteins (Swarts et al., 2014; Carmell et al., 2002). While the AGO clade proteins are expressed ubiquitously in mammals and are known to bind miRNAs, PIWI clade proteins are largely restricted to the germline where they bind piRNAs and protect the genome from the deleterious effects of exuberant transposable element expression (Aravin et al., 2008).

Transposable elements

Beginning with Barbara McClintok's Nobel Prize winning discovery of "jumping genes" in the 1940's (McClintock, 1956), and propelled by recent advances in genome sequencing technology, the sizable proportion of vertebrate genomes that are comprised of transposable elements (TEs) has been revealed. These mobile genetic elements, or so-called "parasitic DNA" can be found in nearly all vertebrate genomes. TEs comprise 37.5 and 45 percent of the mouse and human genomes, respectively (Mouse Genome Sequencing Consortium et al., 2002; Lander et al., 2001). This figure is striking considering that protein coding genes account for less than two percent. Two major classes of transposable elements have been distinguished based on their mechanism of

replication and evolutionary history. Class II elements, or DNA transposons serve as a DNA template and insert into the host DNA genome by an excision-insertion mechanism known as “cut and paste” replication (Finnegan, 1997; Belancio et al., 2008; Wicker et al., 2007). These elements are largely fixed in the human genome, and are no longer mobile. Class I elements, also known as retrotransposons, utilize a reverse transcriptase to copy an RNA template genome before integration in the host DNA. Two subtypes of retroelements have been identified based on the presence or absence of a long-terminal repeat (LTR) (Wicker et al., 2007). Derived from ancient retroviruses, LTR containing transposons integrated into the mammalian genome and acquired mutations ablating their ability to replicate autonomously (Finnegan, 1997). These sequences encode genes recognizable as *Gag* and *Pol* genes of known retroviruses, but notably lack *envelope* genes, eliminating the possibility of cell to cell transfer (Goodier and Kazazian, 2008). The second subtype of retroelements are non-LTR transposons, which are the predominant retrotransposon family in mammals (Wicker et al., 2007). Non LTR elements consist of two subtypes, SINE elements (short interspersed nucleotide elements) and the predominant mammalian TE, LINE elements (long interspersed nucleotide elements). LINE elements contain a 5’ untranslated region (UTR) and two open reading frames encoding proteins necessary for reverse transcription and integration (Slotkin and Martienssen, 2007; Goodier and Kazazian, 2008). Replication relies on an elucidated mechanism known as target-site primed reverse transcription, where

RNA is reverse transcribed at the site of integration into the host genome. Approximately 500,000 copies of LINE elements are contained in the mouse and human genomes accounting for nearly 20 percent of the total genomic sequence (Xing et al., 2007; Lander et al., 2001; Mouse Genome Sequencing Consortium et al., 2002). While many LINE elements are fixed, approximately 100 elements are still capable of retrotransposon in humans and several thousand in mice (Goodier and Kazazian, 2008). Over the course of evolution, retroelement transposition has played an important role in shaping the expression and structure of the genome. Firstly, large scale recombination, addition and deletion events are facilitated by direct repeat structures, and homologous sequences spread across the genome. TEs influence gene expression by generating new promoters and introducing new sites for epigenetic regulation. In addition, it is estimated that at least 47 human genes have evolved directly from transposon sequences (Cordaux and Batzer, 2009; Xing et al., 2007; Lander et al., 2001). Finally, TEs are capable of gene inactivation by insertional mutagenesis, which leads to loss of function mutations (Levin and Moran, 2011; Sedivy et al., 2013). The impact of these mutations can result in a number of different cancers, presenting a major evolutionary conundrum. Hence, while it appears that TEs provide a long-term evolutionary tool, their short term transcription and activity must be controlled to prevent transmission of deleterious mutations. This is particularly important in the mammalian germline, where retroelement transcription is high and risk of vertical inheritance is highly probable. To

minimize the deleterious effects of retroelement expression and protect the integrity of the genome many organisms have evolved specialized restriction systems within the germline to combat TE activity.

piRNA silencing pathway

Studies of *Drosophila* development revealed the diverse set of RNAs derived from repetitive sequences (Aravin et al., 2001; 2003). However, the first clue that transposon sequences were silenced by small RNAs came with the discovery of the protein *Piwi* (P-element induced wimpy testis) during a forward genetic screen for regulators of stem cell division in *Drosophila melanogaster* (Cox et al., 2000). Subsequent work demonstrated that *Piwi* deficiency led to sterility, and the overexpression of transposon sequences in the germline (Cox et al., 2000). It was well appreciated that *Piwi* homologues exist throughout evolution, including in mammals, and were closely related to the Argonaute family of proteins which bind small RNAs (Carmell et al., 2002). The mechanism of transposon repression remained elusive until several groups, working in flies and mice, identified that *Piwi* and *Piwi* homologues associate with a class of small RNAs now known as *Piwi*-interacting RNAs (piRNAs) (Deng and Lin, 2002; Kuramochi-Miyagawa, 2004; Vagin et al., 2006; Girard et al., 2006; Saito et al., 2006).

Despite their identification nearly ten years ago, a complete understanding of the biogenesis, and function of piRNAs has yet to be fully elucidated. There are hundreds of thousands of distinct piRNA sequences within a species and

these sequences differ greatly between species (Aravin et al., 2003). In the mammalian germline, two major waves of piRNAs are produced during developmentally distinct periods in spermatogenesis, pre-pachytene and pachytene. Pre-pachytene piRNAs are derived mainly from transposable elements, while pachytene piRNAs are generated from unannotated non-repeat intergenic regions known as piRNA clusters (Fu and Wang, 2014). During pre-pachytene and pachytene, piRNAs are generated through a primary biogenesis pathway, however during pre-pachytene, piRNAs are also generated by an amplification loop, termed the ping-pong cycle (Aravin et al., 2007). RNA polymerase II and the transcription factor A-MYB generate 5' capped and 3' polyadenylated piRNA precursurs (Li et al., 2013; Fu and Wang, 2014) which are cleaved into shorter so-called piRNA intermediates. This cleavage is independent of the miRNA biogenesis factor Dicer (Vagin et al., 2006; Bernstein et al., 2003), and is likely carried out by the enzyme MitoPLD (also known as Zucchini) (Watanabe et al., 2011; Ipsaro et al., 2012) however, other enzymes are likely involved as MitoPLD deficient mice still have piRNAs (Watanabe et al., 2011). The piRNA is then trimmed by a hypothetical 3'-5' endonuclease known as Trimmer (Saxe et al., 2013), 2'-O-methylated by the enzyme HEN1 and loaded into the Piwi-clade Argonaute protein MILI (during pre-pachytene), or MILI/MIWI (during pachytene) (Ohara et al., 2007; Horwich et al., 2007). piRNA- loaded MILI is recruited to complementary TE RNAs by base pairing, where it slices the target RNA through endogenous cleavage activity, that is in turn trimmed and loaded

into MILI or a third Piwi-clade protein, MIWI2 . While MILI and MIWI are capable of slicing and silencing complementary RNAs in the cytoplasm, MIWI2 when loaded with secondary piRNAs is transported to the nucleus where it binds nascent RNA transcripts of transposable elements and orchestrates transcriptional silencing of TE RNA by reinforcing DNA methylation (Carmell et al., 2007; De Fazio et al., 2011). Unlike miRNA biogenesis and silencing, which is well characterized, the complexity of piRNA silencing is still being elucidated. Several factors have been identified in flies and mice which associate with piRNA complexes (nicely reviewed in ((Iwasaki et al., 2014)). An emerging theme in mammals indicates that piRNA silencing is essential in the male germline, and dispensable for maintenance of female germ cells. Ablation of any of the three piRNA binding proteins in mice, MILI, MIWI, or MIWI2 result in retrotransposon overexpression in spermatogenic precursors, however homozygous deficient females remain fertile (Carmell et al., 2007; Deng and Lin, 2002; Kuramochi-Miyagawa, 2004). This is likely the result of the continued mitotic and meiotic activity specific to the male gametes.

Evidence for a somatic cell role of the piRNA pathway

Despite the focus on the role of the piRNA pathway in the mammalian germline, multiple lines of evidence point to potential somatic cell functions in mammals. Indeed, an active piRNA pathway has been well described in the somatic cells of the *Drosophila* ovary (Ross et al., 2014), but no definitive study to date has been able to elucidate a function for piRNA components in the

vertebrate soma. In *Drosophila,* the piRNA binding protein *Piwi* is critical for stem cell renewal and maintenance (Cox et al., 2000). Given the known role of Piwi proteins as regulators of stem cell activity in *Drosophila*, much of the available data in the soma has focused on the role of piRNA binding proteins in the development of differentiated cells and tissue lineages.

In mammals, there are 3 Piwi-clade proteins in mice, Piwil1/MIWI, Piwil2/MILI, and Piwil4/MIWI2, and 4 in humans, Piwil1/HIWI, Piwil2/HILI, Piwil3/HIWI3 and Piwil4/HIWI2 (Fu and Wang, 2014). A survey of of normal human tissues indicate that Piwil4 is highly expressed in almost all tissues, while Piwil1,2 and 3 are restricted to the testis (Sasaki et al., 2003). Piwil1 and Piwil4 are expressed in hematopoietic progenitors in humans and mice, respectively (Sharma et al., 2001; Nolde et al., 2013; Jacobs et al., 2013). Genetic ablation in mice of Piwil4, or Piwil1,2 and 4 however, have no direct effect on hematopoietic development indicating that these proteins are dispensable for terminal differentiation of the myeloid and lymphoid lineages (Nolde et al., 2013; Jacobs et al., 2013). Piwil1 and Piwil4 are also highly expressed in mouse and human embryonic stem cells, but are not detectable in mouse embryonic fibroblasts (MEFs) or human foreskin fibroblasts (Cheng et al., 2014). Deletion of these proteins had no effect on the ability to reprogram these cells into induced pluripotent stem cells. In addition, embryonic stem cells from Piwil1,2,4, triple knockout mice were able to form all three germ layers (Cheng et al., 2014). Collectively these data indicate that piRNA binding proteins have a negligible

effect on the development of somatic tissues under basal conditions. It should be noted however, that in each of these studies, Piwi clade protein expression was not demonstrated.

Finally, a growing body of evidence hints at a potential role for piRNA binding Piwi proteins in cancer (Suzuki et al., 2012). In recent years several observational and correlative studies have detected dysregulated Piwi protein expression in various human cancers, including breast, cervical, colon, endometrial, esophageal, gastric, Glioma, liver, pancreatic, and seminoma. Several in vitro studies have shown an effect of Piwi protein overexpression or deficiency on the proliferation of transformed cells, hinting at a role in cancer metastisis or drug resistance (Tan et al., 2015; Greither et al., 2012; Su et al., 2012; Wang et al., 2012). The lack of a consensus expression pattern in cancer, where one or multiple Piwi proteins are either increased or decreased in expression relative to normal tissue, emphasizes the need for more rigorous testing of the somatic cell function of Piwi proteins.

RATIONALE

Large-scale genome sequencing has revealed the large proportion of the mammalian genome derived from ancient retroviral elements and transposons, collectively known as retroelements. Control of retroelement expression in mammals is critical, as activation and reinsertion of retroelements into the genome are detrimental to host genome integrity. Retroelements are most highly expressed in the male germline in mammals, however recent evidence suggests that they are also induced in many somatic tissues, particularly during inflammation and infection. This expression is driven by inflammatory transcription factor binding sites encoded on the retroelement promoters (Young et al., 2012; Chambers, 2014). In the mammalian germline, defense against retroelement expression is executed by the piRNA silencing pathway. piRNAs are a family of short, 23-36 nucleotide RNAs generated from distinct genomic clusters (Thomson and Lin, 2009). piRNAs associate with a subtype of Argonaute proteins known as PIWI proteins, which facilitate both transcriptional and post-transcription gene silencing (Hutvagner and Simard, 2008; Deng and Lin, 2002; Kuramochi-Miyagawa, 2004; Carmell et al., 2007). Mice deficient in one or all of the Piwi–clade proteins are viable, however they universally exhibit abnormalities in germ cell function, primarily spermatogenesis, resulting from aberrant retrotransposon expression and causing meiotic arrest. While study of piRNAs and PIWI proteins have mainly focused on the role in the germline, strong evidence exists, at least in *Drosophila*, for a somatic cell function of

piRNAs or piRNA binding proteins. However, exhaustive efforts have been yet unsuccessful in identifying a clear role for piRNA silencing machinery in mammalian somatic cells. Given the role of piRNAs as an immune defense strategy against ancient retroviral elements in germ cells, and the potential that retroelements are induced during inflammation, we sought to determine if the piRNA silencing pathway was active in somatic cells during the innate immune response to bacterial infection.

CHAPTER TWO: MATERIALS AND METHODS

Common Buffers and Reagents

Phosphate- buffered saline (PBS): 1.05 mM KH_2PO_4, 155.17 mM NaCl, 2.97 Na_2HPO_4-$7H_2O$, pH 7.4 (Gibco, Life Technologies)

Dulbecco's modification of phosphate-buffered saline (DPBS): 2.67 KCl, 1.47 mM KH_2PO_4, 137.93 mM NaCl, 8.06 Na_2HPO_4-$7H_2O$, pH 7.0 (Gibco, Life Technologies)

Tris-buffered saline- Tween-20 (TBS-T): 25 mM Tris, 125 mM NaCl, 0.1% Tween-20

Hank's balanced salt solution (HBSS): 5.33 mM KCl, 0.44 mM KH_2PO_4, 4.167 mM $NaHCO_3$, 137.93 mM NaCl, 0.33 mM Na_2HPO_4, 5.56 mM D-Glucose (Gibco, Life Technologies)

Tris acetate- EDTA buffer (TAE): 40 mM Tris, 20 mM acetic acid, 1 mM EDTA

NuPAGE® MOPS SDS running buffer: 50 mM MOPS, 50mM Tris base, 0.1% SDS, 1 mM EDTA, pH 7.7 (Life Technologies)

NuPAGE® Transfer buffer: 25 mM Bicine, 25mM Bis-Tris, 1 mM EDTA, 50% methanol, pH 7.2 (Life Technologies)

FACS buffer: 0.5% HI-FBS (Gibco, Life Technologies), 2 mM EDTA in PBS

FACS sorting buffer: 1% BSA (Sigma Aldrich) in PBS

Immunoblot blocking buffer: 5% non-fat milk in TBS-T

IP lysis buffer: 50 mM Tris–HCl pH 7.4, 150 mM NaCl, 5 mM $MgCl_2$, 15% glycerol, 1 mM DTT, 0.5% sodium deoxycholate, 0.5% Triton X-100, 1x protease inhibitor cocktail

IP wash buffer: 10 mM Tris, pH 8, 150 mM NaCl, 1 mM $MgCl_2$, 0.1% NP-40

Proteinase K buffer: 10 mM Tris, pH 7.5, 0.5% SDS, 5 mM EDTA

Mouse Models

Mouse experiments were performed in accordance with US Federal Law and approved by the Boston University School of Medicine Institutional Animal Care and Use Committee (IACUC) (Permit # 14859). Experiments were performed under approved anesthesia as described below, and all efforts were made to minimize suffering. Mice were housed in a specific pathogen free facility

at Boston University School of Medicine with access to food and water *ad libitum* on a twelve-hour light/dark cycle. Experiments were carried out on 6-12 week old mice unless otherwise indicated.

C57BL/6

C57BL/6 mice were purchased and used directly from the Jackson Laboratory, or from a colony maintained by our laboratory.

Miwi2 deficient mice

Miwi2$^{-/-}$ mice were obtained from Dr. Gregory Hannon at Cold Spring Harbor Laboratory/Howard Hughes Medical Institute and rederived at Boston University. This mouse was generated by insertional mutagenesis that created a duplication of the genomic region containing exons 9-12 of *Miwi2*, resulting in multiple stop codons and the subsequent nonsense-mediated decay of the mutant *Miwi2* transcript (Carmell et al., 2007). These mice were maintained on a C57BL/6 background, and bred as heterozygous x heterozygous crosses, hence generating wildtype littermate controls.

Epitope-tagged Miwi2 mice

Miwi2$^{HA/+}$ mice were generated by and obtained from Dr. Dónal O'Caroll at EMBL Monterontondo. These mice were engineered by CRISPR/CAS9 targeting to contain the HA (hemagglutinin) epitope derived from the influenza virus HA protein inserted immediately following the *Miwi2* start codon resulting in an HA-MIWI2 N-terminal fusion. These mice were maintained on a C57BL/6

background, and bred as Miwi2$^{HA/+}$ x C57BL/6 crosses, hence generating wildtype littermate controls. A full description and targeting strategy will be provided in a forthcoming report by Dr. O'Caroll.

Epithelial specific RelA deficient mice

Mice lacking RelA in lung epithelial cells were generated by crossing Nkx2-1-Cre mice with RelA$^{loxP/loxP}$ mice (Yamamoto et al., 2013) to generate a colony of Nkx2-1^{tg+} RelA$^{loxP/loxP}$ (Ep. RelA$^{\Delta/\Delta}$) and of Nkx2-1^{tg-} RelA$^{loxP/loxP}$ (WT) littermates.

Miwi2 tomato knock-in mice

To generate Miwi2 reporter mice, tdTomato, along with a polyadenylation sequence was engineered into the first exon of the native *Miwi2* locus by CRISPR/Cas targeting by Dr. Dónal O'Caroll (MRC). The full targeting scheme will be described in a later report.

Cell Lines

General Information

E10 cells are a murine lung epithelial cell line and were obtained from the BU Pulmonary Center cell bank and originally a gift of Dr. A. Malkinson (University of Colorado) (Kathuria, 2004). Cells were maintained in CMRL 1066 medium supplemented with 10% FBS, 0.5 mM L-glutamine, 100 units/mL penicillin G, and 100 μg/mL streptomycin sulfate (all from Life Technologies) and

grown at 37 °C 5% CO_2 in a humidified incubator. When necessary, media was supplemented with 2 μg/mL of puromycin.

Generation of stable shRNA cell lines

Replication incompetent lentiviruses used to generate stably expressing shRNA cells were generated as previously described. Miwi2 shRNA vectors or control shRNA were acquired from Dharmacon. Briefly, 293T cells were transfected with the shRNA containing backbone vector together with 2 expression vectors encoding the packaging proteins Gag-Pol, Rev, Tat, and the G protein of the vesicular stomatitis virus (VSV-G) using TransIT transfection reagent. Cell supernatants were collected for 3 days post transfection, filtered and ultracentrifugated at 48,960 x *g* for 30 minutes at 4 °C. To generate a stably transduced E10 cell line, cells were seeded into 6 well tissue culture plates and grown at 37 °C 5% CO_2 in a humidified incubator overnight. The next day, 20 μL of Miwi2 targeting or control lentivirus was added along with 5 μg/mL polybrene (Santa Cruz Biotechnology). 24 hours post infection, CMRL complete media supplemented with 2ug/mL puromycin was added.

Cell fixation for immunofluorescence

Stable shRNA expressing E10 cells were grown on a 35mm glass bottom culture dish (Mat Tek) at 37 °C 5% CO_2 in a humidified incubator overnight. The next day, media was replaced with complete CMRL supplemented with 10 ng/mL TNFa or vehicle for 6 hours. Glass slides were fixed in 2% (vol/vol)

paraformaldehyde for 10 minutes at room temperature before staining. Staining was performed as described below, using a Miwi2 antibody provided by Dr. Ramesh Pillai (EMBL Grenoble).

Bacterial Procedures

Generation of bacterial stocks

To generate frozen stocks, *Streptococcus pneumoniae* serotype 19F (Sp19, strain EF3030 provided by Dr. M. Lipsitch, Harvard School of Public Health, Boston, MA) was grown on trypticase soy agar supplemented with 5% sheep blood and incubated at 37 °C 5% CO_2 until mid-logarithmic growth. A bacterial suspension was made in Brain Heart Infusion broth containing 16% sterile glycerol and snap frozen in a dry ice-ethanol bath in single use aliquots and stored at -80 °C.

Preparation of bacteria for in vivo experiments

For intratracheal infection experiments, bacteria were streaked on trypticase soy agar supplemented with 5% sheep blood and incubated at 37 °C 5% CO_2 overnight. Four hours prior to infection, bacteria were restreaked on trypticase soy agar supplemented with 5% sheep blood and incubated at 37 °C 5% CO_2. Target instillation was estimated by optical density and confirmed by serial dilution on agar plates.

Experimental infections

For intratracheal instillations mice were anesthetized by an intraperitoneal (i.p.) injection of ketamine (50 mg/kg) and xylazine (5mg/kg) diluted in sterile saline. The tracheas were surgically exposed and cannulated using a 24 gauge angiocatheter that was directed to the left bronchus. A 50 μL bolus of bacteria suspended in sterile saline was instilled using a micropipetter. Mice were placed in the right lateral decubitus position until they were sternally recumbent. A target instillation of $5x10^6$ CFU of bacteria was estimated by optical density and verified by quantifying serial dilutions grown on trypticase soy agar supplemented with 5% sheep blood agar plates (SBA) at 37 °C overnight.

Bronchoalveolar lavage

Mice were sacrificed by overdose of isoflourane. After skin decontamination with 70% isopropanol, the mouse was placed supine and a midline abdominal incision was made and extended from the level of the bladder cephalad into a midline sternotomy. Exsangunation was performed by ligating the inferior vena cava. The trachea was identified and marked with silk suture and the cardiopulmonary trunk was removed *en bloc*. The trachea was cannulated with a 20-gauge blunted stainless steel catheter and secured with silk suture. Serial 1 mL lavage samples were taken with ice-cold PBS. The lavage fluid was centrifuged at 300 x *g* for 5 minutes at 4°C, and cell pellets were utilized for differential counts. BAL cell counts were performed as previously described

(Hyatt et al., 2014), with cytocentrifuged slides stained with the Diff-Quick staining kit (Dade Behring) after counting suspended cells using a hemocytometer. For BAL cytokine measurement, the supernatant of the first 1 mL lavage sample was saved separately at -80 °C for protein analysis.

Bacterial burden measurements

At the indicated time points, mice were sacrificed by overdose of isoflourane. After skin decontamination with 70% isopropanol, the mice were placed supine and a midline abdominal incision was made and extended from the level of the bladder cephalad into a midline sternotomy. Exsangunation was performed by ligating the inferior vena cava. The lung lobes were removed individually and placed into 5 mL capacity tubes containing sterile 3.2-mm diameter stainless steel beads (Next Advance) and 300 µL of sterile water supplemented with 1x protease inhibitor (Roche). Once homogenized using the Bullet Blender (Next Advance), lung homogenates were brought up to 5 mL with PBS containing 1x protease inhibitor (Roche). Homogenates were serially diluted in PBS and plated on sheep blood agar plates. After an overnight incubation at 37 °C, colonies were enumerated and expressed as total CFU per lung.

Lung Digestion

Mice were sacrificed by overdose of isoflourane. After skin decontamination with 70% isopropanol, the mouse was placed supine and a

midline abdominal incision was made and extended from the level of the bladder cephalad into a midline sternotomy. Exsangunation was performed by ligating the inferior vena cava. A 24 gauge angiocatheter was inserted into the right ventricle and the lungs perfused via the pulmonary artery with 10 mL of HBSS to remove red blood cells. A silk tie was placed around the heart to maintain pulmonary pressure. The trachea was identified, marked with silk suture and the cardiopulmonary trunk was removed *en bloc*. The trachea was cannulated with a 20-gauge blunted stainless steel catheter and secured with silk suture. Lavage samples, a total of 10 mL, in 1 mL increments were taken with ice-cold DPBS containing 5 mM of EDTA. Lungs were then serially lavaged with 1 mL of RPMI1640 with 100 U/mL DNAse I (Qiagen), followed by 1 mL of porcine elastase (4.5 U/mL; Roche Diagnostics) dissolved in RPMI1640 medium. An additional 1 mL of elastase solution was instilled followed by 0.5 mL low melting agarose solution warmed to 55 °C. Lungs were immediately covered with ice for 2 min to polymerize the agarose and then incubated in 2 mL elastase solution for 45 min at 37 °C. After this incubation, lung lobes were gently separated from the trachea and cardiac tissue and minced in RPMI1640 medium containing 50% FBS and 100 U/mL DNase I using a sterile razor blade. Cells were separated by serial filtration through 100, 70, and 40 μM filters, and collected by centrifugation at 300 x *g* for 10 minutes. Lung single-cell suspensions were subjected to FACS.

Flow Cytometry

Cells isolated from lung digests were pelleted by centrifugation for 5 minutes at 300 x *g* at 4°C, and resuspended in 100 μL of FACS buffer for staining. Surface antigens were stained by adding 20 μL of diluted antibody and Fc Block (BD Biosciences), and incubating on ice in the dark for 30 minutes. Cells were washed by adding 4 mL of PBS to each tube, followed by pelleting by centrifugation. Cells were then resuspended in 300 μL FACS buffer. Single stained bead controls were utilized for gating and compensation. Antibodies and stains are available in Table 1. Cells were sorted using the BD FACS AriaII and collected in PBS containing 1% BSA, centrifuged at 300 x *g* for 5 minutes at 4 °C and then resuspended in 1 mL of Trizol. RNA was isolated following the manufacturer's protocol.

Table 1: Antibodies used for flow cytometry (FACS)

Antigen	Species	Clone	Conjugate	Supplier	Dilution	Use
EpCAM (CD326)	Rat	G8.8	APC, APC-Cy7	G8.8	1:300	FC
CD45	Rat	30-F11	PE-Cy7	Biolegend	1:500	FC
CD24	Rat	M1/69	PE, APC	BD Pharmagin	1:50	FC
Ly6G	Rat	1A8	APC-Cy7	Biolegend	1:200	FC
F4/80	Rat	BM8	PE-eflour 610	Biolegend	1:50	FC

RNA Isolation, and Quantitative Reverse Transcriptase-PCR

Total Lung RNA Isolation

Lung lobes were isolated, snap frozen in liquid nitrogen and stored at -80 °C until RNA preparation. Tissue was placed into 5 mL capacity tubes containing sterile 3.2-mm diameter stainless steel beads (Next Advance) and homogenized in buffer RLT (from Qiagen RNeasy kit) and RNA was isolated using the Qiagen RNeasy kit following the manufacturers instructions.

Cell line RNA isolation

Cells were collected via trypsin dissociation, washed in PBS and centrifuged at 300 x *g* for 5 minutes at 4 °C. Cells were lysed in RLT (from Qiagen RNeasy kit) and RNA was isolated using the Qiagen RNeasy kit following the manufacturers instructions.

qRT-PCR

Quantitative real time PCR (qRT-PCR) was performed on 100 ng of extracted RNA using a CFX96 Real-Time System (Bio-Rad) and TaqMan RNA-to-C_T 1-step kit (Applied Biosystems). Primer and probes for *Miwi2* (Mm01144775) and 18s (Mm03928990) rRNA were obtained from Life Technologies. Fold induction was calculated using the $2^{\Delta\Delta Ct}$ method (Livak and Schmittgen, 2001).

Microarray analysis

Microarray analysis was performed by the Boston University Medical Campus Microarray Core. Affymetrix GeneChip Mouse Gene 2.0 CEL files were normalized to produce gene-level expression values using the implementation of the Robust Multiarray Average (RMA) (Irizarry et al., 2003) in the *affy* package (version 1.36.1) (Gautier et al., 2004) included in the Bioconductor software suite (version 2.12) (Gentleman et al., 2004) and an Entrez Gene-specific probeset mapping (17.0.0) from the Molecular and Behavioral Neuroscience Institute (Brainarray) at the University of Michigan (Dai et al., 2005). Array quality was assessed by computing Relative Log Expression (RLE) and Normalized Unscaled Standard Error (NUSE) using the *affyPLM* package (version 1.34.0) (Brettschneider et al., 2008). Principal Component Analysis (PCA) was performed using the *prcomp* R function with expression values that had been normalized across all samples to a mean of zero and a standard deviation of

one. Re-normalization of the array to interrogate probesets unique to endogenous retroelements was performed using a custom mapping (Young et al., 2014). Differential expression was assessed using the moderated (empirical Bayesian) and t test implemented in the *limma* package (version 3.14.4) (i.e., creating simple linear models with *lmFit*, followed by empirical Bayesian adjustment with *eBayes*). Correction for multiple hypothesis testing was accomplished using the Benjamini-Hochberg false discovery rate (FDR) (Benjamini and Hochberg, 1995). Human homologs of mouse genes were identified using HomoloGene (version 68) (NCBI Resource Coordinators, 2016). All microarray analyses were performed using the R environment for statistical computing (version 2.15.1). Heatmaps were generated using a method previously described (Pavlidis and Noble, 2003).

Tissue fixation, immunohistochemistry and immunofluorescence

For immunohistochemistry, mice were sacrificed by overdose of isoflourane. After skin decontamination with 70% isopropanol, the mouse was placed supine and a midline abdominal incision was made and extended from the level of the bladder cephalad into a midline sternotomy. Exsangunation was performed by ligating the inferior vena cava. A silk tie was placed around the heart. The trachea was identified, marked with silk suture and the cardiopulmonary trunk was removed *en bloc*. The trachea was cannulated with an 18-gauge angiocatheter and secured with silk suture. Freshly prepared 4%

(vol/vol) paraformaldehyde (PFA) diluted in PBS was instilled at 20 cm H_2O pressure. PFA inflated lungs were fixed, submerged in 10 mL of 4% paraformaldehyde at 4 °C overnight. The following day, samples were embedded in paraffin using the protocol described in **Table 2**. 5 μM sections were prepared with a microtome, and the slides cured on a heating block at 55 °C for 12 hours, before storage at 4 °C. Slides were deparaffinized by standard treatment in xylenes and ethanol and quenched with 3% (vol/vol) hydrogen peroxide in methanol for 30 min. Sections were blocked with 5% normal donkey serum in PBS and incubated with primary antibody overnight at 4 °C. Secondary antibody, diluted in PBS was added for 1 hour at 23 °C. Bound antibody was detected using the Vectastain ABC peroxidase kit (Vector Laboratories) and visualized using 3,3′-diaminobenzidine (DAB). Slides were counterstained with hematoxylin, sealed with Cytoseal XYL (Thermo Fisher) and imaged using a Zeiss Axioskop microscope. For immunofluorescence, sections were prepared as above except with the following modification. A 22 gauge angiocatheter was inserted into the right ventricle and the lungs perfused via the pulmonary artery with 10 mL HBSS to remove red blood cells before placing a tie around the heart to maintain pulmonary pressure during inflation. Images were acquired using a Zeiss LSM-700 confocal microscope, and ZEN software. Primary and secondary antibodies used are available in **Table 3.**

Table 2: Paraffin embedding protocol

Solution	Incubation Time	Temperature
PBS	30 min	on ice
0.85% NaCl	30 min	on ice
1:1 ethanol: 0.85% NaCl	30 min	RT
70% ethanol	30 min	RT
70% ethanol	30 min	RT
80% ethanol	45 min	RT
90% ethanol	45 min	RT
100% ethanol	30 min	RT
100% ethanol	30 min	RT
100% ethanol	30 min	RT
xylene	30 min	RT
xylene	30 min	RT
xylene	30 min	RT
1:1 xylene: paraffin	1.5 h	60 °C
paraffin	1h	60 °C vacuum
paraffin	1h	60 °C vacuum

Table 3: Antibodies used for IF

Antigen	Species	Clone	Conjugate	Supplier	Dilution	Use
HA epitope	Rabbit	C29F4	N/A	Cell Signaling	1:1000/ 1:100/ 1:100	IB/IF/IHC
Foxj1	Mouse	2A5	N/A	eBioscience	1:300	IF
Scgb1A1 (CC10)	Goat	Polyclonal	N/A	Santa Cruz	1:500	IF
Acetylated alpha tubulin	Mouse	6-11B-1	N/A	Sigma Aldrich	1:1000	IF
RFP	Rabbit	Polyclonal	N/A	Rockland	1:500	IF
Mouse IgG	Donkey	Polyclonal	Alexa Fluor 488	Life Technologies	1:500	IF
Rabbit IgG	Donkey	Polyclonal	Alexa Fluor 647	Life Technologies	1:300	IF
Goat IgG	Donkey	Polyclonal	Alexa Fluor 555	Life Technologies	1:300	IF

Protein Measurements

Enzyme-Linked Immunosorbent Assays (ELISAs)

IL-6, CXCL1, CXCL2, and CXCL5 DuoSet kits were purchased from R&D Systems and were performed according to the manufacturer's instructions.

Multi-Plex Bead Array

BALF cytokine concentrations were quantified using a Bio-plex cytokine bead array and analyzed on a Bioplex 200 workstation (Bio-Rad) according to the manufacturer's protocol.

Bicinchoninic Acid (BCA) Assay

Total protein concentrations were determined using the BCA assay (Sigma-Aldrich). BSA was used as the protein standard at four different concentrations, 0, 0.2, 0.6, and 0.9 mg/ml, and protein concentration calculated by generating a standard curve.

Immunoblot analysis

Total protein concentrations were measured by BCA assay (Sigma Aldrich) using the manufacturers suggested protocol. 40 μg of protein, or a predefined proportion of immunoprecipitate was suspended in 1x LDS sample loading buffer plus reducing agent (Life Technologies) and heated for 10 minutes at 70 °C before loading onto a 4-12% Bis-Tris gel, along with 10 μL of the Novex Sharp pre-stained protein ladder. 1x MOPS SDS running buffer was added and

the gel was resolved for 50 min at 200V. Protein was then transferred onto an Immobilon-P polyvinylidene fluoride (PVDF) membrane (Millipore) in 1X NuPage transfer buffer (Life Technologies) with 10% methanol at 30 V for 1 hour using the X-Cell Blot II system. Following transfer, membranes were blocked in 5% non-fat milk in TBS-T with agitation at room temperature. Primary antibody (rabbit anti-HA epitope, Cell Signaling Clone: C29F4) was diluted in 5% non-fat milk in TBS-T and incubated at room temperature for 2 hours with agitation. The membrane was washed 3 times in TBS-T and incubated with secondary antibody (anti-rabbit IgG-HRP, Cell Signaling) diluted in 5% non-fat milk in TBS-T at room temperature for 1 hour with agitation. Membranes were washed 3 times in TBS-T and treated with ECLPlus for 3 minutes (GE Healthcare) before exposure exposure to film (GE Healthcare).

Isolation of Miwi2 bound RNA

Lungs from uninfected or infected *Miwi2*$^{+/+}$ or *Miwi2*$^{HA/+}$ mice were harvested as above and homogenized in 20 mM Tris–HCl pH 7.4, 100 mM NaCl, 2.5 mM MgCl2, 0.1% NP-40 with a protease inhibitor cocktail (Sigma) and RNaseOUT(Life Technologies) using a polytron homogenizer. The homogenate was centrifuged at 15,000 x g for 10 min at 4 °C, and total protein concentration measured by BCA (Sigma Aldrich). 10 mg of supernatant was pre-incubated with 100 μL of protein G coupled magnetic beads (Invitrogen), and immunoprecipitation was carried out with 100 μL of magnetic beads coupled to

12 μg α−HA antibody (Thermo Fisher #26183). Beads were washed 3 times with IP wash buffer and an aliquot saved for western blot analysis. The remaining beads were resuspended in protease K buffer, treated with proteinase K and RNA prepared from the supernatants using Trizol LS according to the manufactures recommendations. Isolated RNA was dephosphorylated using thermosensitive alkaline phosphatase (TSAP, Promega) for 30 min at 37 °C. To inactivate TSAP, the reaction was incubated at 74 °C for 15 min. 5′ labeling was performed with [γ-^{32}P]ATP (8,000 Ci mmol−1) and T4 PNK. Reactions were mixed with an equal volume of 2× urea loading buffer, and products were resolved on a 15% TBE-Urea gel.

Statistical Analysis

All statistical analyses were performed using GraphPad Prism 6.0 (GraphPad). Data are displayed as either arithmetic means ± standard error of the mean (SEM), or medians as indicated in the figure legends. Two groups were compared using either a student's t test (parametric) or a Mann-Whitney test (non-parametric), while multiple group comparisons were conducted using either a one- or two-way analysis of variance (ANOVA), followed by specific post hoc tests as indicated in the figure legend. Values were log-transformed prior to analysis if they did not pass the F test for equal variance. Data were considered significant if $P \leq 0.05$ for all experiments. For microarray data, statistical

significance was determined by false discovery rate (*q)* to correct for multiple comparisons.

CHAPTER THREE: RESULTS

3.1 Miwi2, a piRNA binding protein is induced in the lungs during pneumococcal pneumonia

Our laboratory group has previously reported a novel digestion and sorting strategy to isolate single cell suspensions from the mouse lung on the basis of relative expression of CD45 and CD326, also known as epithelial cell adhesion molecule (EpCAM). Epithelial cells are identified as $CD45^-$ $EpCAM^+$, leukocytes as $CD45^+$ $EpCAM^-$, and other cell-types being $CD45^-$ $EpCAM^-$ (Yamamoto et al., 2013). In a report by Kamata and colleagues currently in revision, we expand our understanding of epithelial-specific gene expression during *Streptococcus pneumoniae* pneumonia. Epithelial and non-epithelial cells were transcriptionally profiled using microarray to identify genes induced by pneumonia selectively in epithelial cells. Mice were instilled with pneumococcus or vehicle and left lungs were collected 15 hours after infection. Single cell suspensions were generated and sorted into 2 separate populations, epithelial cells ($CD45^-$ $EpCAM^+$) and others (all non-epithelial cells) **(Figure 1A)**. Genome-wide expression profiling revealed 196 genes specific to the epithelium, significantly induced greater than two fold in epithelial cells from pneumonic mice as compared to vehicle treated mice(**Figure 1B)**. Among the mRNAs significantly induced during lung infection, we were surprised to observe that the transcript encoding for Miwi2, a piRNA binding protein, was induced approximately 3 fold (Log_2) (**Figure 2A)**. The transcriptomic dataset was subsequently queried to determine if other proteins

known to be involved in piRNA biogenesis or silencing were induced during bacterial infection in lung epithelial cells. Using an FDR cutoff of q <0.05, we observed that none of the proteins involved in primary biogenesis including, MIWI, MILI, MOV10L1, TDRD1, TDRKH, PLD6, GASZ, GPAT2, or MAEL were significantly induced (Fu and Wang, 2014; Iwasaki et al., 2014). Nor were any of the piRNA proteins involved in secondary piRNA biogenesis (MILI, MVH, TDRD9, TDRD12, MAEL, FKBP6) differentially expressed (**Figure 2A)**. Similar to the majority of the components of the piRNA silencing machinery, expression of the miRNA binding family of Argonautes remained unchanged during infection. We next confirmed the induction of *Miwi2* RNA using quantitative reverse transcriptase polymerase chain reaction (qRT-PCR) on the original RNA samples used in the microarray analysis (**Figure 2B).** Results indicate that *Miwi2* mRNA was significantly induced approximately 4 fold in $CD45^-$ $EpCAM^+$ epithelial cells 15 hours after infection with pneumococcus.

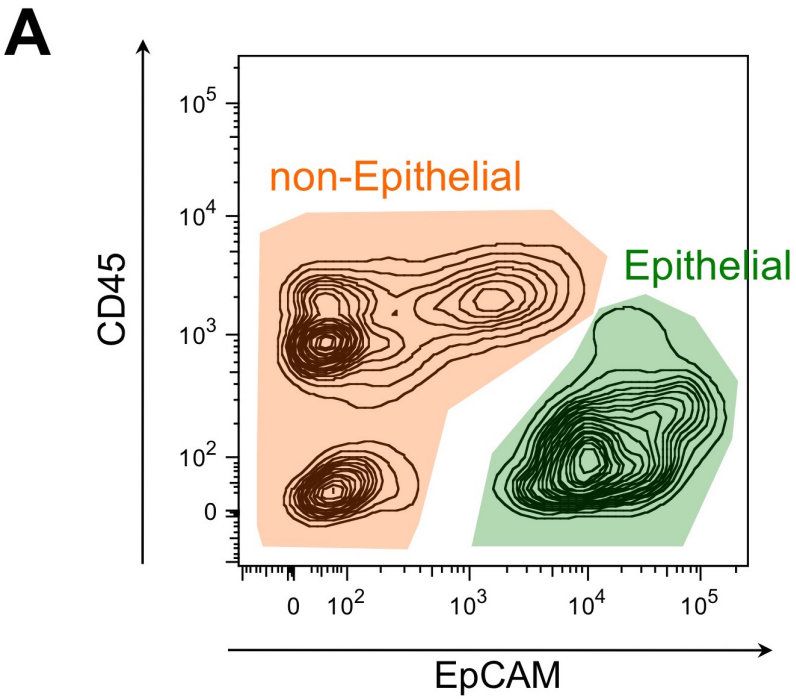
A
CD45
EpCAM
non-Epithelial
Epithelial
10^5
10^4
10^3
10^2
0
0
10^2
10^3
10^4
10^5

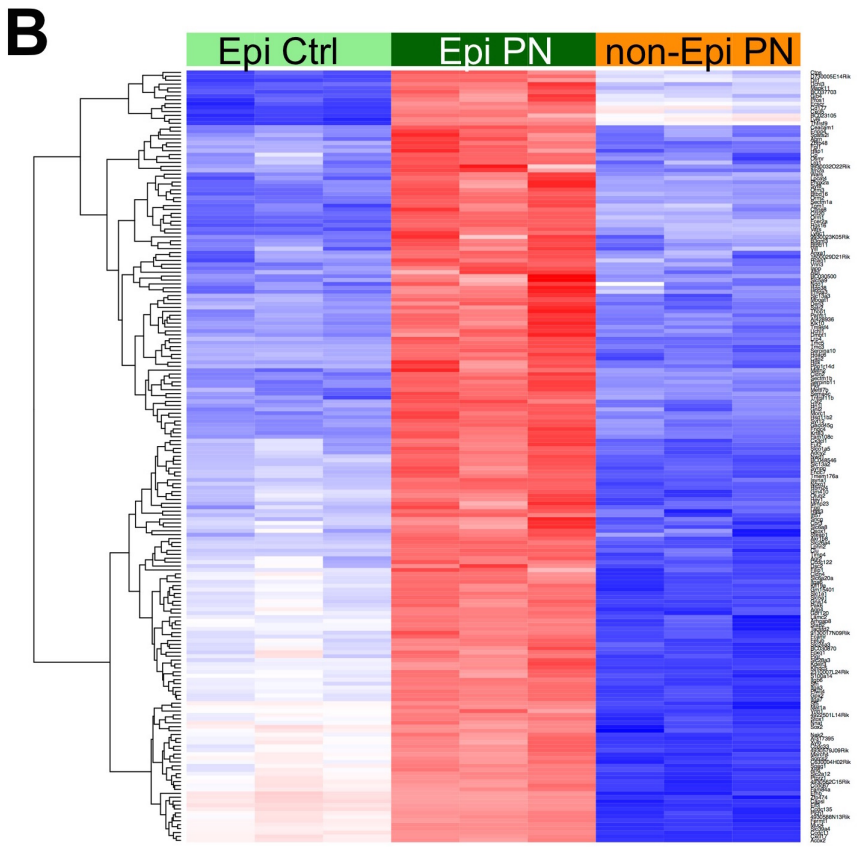
B
Epi Ctrl
Epi PN
non-Epi PN

Figure 1: Identification of epithelial induced genes during pneumococcal pneumonia

C57BL/6 mice were infected with $2x10^6$ CFU of *Streptococcus pneumoniae*, intratracheally for 15 hours. Lungs were harvested and digested with elastase to generate single cell suspensions. **(A)** Representative flow cytometry plot pre-selected for live cells. Delineation of sorted populations indicated by colored shading, green=epithelial, orange= non-epithelial **(B)** Expression heatmap of filtered genes induced greater than 2 fold with respect to pneumonia and enrichment in epithelial cells. FDR< 0.05.

A

	Symbol	Description	Common Name	epithelial pneumonic vs epithelial uninfected fold change	Student FDR q
Primary Processing	Piwil1	piwi-like homolog 1 (Drosophila)	Miwi	-1.03	0.6806
	Mov10l1	Moloney leukemia virus 10-like 1	Mov10L1	1.00	0.9878
	Pld6	phospholipase D family, member 6	MitoPLD/ Zucchini	-1.06	0.0774
	Piwil2	piwi-like homolog 2 (Drosophila)	Mili	-1.04	0.4916
	Tdrkh	tudor and KH domain containing protein		1.12	0.05640
Secondary Processing	Tdrd1	tudor domain containing 1		1.03	0.5307
	Fkbp6	FK506 binding protein 6		1.01	0.5498
	Tdrd12	tudor domain containing 12		1.13	0.2877
	Piwil4	piwi-like homolog 4 (Drosophila)	Miwi2	2.86	0.0025
	Ddx4	DEAD (Asp-Glu-Ala-Asp) box polypeptide 4	Mvh	-1.03	0.5508
	Tdrd9	tudor domain containing 9		-1.05	0.2168
	Tdrd5	tudor domain containing 5		-2.33	0.0110
	Mael	maelstrom homolog (Drosophila)		1.00	0.9971
Ago Family	Eif2c1	eukaryotic translation initiation factor 2C, 1	Ago1	-1.73	0.0027
	Eif2c2	eukaryotic translation initiation factor 2C, 2	Ago2	1.09	0.4610
	Eif2c3	eukaryotic translation initiation factor 2C, 3	Ago3	1.03	0.5375
	Eif2c4	eukaryotic translation initiation factor 2C, 4	Ago4	-1.61	0.0027

B

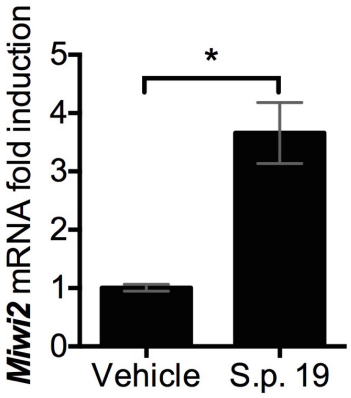

Figure 2: The piRNA binding protein MIWI2 is induced during pneumococcal pneumonia

C57BL/6 mice were infected with $2x10^6$ CFU of *Streptococcus pneumoniae*, intratracheally for 15 hours. Lungs were harvested and digested with elastase to generate single cell suspensions sorted by FACS. **(A)** Microarray expression results for selected piRNA silencing pathway components and Argonaute family proteins. Classification was based off of (Fu and Wang, 2014) **(B)** qRT-PCR of RNA from sorted Live $CD45^-$ $EpCAM^+$ epithelial cells from mice treated with vehicle or *S. pneumoniae* serotype 19F. Results indicate fold change relative to vehicle treated mice (*n*= 4 mice per group, means ± s.e.m. $P< 0.05$ as determined by unpaired t-test).

3.2 Miwi2 induction is specific to epithelial cells

Several previous studies have detected piRNA binding protein mRNAs in various tissues and cell types (Jacobs et al., 2013; Sharma et al., 2001; Sasaki et al., 2003). To determine if lung epithelial cells are the predominant source of *Miwi2* in lungs during pneumococcal pneumonia, major cell populations were isolated from lung digests and bronchoalveolar lavage by FACS from mice infected for 24 hours with $5x10^6$ CFU of *S. pneumoniae* serotype 19. RNA was prepared from total epithelial cells ($CD45^-$ $EpCAM^+$), leukocytes ($CD45^+$ $EpCAM^-$), other cells (including endothelial, lymphatic, and smooth muscle cells) ($CD45^-$ $EpCAM^-$) airspace macrophages ($CD45^+$ $EpCAM^-$ $Ly6G^-$ $F4/80^+$) and airspace neutrophils ($CD45^+$ $EpCAM^-$ $Ly6G^+$ $F4/80^-$) and qRT-PCR was used to quantitate relative abundance (**Figure 3A,B)**. *Miwi2* expression was enriched 40 fold in the $EpCAM^+$ $CD45^-$ population, indicating that epithelial cells are the major producers of *Miwi2* mRNA in the lung (**Figure 3C)**.

Multiple cytokine signals produced during pneumonia activate lung epithelial gene programs, which are necessary for competent host defense to pneumococcus (Yamamoto et al., 2013; 2012; Whitsett and Alenghat, 2014). Previous studies from our lab and others have demonstrated the important role of epithelial RelA signaling in the elaboration of lung epithelial gene expression during pneumococcal pneumonia (Yamamoto et al., 2013). In order to determine if *Miwi2* was induced in lung epithelial cells in a RelA dependent manner, we utilized a previously described mouse model where a critical exon of RelA is

flanked by loxP sites and can be deleted specifically in the lung epithelium via Cre recombinase expression driven the transcription factor Nkx2-1. Wildtype or Epithelial RelA$^{\Delta/\Delta}$ mice were infected with pneumococcus intratracheally, and epithelial cells were collected by FACS 15 hours post infection. qRT-PCR revealed that Miwi2 RNA was induced in epithelial cells in the absence of functional RelA indicating that *Miwi2* induction is independent of RelA activation during pneumococcal pneumonia *in vivo* **(Figure 3D**).

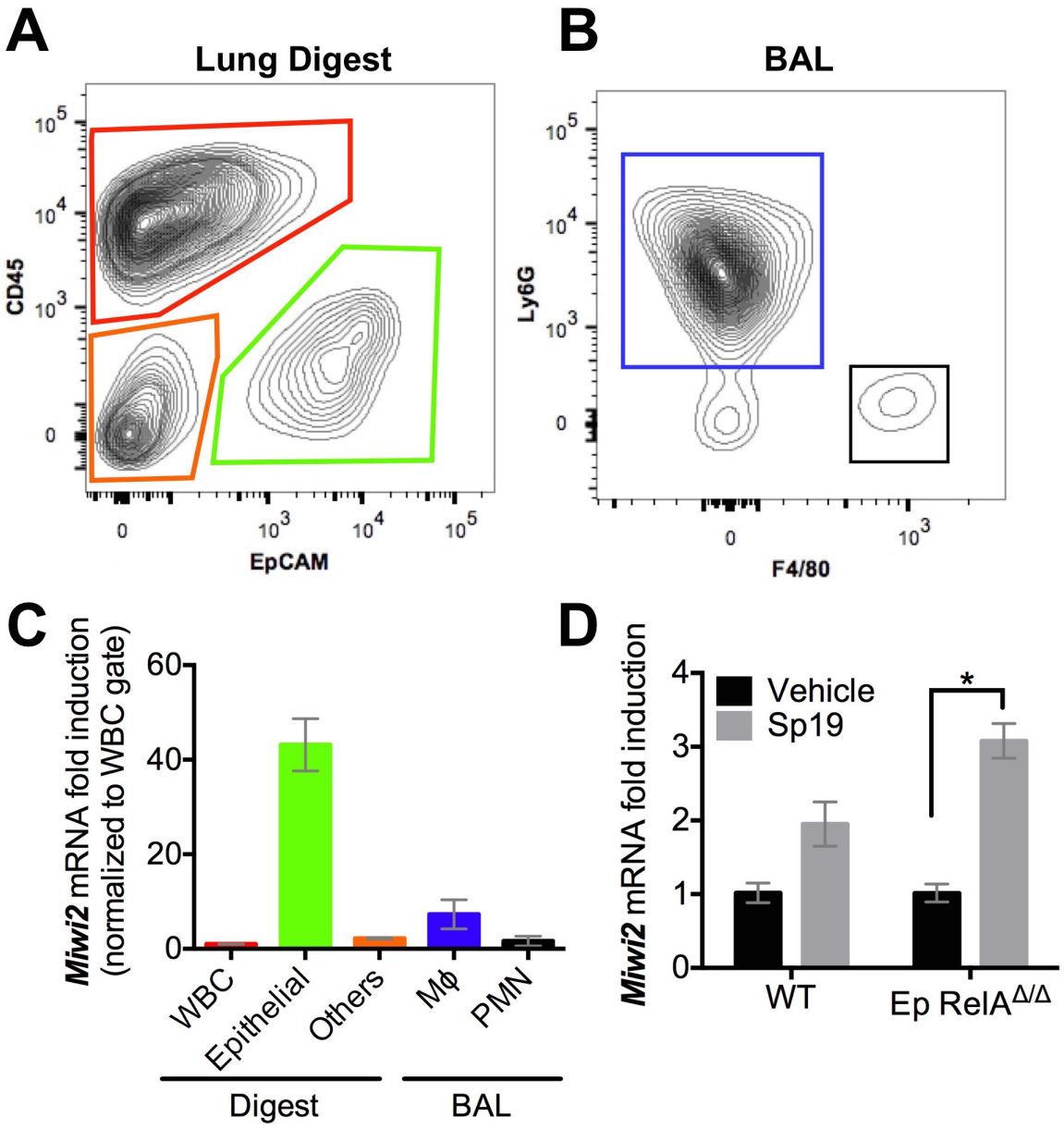
A
Lung Digest
CD45
EpCAM
B
BAL
Ly6G
F4/80
C
Miwi2 mRNA fold induction
(normalized to WBC gate)
WBC
Epithelial
Others
Mφ
PMN
Digest
BAL
D
Miwi2 mRNA fold induction
Vehicle
Sp19
*
WT
Ep RelA Δ/Δ

Figure 3: Miwi2 mRNA is specifically induced in lung epithelium during pneumococcal pneumonia

C57BL/6 mice were infected with $2x10^6$ CFU of *Streptococcus pneumoniae*, intratracheally for 24 hours. Lungs were lavaged and then harvested and digested with elastase to generate single cell suspensions. **(A)** Representative flow cytometry plot indicating sorted populations from lung digest, Live $CD45^-$ $EpCAM^+$ (Epithelial cells-green gate) Live $CD45^+$ $EpCAM^-$ (white blood cells-red gate) and Live $CD45^-$ $EpCAM^-$ (other cells-orange gate) **(B)** Representative flow cytometry plot from BAL, Plot already selected for Live $CD45^+$ cells. Sorted populations include $Ly6G^+F4/80^-$ (PMN,neutrophils-blue gate) and $Ly6G^-F4/80^+$ (macrophages-black gate) (*n*= 3 mice per group) **(C)** qRT-PCR of RNA from sorted populations. Results indicate fold change relative to cells collected from WBC gate (*n*= 3 mice per group, means ± s.e.m) **(D)** qRT-PCR of RNA from sorted Live $CD45^-$ $EpCAM^+$ epithelial cells from $Nkx2\text{-}1^{tg+}$ $RelA^{loxP/loxP}$ (Ep. $RelA^{\Delta/\Delta}$) and of $Nkx2\text{-}1^{tg-}$ $RelA^{loxP/loxP}$ (WT) mice treated with vehicle or *S. pneumoniae* serotype 19F. Results indicate fold change relative to vehicle treated mice (*n*= 3 mice per group, means ± s.e.m. *P< 0.05 as determined by unpaired t-test).

3.3 Miwi2 RNA is induced by various inflammatory stimuli

We next sought to determine the inflammatory stimuli that drove *Miwi2* induction. E10 murine alveolar epithelial cells were stimulated with TNF-α, LPS, IFN-β, or live bacteria. Total cellular RNA was collected and qRT-PCR used to evaluate *Miwi2* induction. *Miwi2* mRNA was not significantly induced by direct stimulation with *S. pneumoniae, K. pneumoniae, or E. coli* **(Figure 4B),** nor by the toll like receptor agonists LPS, or Pam3CSK4 **(Figure 4C,D)**. However *Miwi2* mRNA was significantly induced following stimulation with recombinant TNFα, and IFN-β, both cytokines produced during pneumococcal pneumonia, and known to affect epithelial gene expression **(Figure4D, E)**. Collectively these results indicate that *Miwi2* responds to multiple upstream inflammatory activators in epithelial cells. More broadly, our data show that lung epithelial cells respond to inflammation or infection by inducing the expression of *Miwi2* mRNA both in vitro and in vivo.

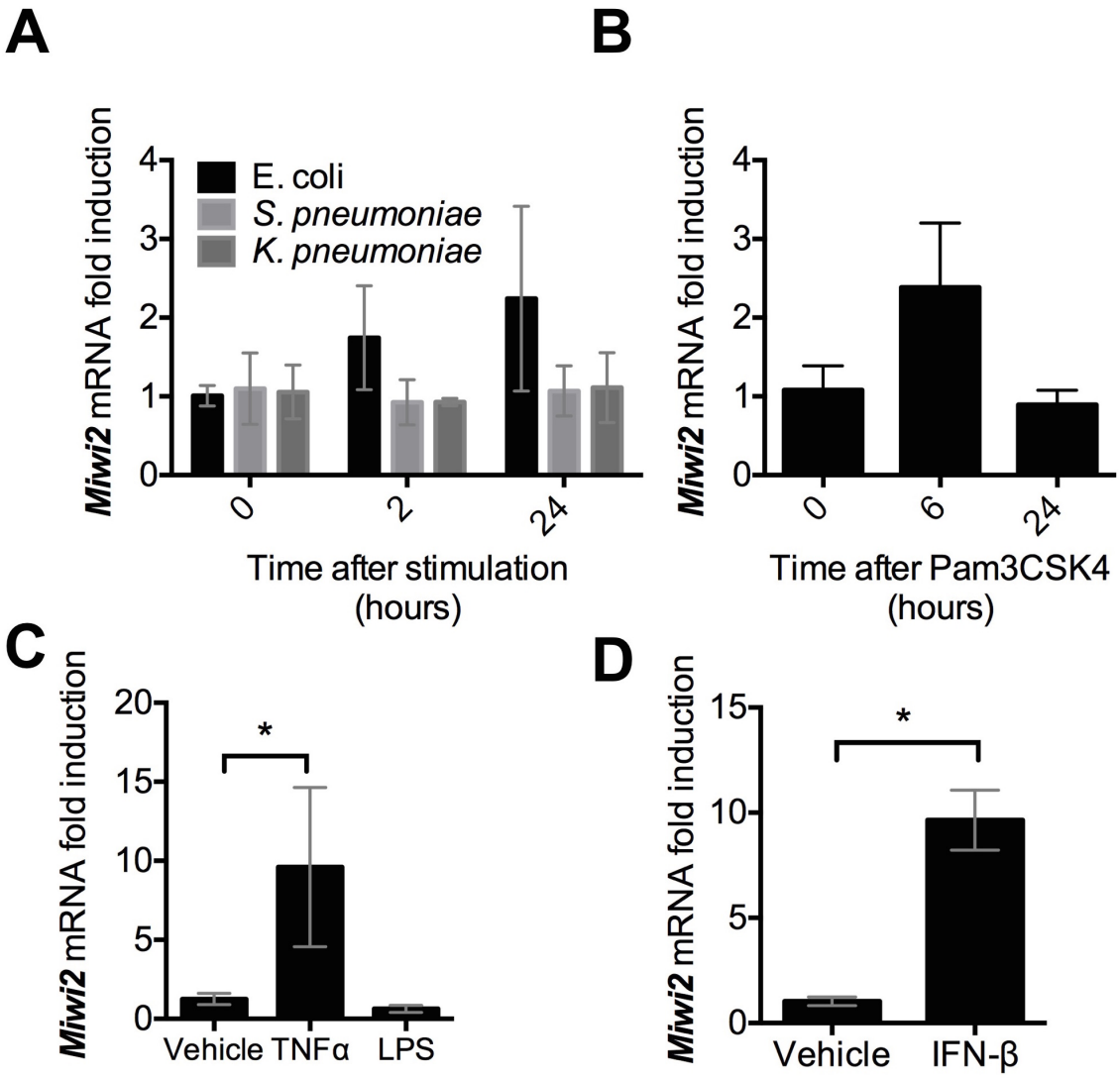
A
B
Miwi2 mRNA fold induction
E. coli
S. pneumoniae
K. pneumoniae
0
1
2
3
4
0
2
24
Time after stimulation (hours)
Miwi2 mRNA fold induction
0
1
2
3
4
0
6
24
Time after Pam3CSK4 (hours)
C
D
Miwi2 mRNA fold induction
0
5
10
15
20
*
Vehicle
TNFα
LPS
Miwi2 mRNA fold induction
0
5
10
15
*
Vehicle
IFN-β

Figure 4: Miwi2 mRNA is induced by inflammatory stimuli

qRT-PCR analysis of RNA prepared from Murine alveolar epithelial E10 cells stimulated with **(A)** live bacteria **(B)** 100 ng/mL of recombinant PAM3CSK4 **(C)** 10 ng/mL recombinant TNF-α or 100 ng/mL LPS for 6 hours (**D)** 1000U recombinant IFN-b for 6 hours. Results indicate fold change relative to *E. coli* stimulated, or vehicle treated (*n*= 3 independent experiments, means ± s.e.m, *P<0.05 as determined by unpaired t-test).

3.4 Miwi2 protein is expressed outside of the germline in lung epithelium

To our knowledge there is no report providing evidence for *Miwi2* protein expression in somatic cells. Despite detection of the mRNA encoding *Miwi2* in the lung, it was unclear whether the protein was also produced. We thus collaborated with Dr. Dónal O'Caroll of the Medical Research Council, Centre for Regenerative Medicine who used CRISPR/Cas9 genome editing technology to engineer a novel mouse model through recombination at the endogenous *Miwi2* locus to insert an in-frame influenza virus hemagglutinin (HA) epitope tag immediately downstream of the *Miwi2* start codon. The resulting HA-MIWI2 fusion protein is expressed at normal levels and does not disrupt normal MIWI2 function as evidenced by fertile homozygous *Miwi2*$^{HA/HA}$ male mice. Given our mRNA expression data, we hypothesized that Miwi2 protein would be present in lung epithelial cells. To test this, we performed immunohistochemical analysis of lung sections from uninfected *Miwi2*$^{+/+}$ and *Miwi2*$^{HA/+}$ mice. Results indicate that MIWI2 expression was exclusively localized to large and intrapulmonary airways **(Figure 5, top panel)**. Expression was not ubiquitous, with immunoreactivity limited to only several cells per airway, and only some airways contained positive cells. Staining was notably enhanced at airway-airway branch points (**Figure 5, bottom panel),** and absent from alveoli.

Given the increase in *Miwi2* RNA in total epithelial cells, we next determined if *Miwi2* protein expression was induced during infection. Immunohistochemistry was performed on lung sections from *Miwi2*$^{+/+}$ and

Miwi2$^{HA/+}$ mice were infected with 5x10^6 CFU of *S. pneumoniae* serotype 19 intratracheally for 24 hours. In infected mice, MIWI2 positive cells were again apparent in the intrapulmonary and large airways. The staining pattern within airways was consistent with uninfected mice, where an interrupted pattern was appreciated **(Figure 6A)**. Noticeably, more airways contained immunopositive cells 24 hours post infection. This was quantified by identifying the number of intrapulmonary airways that contained at least 1 positive cell, demonstrating a statistically significant increase in MIWI2 expression after infection with pneumococcus **(Figure 6B)**. These results compliment our previous expression data that both *Miwi2* RNA and protein are induced during inflammation.

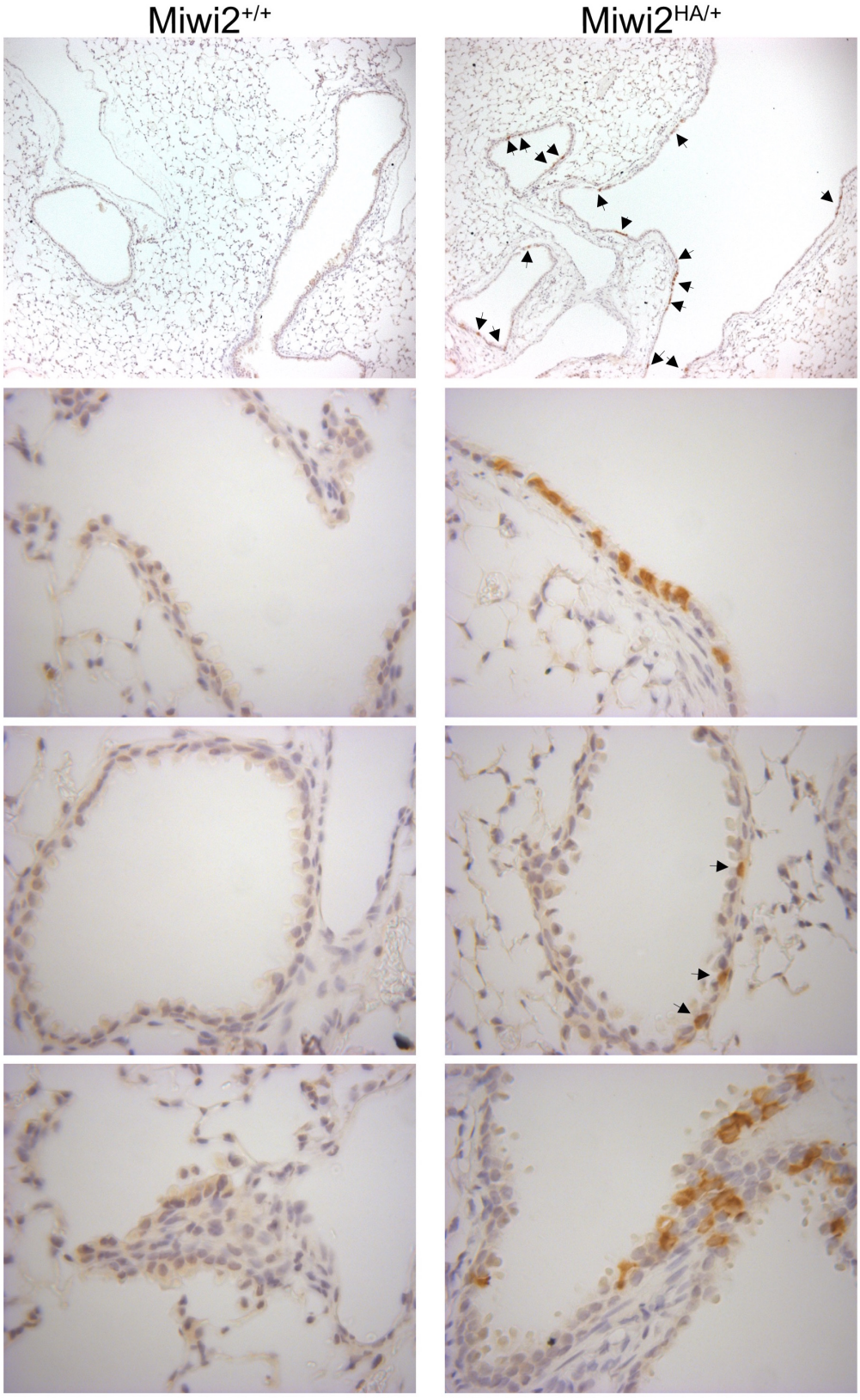
Miwi2+/+
Miwi2HA/+

Figure 5: MIWI2 protein is expressed in the lung

Immunohistochemical analysis of lung sections from uninfected *Miwi2*$^{+/+}$ or *Miwi2*$^{HA/+}$ mice stained with a monoclonal antibody against the HA epitope. Representative results are shown from staining performed on at least 5 sections from 3 mice of each genotype. Top panel, 5x objective Bottom panel 40x objective. Arrows emphasize some but not all positive cells.

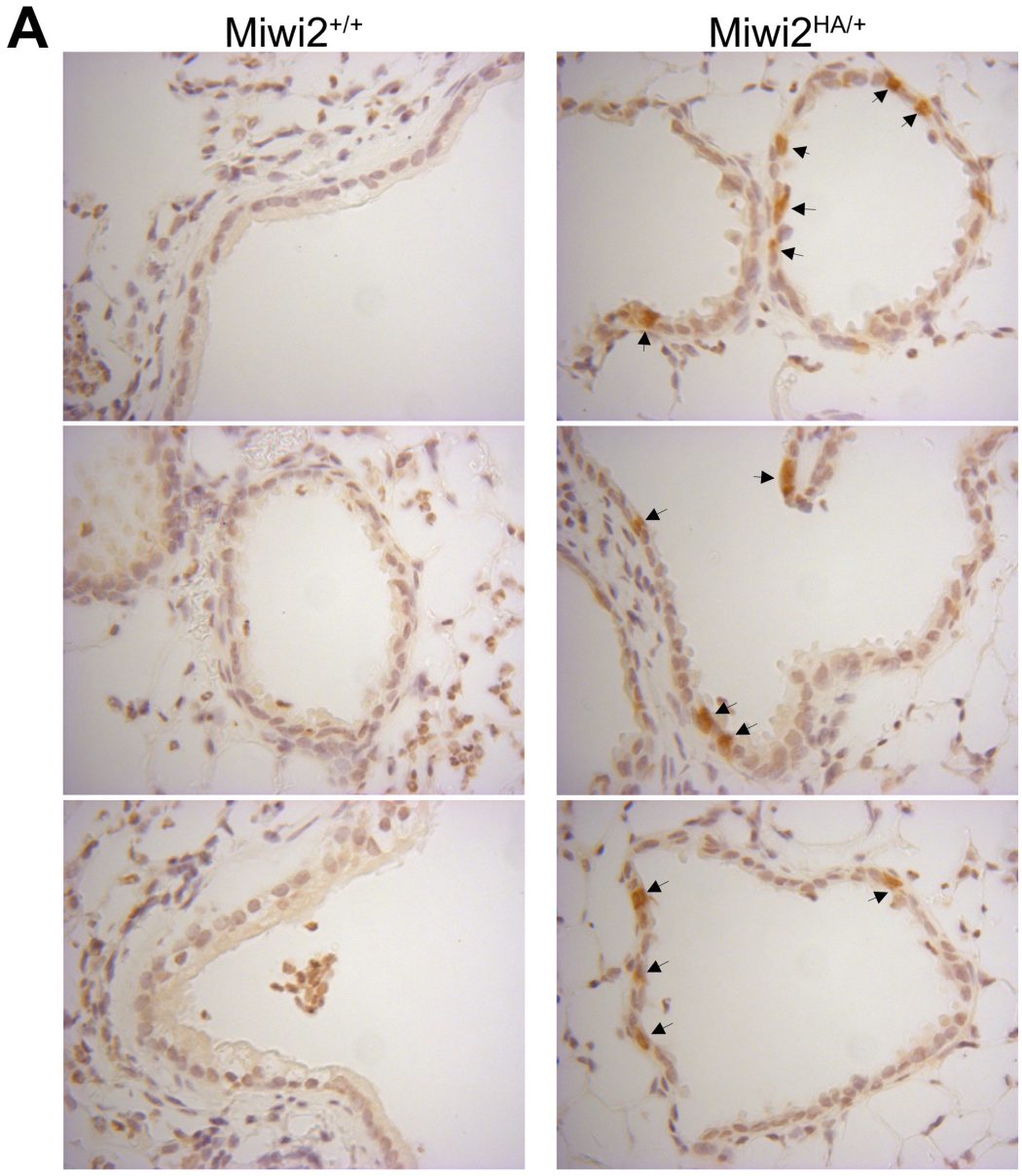
A
Miwi2+/+
Miwi2HA/+

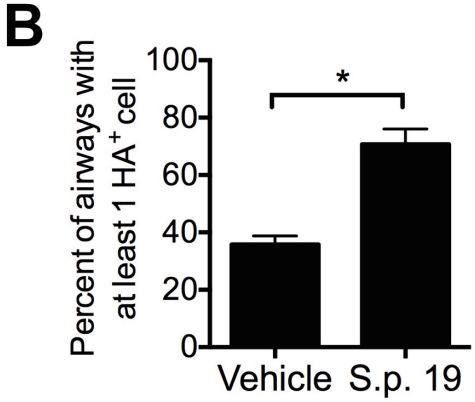
B
Percent of airways with at least 1 HA+ cell
100
80
60
40
20
0
*
Vehicle
S.p. 19

Figure 6: MIWI2 protein expression is induced during pneumococcal pneumonia

(A) Immunohistochemical analysis of lung sections from *Miwi2*$^{+/+}$ or *Miwi2*$^{HA/+}$ mice infected intratracheally with 5x10^{6} CFU of Sp19 for 24 hours. Sections were stained with a monoclonal antibody against the HA epitope. Representative results are shown from staining performed on at 2 least sections from 3 mice of each genotype. Arrows emphasize some but not all positive cells. Scale bars, 10 μm. **(B)** Morphometric quantitation of IHC was performed by counting the number of airways which express at least 1 MIWI2^{+} cell, normalized to the total number of airways counted (*n*= 3 mice per group, means ± s.e.m., *P<0.05 as determined by unpaired t-test).

3.5 Miwi2 is expressed exclusively in the airway lumen

The pseudostratified epithelium of the airway in mice and humans is comprised of several different cell types with specific functions (Rock and Hogan, 2011a; Rackley and Stripp, 2012). In both humans and in mice a specialized subset of cells resides in the basal lamina and are not in direct contact with the airway lumen. Numerous studies have identified that this population of basal cells are crucial in the maintenance of the luminal epithelium and participate in injury repair. Characteristically, basal cells express the cytokeratin protein KRT5, whereas luminal epithelial cells express the cytokeratin protein KRT8 (Rock and Hogan, 2011b; Hogan et al., 2014; Wansleeben et al., 2012). Our immunohistochemical analysis suggested that MIWI2 was expressed in cells in the lumen, hence in order to determine which epithelial cell type(s) express MIWI2, we stained lung sections from uninfected and Sp19 infected *Miwi2*$^{+/+}$ and *Miwi2*$^{HA/+}$ mice for various markers of lung differentiation. In both uninfected and infected mice, MIWI2 co-stained cells also expressing the cytokeratin KRT8 and not KRT5 thus indicating that Miwi2 is expressed in differentiated airway luminal cells and not basal cells **(Figure 7A,B)**.

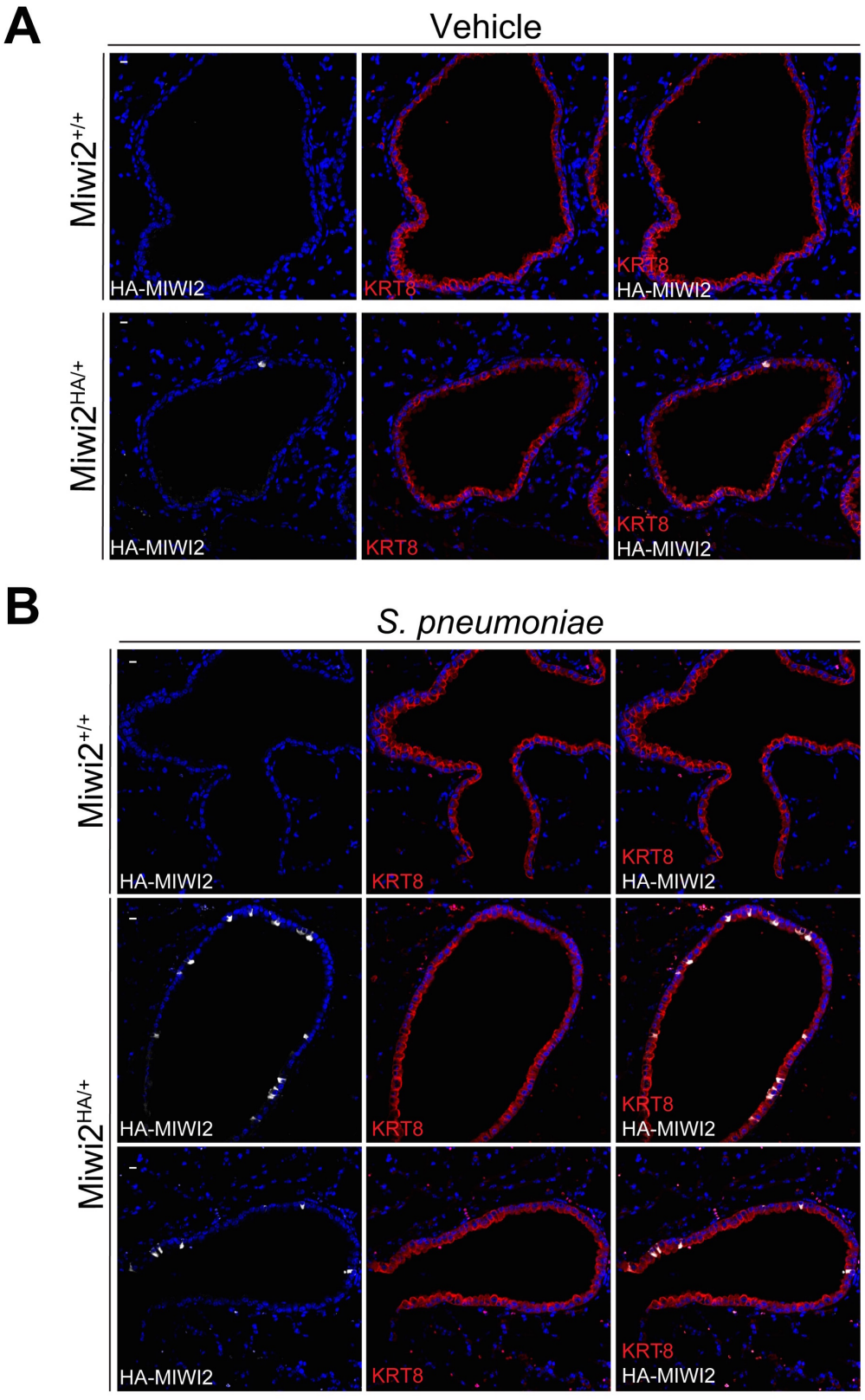
A
Vehicle
Miwi2+/+
Miwi2HA/+
HA-MIWI2
KRT8
KRT8
HA-MIWI2
B
S. pneumoniae
Miwi2+/+
Miwi2HA/+
HA-MIWI2
KRT8
KRT8
HA-MIWI2

Figure 7: MIWI2 is expressed in airway luminal cells in the adult lung

Immunostaining for *Krt8* (red) HA epitope (white) or Hoechst (blue) on paraffin lung sections from *Miwi2*$^{+/+}$ or *Miwi2*$^{HA/+}$ mice infected with **(A)** vehicle or **(B)** 5x10^{6} CFU of Sp19 for 24 hours. Representative results are shown from staining performed on at least 2 sections from 3 mice of each genotype. Scale bars, 10 μm.

3.6 Miwi2 is expressed exclusively in a subset of ciliated cells

The cell types that comprise the airway lumen include club cells ($CC10^+$), ciliated cells ($Foxj1^+$) and pulmonary neuroendocrine cells (PNECs, $CGRP^+$) that cluster together to form neuroendocrine bodies (Johnson and Georgieff, 1989). In order to determine if MIWI2 was expressed in a single lung epithelial lineage, we staining lung sections from uninfected *Miwi2*$^{+/+}$ and *Miwi2*$^{HA/+}$ mice with antibodies to known lineage markers. Immunostaining revealed that MIWI2 expression was restricted to cells also expressing the major ciliated cell transcription factor FOXJ1 **(Figure 8A)**. Moreover, MIWI2 was only expressed in a subset of $FOXJ1^+$ cells **(Figure 8B)** as determined from morphometric quantification. No $MIWI2^+$ cells were identified in any adult airways that were expressed outside of the ciliated lineage. Given these results, we next sought to determine if during infection, MIWI2 protein was induced in additional lung epithelial lineages. We stained lung sections from *Miwi2*$^{+/+}$ and *Miwi2*$^{HA/+}$ mice infected for 24 hours with Sp19. Results confirmed that MIWI2 expression is indeed still restricted to ciliated cells. In addition, under these conditions MIWI2 expression remained in only a subset of the total $FOXJ1^+$ cells **(Figure 9A)**.

It is well described that the specification of airway epithelial cells develops in a proximal to distal pattern, and there are several differences in the cell type and functioning between proximal and distal airway cells. To determine if MIWI2 expression is restricted to distal airways, we stained tracheal sections from

Miwi2$^{+/+}$ and *Miwi2*$^{HA/+}$ mice. We detected an identical staining pattern (**Figure 9B)** in tracheal sections when compared to distal airways.

To this point, we have based our conclusions that MIWI2 is expressed in ciliated cells using a the well defined marker, FOXJ1. However, Foxj1 is the master transcription factor that drives the ciliated cell fate, yet its expression precedes the formation of mature cilia. To test if Miwi2^{+} cells also express cilia, we stained lung and trachea sections from infected *Miwi2*$^{+/+}$ and *Miwi2*$^{HA/+}$ mice for acetylated alpha tubulin. Without exception, all MIWI2^{+} cells in both proximal and distal airways express cilia **(Figure 10)** indicating that MIWI2 does not mark an immature population of ciliated cells.

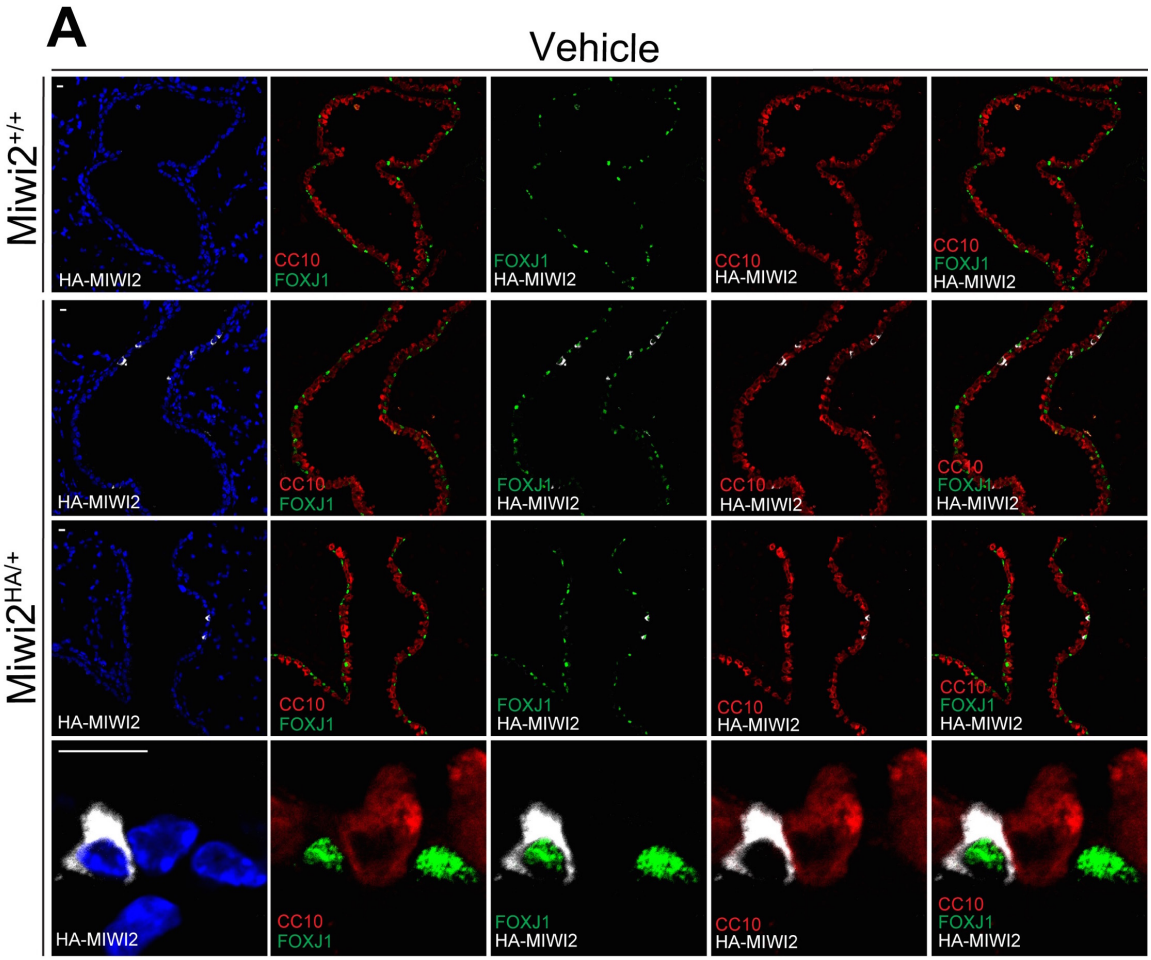
A
Vehicle
Miwi2+/+
Miwi2HA/+
HA-MIWI2
CC10
FOXJ1
CC10
FOXJ1
HA-MIWI2
FOXJ1
HA-MIWI2
CC10
HA-MIWI2
CC10
FOXJ1
HA-MIWI2

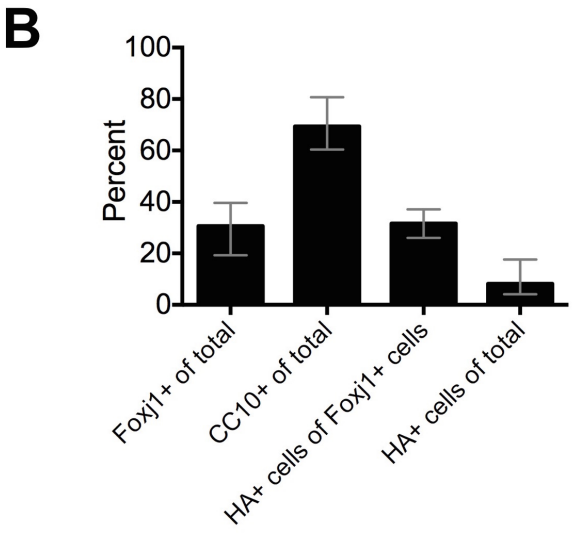
B
Percent
100
80
60
40
20
0
Foxj1+ of total
CC10+ of total
HA+ cells of Foxj1+ cells
HA+ cells of total

Figure 8: MIWI2 is expressed exclusively in a subset of ciliated epithelial cells in uninfected mice

(A) Immunostaining for CC10 (red) HA epitope (white) FOXJ1 (green) or Hoechst (blue) on paraffin lung sections from vehicle treated *Miwi2*$^{+/+}$ or *Miwi2*$^{HA/+}$ mice Representative results are shown from staining performed on at least 2 sections from 3 mice of each genotype. Scale bars, 10 μm. **(B)** Morphometric quantitation of IF was performed by counting the number of FOXJ1^{+}, CC10^{+} and HA^{+} cells normalized to the total number of nuclei in the airway (*n*= 3 mice, means ± s.e.m).

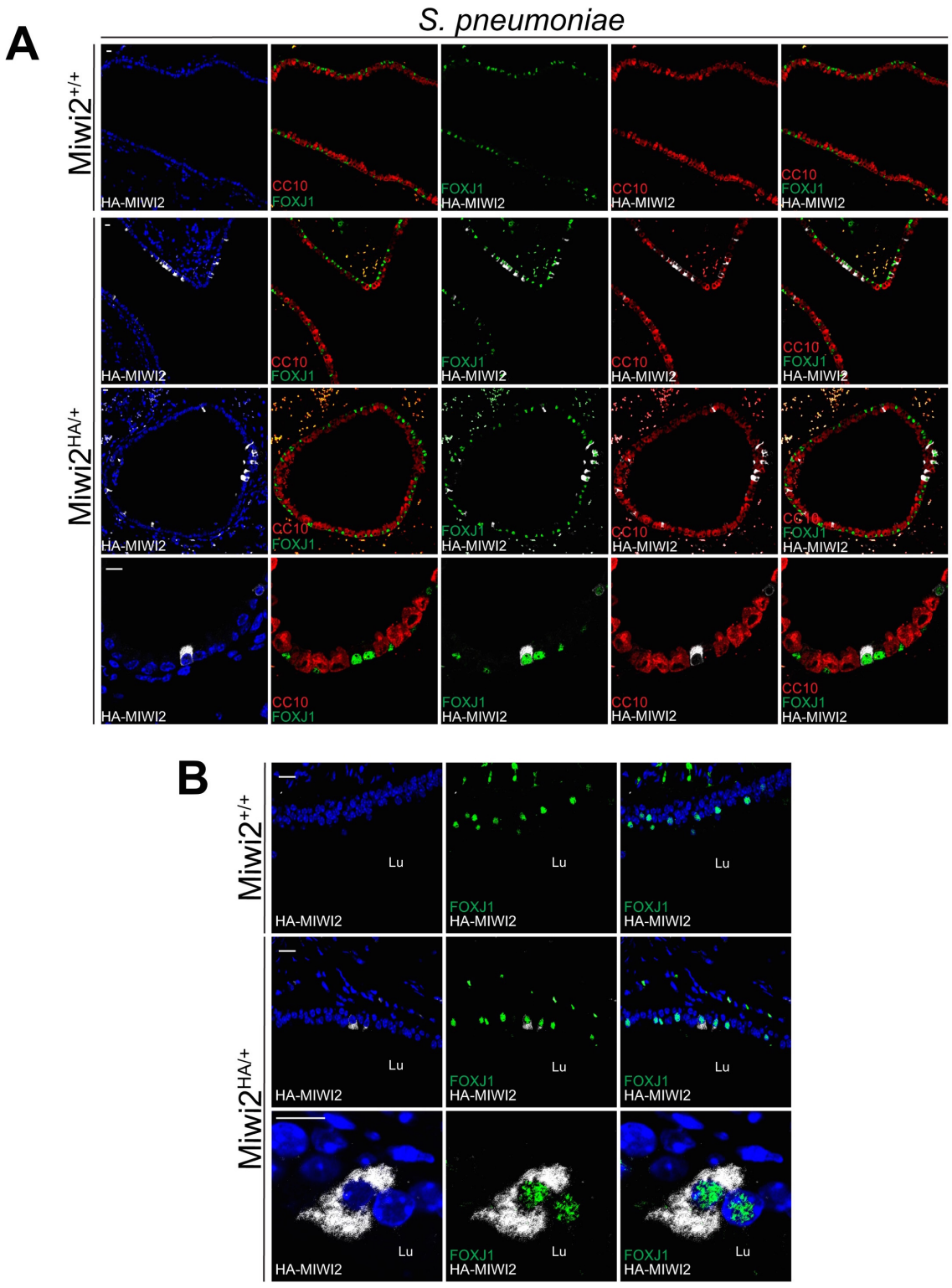
A
S. pneumoniae
Miwi2+/+
Miwi2HA/+
CC10
FOXJ1
HA-MIWI2
B
Lu

Figure 9: MIWI2 is expressed exclusively in a subset of ciliated epithelial cells in intrapulmonary and trachea of mice infected with pneumococcus

(A) Immunostaining for CC10 (red) HA epitope (white) FOXJ1 (green) or Hoechst (blue) on paraffin lung sections from *Miwi2*$^{+/+}$ or *Miwi2*$^{HA/+}$ mice infected intratracheally with 5x10^{6} CFU of Sp19 for 24 hours. Representative results are shown from staining performed on at least 2 sections from 3 mice of each genotype. Scale bars, 10 μm. **(B)** Immunostaining for HA epitope (white) FOXJ1 (green) or Hoechst (blue) on paraffin embedded tracheal sections from *Miwi2*$^{+/+}$ or *Miwi2*$^{HA/+}$ mice infected intratracheally with 5x10^{6} CFU of Sp19 for 24 hours. Representative results are shown from staining performed on at least 2 sections from 2 mice of each genotype. Lu, indicated airway lumen. Scale bars, 10 μm.

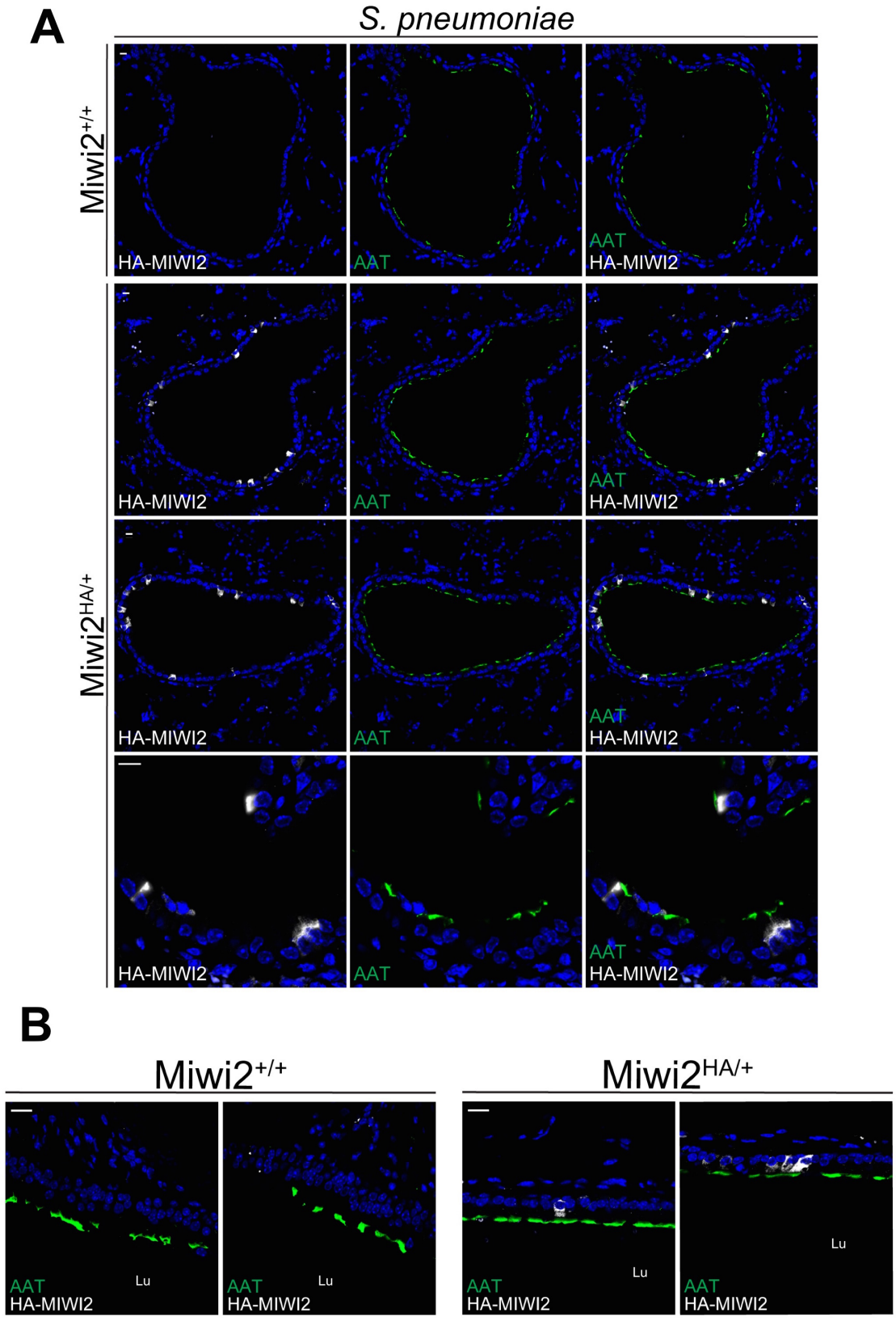
A
S. pneumoniae
Miwi2+/+
Miwi2HA/+
HA-MIWI2
AAT
AAT
HA-MIWI2
B
Miwi2+/+
Miwi2HA/+
AAT
HA-MIWI2
Lu

Figure 10: MIWI2^{+} ciliated cells express multicilia

Immunostaining for HA epitope (white) acetylated alpha-tubulin (green) or Hoechst (blue) on paraffin embedded **(A)** lung sections or **(B)** trachea from *Miwi2*$^{+/+}$ or *Miwi2*$^{HA/+}$ mice infected intratracheally with 5x10^{6} CFU of Sp19 for 24 hours. Representative results are shown from staining performed on at least 2 sections from 3 mice of each genotype. Lu, indicated airway lumen. Scale bars, 10 μm.

3.7 MIWI2 expression precedes the ciliated cell program

The specification of FOXJ1^{+} ciliated cells from NKX2-1^{+} progenitor cells occurs in a proximal to distal patterning beginning around E14.5 in mice, and continues postnatally (Rawlins and Hogan, 2008). We next sought to determine whether MIWI2 is expressed at earlier time points in epithelial development, perhaps providing insight into its origin or function. Additionally, was the cell type or number of MIWI2 expressing cells dynamic with respect to lung development? We collected *Miwi2*$^{+/+}$ and *Miwi2*$^{HA/+}$ embryonic lungs between E15.5 and E17.5 and stained for MIWI2 and FOXJ1 expression. At this time point, few to no club cells have developed, and patterning of the ciliated cells is not complete. In embryonic lungs, FOXJ1 expression was noted in trachea and large airways, however no expression was seen in distal lung saccules. MIWI2 was again expressed in a sporadic pattern, with MIWI2^{+} FOXJ1^{+} cells identified in large airways and trachea **(Figure 11A, top panel).** Interestingly, MIWI2^{+} FOXJ1^{-} cells were identified in distal lung **(Figure 11A, bottom panel)**, indicating that MIWI2 expression is not dependent on the ciliated cell transcription program. Staining of lungs collected from post natal day 7 mice mirror the expression pattern of adult lung, where all MIWI2^{+} cells are also Foxj1^{+}**(Figure 11B**).

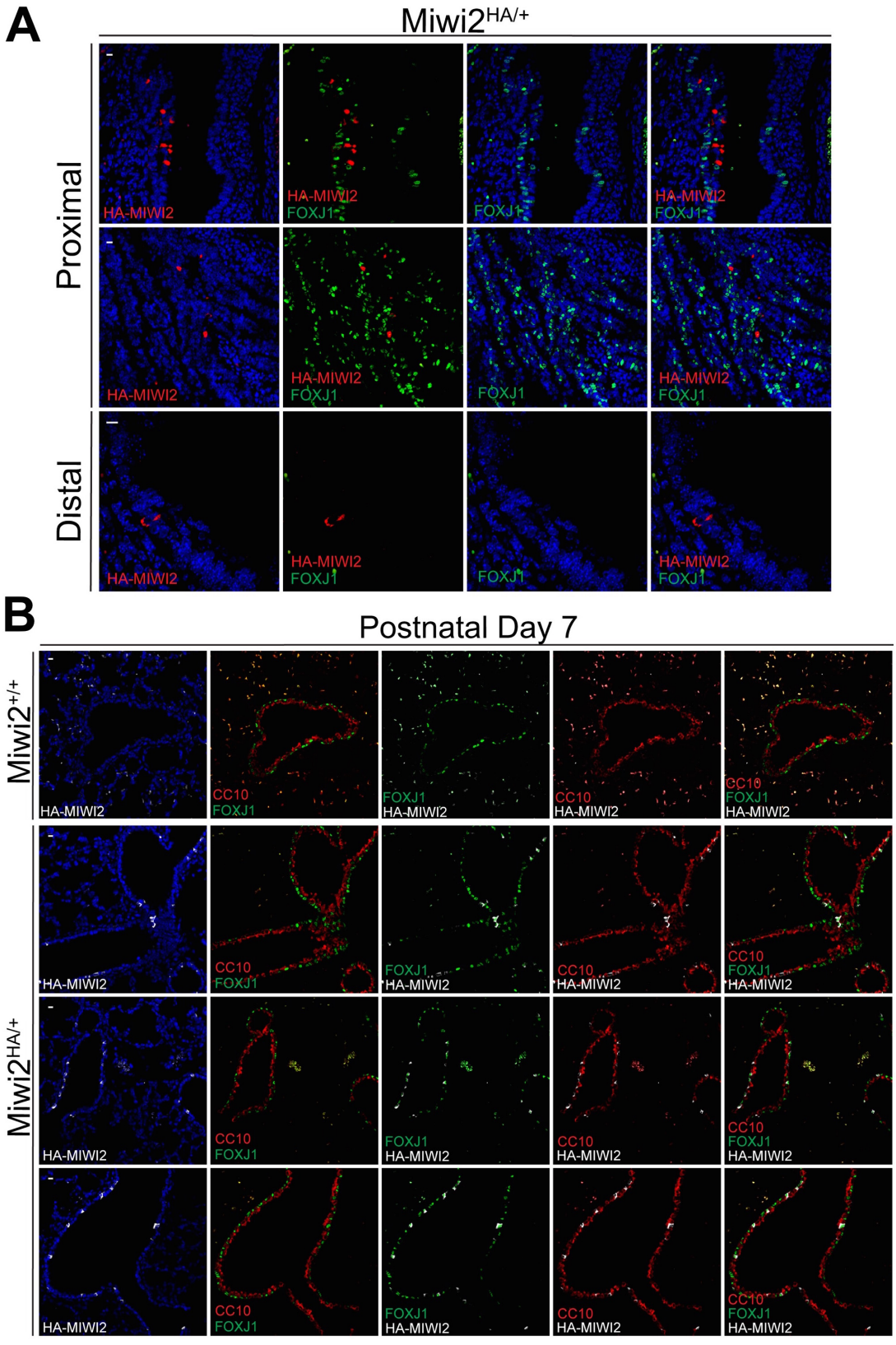
A
Miwi2HA/+
Proximal
Distal
HA-MIWI2
FOXJ1
B
Postnatal Day 7
Miwi2+/+
Miwi2HA/+
CC10
FOXJ1
HA-MIWI2

Figure 11: MIWI2 expression precedes the expression of FOXJ1

(A) Immunostaining for CC10 (red) HA epitope (white) FOXJ1 (green) or Hoechst (blue) on paraffin embryonic lung sections from *Miwi2*$^{HA/+}$ mice. Representative results are shown from staining performed on at least 3 sections from 2 mice of each genotype. Scale bars, 10 μm. **(B)** Immunostaining for CC10 (red) HA epitope (white) FOXJ1 (green) or Hoechst (blue) on paraffin lung sections from post natal day 7 *Miwi2*$^{+/+}$ or *Miwi2*$^{HA/+}$ mice. Representative results are shown from staining performed on at least 3 sections from 2 mice of each genotype. Scale bars, 10 μm.

3.8 Lung MIWI2 function is independent of the piRNA silencing pathway

The function of the piRNA silencing system is well described in germ cells, however expression of piRNAs, or piRNA binding proteins in somatic cells in mammals is controversial. Several deep sequencing studies have identified small RNAs homologous to murine piRNAs found in testis, however these studies had several limitations (Ross et al., 2014; Yan et al., 2011). In addition, the defining characteristic of a piRNA is the association of the RNA with any of the three piRNA binding proteins, MILI, MIWI, or MIWI2, and no study to date has identified a somatic piRNA meeting this standard. In the germline, MIWI2 acts as the effector of the piRNA silencing pathway by recruiting methylation machinery to piRNA promoters. Specificity for this activity is derived through complementary base pairing between the retroelement derived piRNA bound to MIWI2 loaded in the cytoplasm and the retroelement nascent mRNA transcript in the nucleus. The current model in germ cells proposes that MIWI2, when unbound by piRNAs is located in distinct peri-nuclear granules termed piP bodies (Aravin et al., 2008). When associated with a piRNA, a nuclear localization signal is exposed and MIWI2 relocalizes to the nucleus (Aravin et al., 2008). Our immunofluorescence data strongly demonstrates MIWI2 expression in a somatic cell. The cellular localization, however, is in staunch contrast to that in the male germline. Hence, we sought to determine if somatic cell MIWI2 is bound to a small RNA species in lung epithelium. We infected *Miwi2*$^{+/+}$ and *Miwi2*$^{HA/+}$ mice with Sp19 for 24 hours and prepared total lung lysates. Immunoprecipitation of the HA epitope followed

by immunoblotting revealed a protein of the predicted size of Miwi2 (~98 kDa) **(Figure 12A).** To identify MIWI2 bound RNAs, immunoprecipitates were treated with proteinase K followed by dephosphorylation and labeling with $[\gamma]^{32}$P-ATP, before resolution on a 15% TBE Urea gel and exposure to film. The data demonstrate that somatic MIWI2 is not bound to a 25-31nt RNA as would be expected in testis but rather a 50nt RNA species **(Figure 12B)**. Numerous attempts were made to clone MIWI2 associated RNAs, however library preparation was unsuccessful. This could be for several reasons, however the most likely explanation is that MIWI2 associated RNA is modified, preventing RNA adapter ligation. The origin of this RNA aside, collectively these data indicate that full length MIWI2 protein is expressed in somatic cells, and is bound to a non-classical piRNA species.

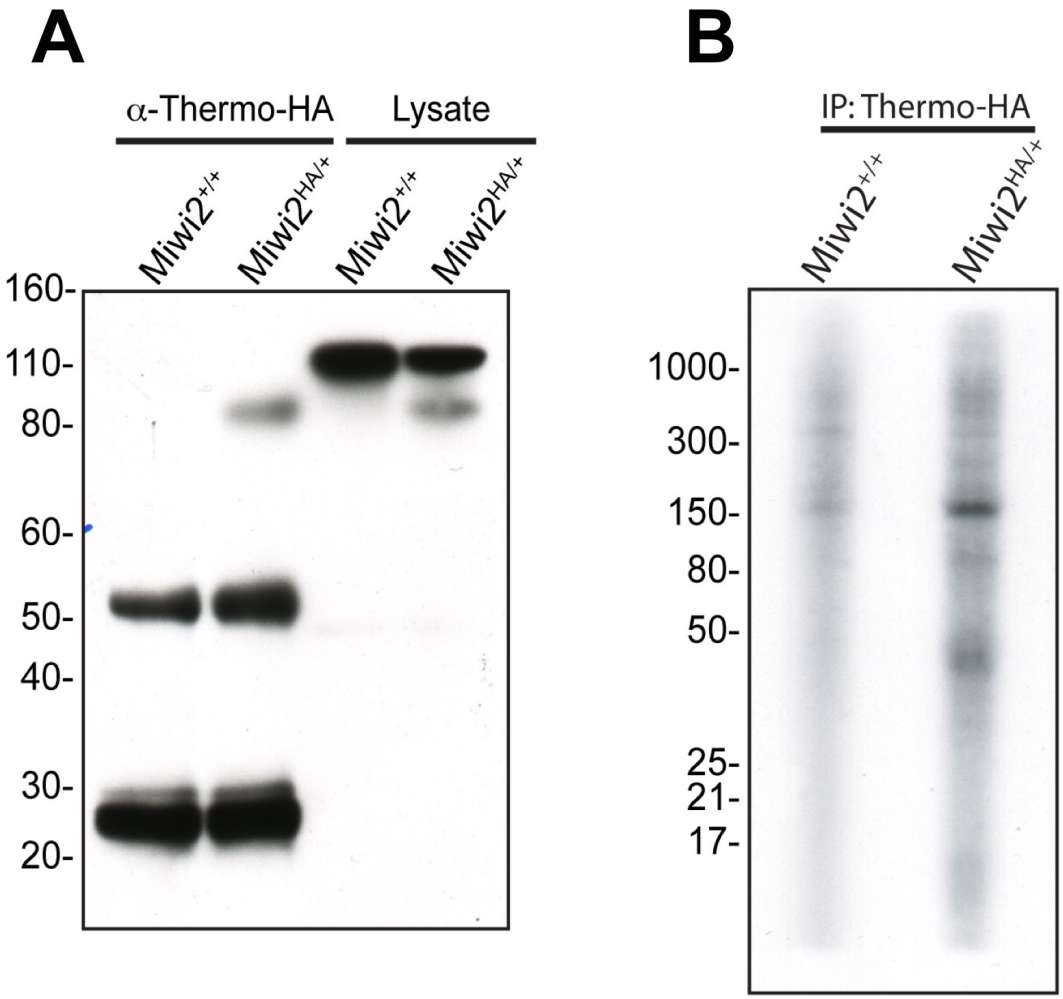
A
α-Thermo-HA
Lysate
Miwi2+/+
Miwi2HA/+
Miwi2+/+
Miwi2HA/+
160-
110-
80-
60-
50-
40-
30-
20-
B
IP: Thermo-HA
Miwi2+/+
Miwi2HA/+
1000-
300-
150-
80-
50-
25-
21-
17-

Figure 12: Lung MIWI2 is full length and bound to an RNA

Lung lysates were prepared from *Miwi2*$^{+/+}$ or *Miwi2*$^{HA/+}$ mice infected with 5x10^{6} CFU of *Streptococcus pneumoniae* intratracheally for 24 hours. **(A)** Immunoblot analysis of HA immunoprecipitation or total lung lysates. IP: Thermo HA antibody, IB: Cell Signaling HA antibody. Results are representative of experiments performed on *n*= 6 mice per group. Protein expected sizes, MIWI2: ~98 kDa, IgG heavy chain: ~55 kDa, IgG light chain: ~25 kDa, a nonspecific band is recognized by IB at ~110 kDa **(B)** Autoradiograph of RNA **i**solated from IP in (A) after proteinase K digestion and radioactive labeling with ^{32}P-ATP and resolution on a 15% TBE-Urea gel. Results are representative of experiments performed on *n*= 3 mice per group.

Expression of retroelement RNA in somatic cells under various conditions has been extensively described in recent reports (Chambers, 2014). To determine if lung MIWI2 regulates retroelement RNA during inflammation, we utilized both an *in vitro* and *in vivo* approach to deplete cells of MIWI2 and assess retreoelement expression. We have demonstrated that *Miwi2* mRNA is induced in E10 cells, a murine epithelial cell line in response to inflammatory stimuli. We transduced E10 cells with lentivirus expressing either non-targeting or Miwi2 specific shRNA and verified *Miwi2* mRNA expression by qRT-PCR, and MIWI2 protein expression by immunofluorescence using an antibody kindly provided by Dr. Ramesh Pillai at the European Molecular Biology Laboratory in Grenoble, France. Results indicate a statistically significant decrease in *Miwi2* mRNA expression in cells expressing a *Miwi2* specific shRNA versus a control shRNA, when treated with recombinant TNFα **(Figure 13A)**. Immunofluorescence imaging confirms expression of MIWI2 in E10 cells, however we achieved an incomplete reduction in MIWI2 protein expression **(Figure 13B, C)**. Total RNA was prepared from stable shRNA E10 cells treated with vehicle or recombinant TNFα for 6 hours and gene expression was measured by Affymetrix Gene 2.0 ST microarray. Sensitivity of the array to determine true differential gene expression was determined by examining mRNA expression of sex linked genes. E10 cells are derived from female mice (Kathuria, 2004), and this is demonstrated by higher $\log_2$ expression values of the female specific gene *Xist*, and the lack of expression of the male specific

gene *Eif2s3y* (Kay et al., 1994; Kobayashi et al., 2006). *Miwi2 (Piwil4)* expression was at the level of detection for the array, and the effect of shRNA was non-significant **(Figure 13D)**. Profiling of retroelements was carried out using a method described by Young and colleagues (Young et al., 2014). Individual probes on the Gene 2.0 ST array mapping to retroelements were identified by RepeatMasker and RepBase using a published R script (Young et al., 2014). While many probes may potentially map to highly repetitive regions, the vast majority of retroelement-mapping probes match uniquely to the genome and hence are fairly sensitive measure of retroelement expression, in contrast to PCR based methods which have dominated the literature. 1025 probesets each recognizing a separate retroelement, containing between 1 and 11 individual probes in each set were identified. No statistically significant differences in expression of any of the retroelements were discovered. Specifically, the major target of MIWI2 repression in the germline, LINE1 retroelements, were expressed in these cells (**Figure 13E, left panel)**, however no genotypic differences were noted **(Figure 13E, right panel)**. Other classes of retroelements were analyzed and there was no genotypic effect on RE expression. From these results, we conclude that depletion of MIWI2 has no effect on retroelement expression *in vitro*.

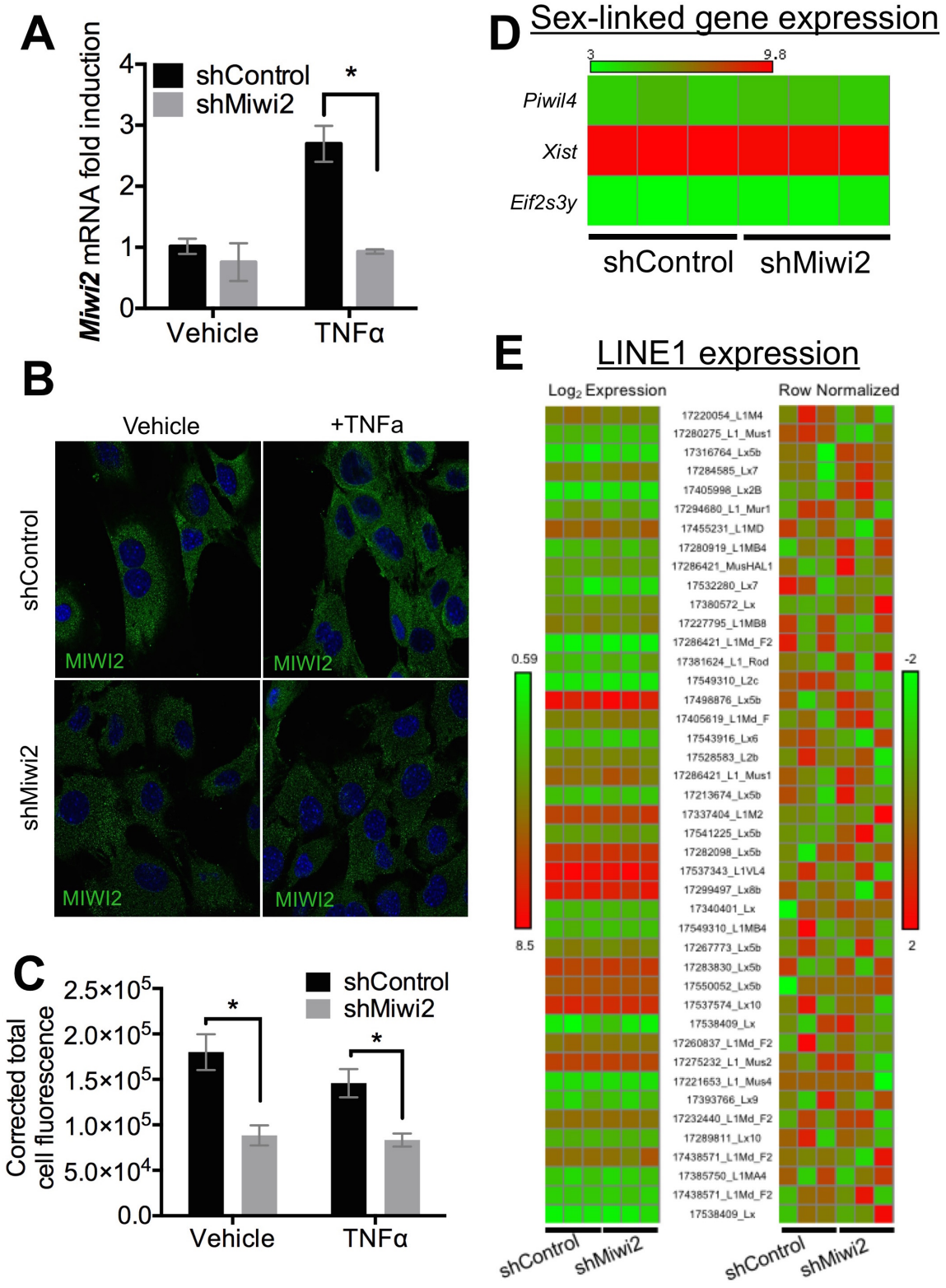
A
Miwi2 mRNA fold induction
shControl
shMiwi2
*
Vehicle
TNFα
B
Vehicle
+TNFa
shControl
shMiwi2
MIWI2
C
Corrected total cell fluorescence
shControl
shMiwi2
Vehicle
TNFα
D
Sex-linked gene expression
Piwil4
Xist
Eif2s3y
shControl
shMiwi2
E
LINE1 expression
Log2 Expression
Row Normalized
shControl
shMiwi2

Figure 13: Lung MIWI2 does not regulate retrotransposon expression, in vitro

(A) qRT-PCR analysis of RNA prepared from Murine alveolar epithelial E10 cells stably expressing non-targeting or *Miwi2* targeting shRNA stimulated with 10 ng/mL recombinant TNFα for 6 hours. Results indicate fold change relative to vehicle treated, non-targeting shRNA. (*n*= 3 independent experiments, data displayed as means ± s.e.m, *P<0.05 as determined by unpaired t-test) **(B)** Immunostaining for MIWI2 (green) or Hoechst (blue) of E10 cells stably expressing non-targeting or *Miwi2* targeting shRNA stimulated with 10 ng/mL recombinant TNFα for 6 hours **(C)** Quantification of (B) using the method described in (Gavet and Pines, 2010; Burgess et al., 2010). (*n*= 3 independent experiments, data displayed as means ± s.e.m, *P<0.05 as determined by two-way ANOVA, followed by Sidak's multiple comparisions test) (**D)** Log_2 expression values as determined by microarray for control mRNAs and Miwi2 (Piwil4) mRNA in RNA prepared from E10 cells stably expressing non-targeting or *Miwi2* targeting shRNA stimulated with 10 ng/mL recombinant TNFα for 6 hours. Columns represent data collected from *n=3* biological replicates per group **(E)** LINE1 element expression is displayed as raw log_2 expression (left) as determined by the microarray, or as relative expression within a row by establishing a row mean of 0 and a variance of 1 (right) from RNA prepared in (D). Columns represent data collected from *n=3* biological replicates per group.

Murine E10 cells were generated from lung culture explants, are likely derived from type II pneumocytes, and express markers of type I pneumocytes. However, our data clearly demonstrate that MIWI2 is expressed in a subset of ciliated cells *in vivo*, and hence we wanted to determine if MIWI2 regulated retroelement expression in murine lungs. We acquired *Miwi2*$^{-/-}$ mice from Dr. Gregory Hannon of the Cold Spring Harbor Laboratory and rederived these mice in our specific pathogen free facility at Boston University. After rederivaton, these mice demonstrated the previously reported hypomorphic testis phenotype **(Figure 14A)**. To evaluate retroelement expression, we infected *Miwi2*$^{+/+}$ and *Miwi2*$^{-/-}$ mice with 5x10^{6} CFU of *S. pneumoniae* for 24 hours and prepared total left lobe RNA. qRT-PCR revealed that genetic disruption of *Miwi2* severely reduced *Miwi* mRNA expression in lungs **(Figure 14B)**. Genome wide RNA profiling was carried out as above, using the method described by Young and colleagues on an Affymetrix Gene 2.0 ST array. Sensitivity of the array to decipher true differential expression was assessed by analyzing sex linked genes, as also described above. As expected the array accurately demonstrated the expression of *Xist* in female mice, and *Eif2s3y* in male mice. The expression of *Miwi2(Piwil4)* was again near the detection limit of the array but was decreased 1.6 fold in *Miwi2*$^{-/-}$ versus *Miwi2*$^{+/+}$ mice **(Figure 14C)**. Several LINE1 elements were highly expressed in lungs of infected *Miwi2*$^{-/-}$ and *Miwi2*$^{+/+}$ mice **(Figure 14D, left panel)**, however no LINE1 or other retroelements were significantly differentially expressed **(Figure 14D, right panel)**. From this, we

conclude that MIWI2 deficiency does not regulate retroelement expression *in vivo.* Given the findings that MIWI2 is expressed exclusively in the cytoplasm, is bound to an RNA species much longer than a traditional piRNA, and does not regulate the expression of retroelements *in vitro,* or *in vivo,* we conclude that lung somatic cell MIWI2 is independent of the piRNA silencing system.

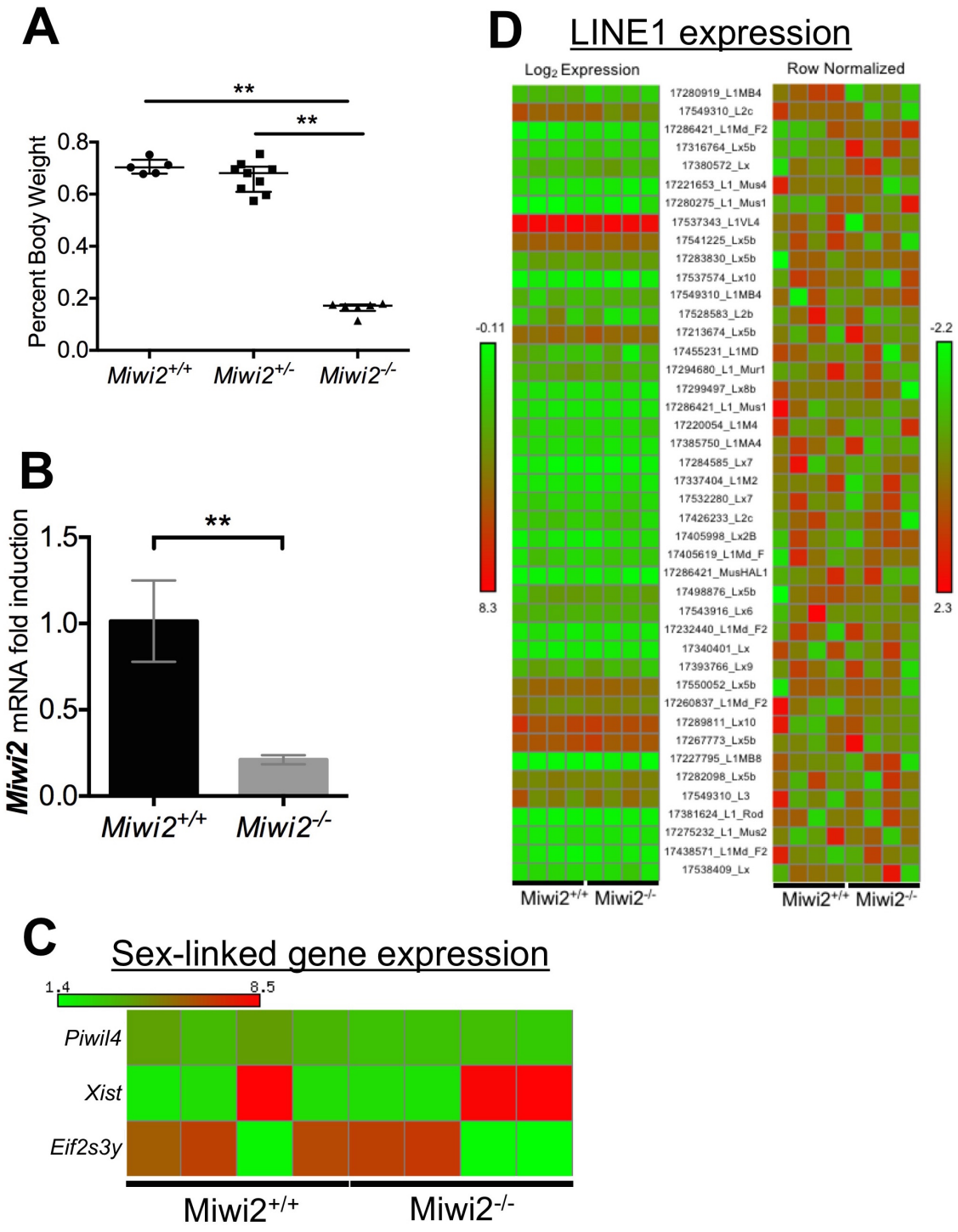
A
**
**
Percent Body Weight
0.8
0.6
0.4
0.2
0.0
Miwi2+/+
Miwi2+/-
Miwi2-/-
B
**
Miwi2 mRNA fold induction
1.5
1.0
0.5
0.0
Miwi2+/+
Miwi2-/-
D
LINE1 expression
Log2 Expression
Row Normalized
-0.11
8.3
-2.2
2.3
17280919_L1MB4
17549310_L2c
17286421_L1Md_F2
17316764_Lx5b
17380572_Lx
17221653_L1_Mus4
17280275_L1_Mus1
17537343_L1VL4
17541225_Lx5b
17283830_Lx5b
17537574_Lx10
17549310_L1MB4
17528583_L2b
17213674_Lx5b
17455231_L1MD
17294680_L1_Mur1
17299497_Lx8b
17286421_L1_Mus1
17220054_L1M4
17385750_L1MA4
17284585_Lx7
17337404_L1M2
17532280_Lx7
17426233_L2c
17405998_Lx2B
17405619_L1Md_F
17286421_MusHAL1
17498876_Lx5b
17543916_Lx6
17232440_L1Md_F2
17340401_Lx
17393766_Lx9
17550052_Lx5b
17260837_L1Md_F2
17289811_Lx10
17267773_Lx5b
17227795_L1MB8
17282098_Lx5b
17549310_L3
17381624_L1_Rod
17275232_L1_Mus2
17438571_L1Md_F2
17538409_Lx
Miwi2+/+
Miwi2-/-
Miwi2+/+
Miwi2-/-
C
Sex-linked gene expression
1.4
8.5
Piwil4
Xist
Eif2s3y
Miwi2+/+
Miwi2-/-

Figure 14: Lung MIWI2 does not regulate retroelement expression in vivo

(A) Testis weights from wildtype, functional heterozygotes, or homozygous deficient mice. (*n=5,8,6* mice per group, data are displayed as medians ± interquartile range, **P<0.01 as determined by one-way ANOVA followed by Tukey's multiple compassion test) **(B)** qRT-PCR analysis of whole lung RNA collected from *Miwi2*$^{+/+}$ and *Miwi2*$^{-/-}$ mice infected intratracheally with 5x10^{6} CFU of Sp19 for 24 hours. Results indicate fold change relative to wildtype mice. (*n*= 4,4 mice per group, means ± s.e.m., **P<0.01 as determined by unpaired t-test). **(C)** Raw $\log_2$ expression of control mRNA and *Miwi2*(*Piwil4*) mRNA from microarray analysis of samples generated in (B) Columns represent data collected from *n=3* mice per group, where each column is a single mouse (**D)** LINE1 element expression is displayed as raw $\log_2$ expression (left) as determined by the microarray, or as relative expression within a row by establishing a row mean of 0 and a variance of 1 (right) from RNA prepared in (B). Columns represent data collected from *n=3* mice per group, where each column is a single mouse.

3.9 Miwi2 deficiency impacts airway cell composition

Our data clearly demonstrate that MIWI2 is expressed in a subtype of ciliated cells in adult airways and is induced during bacterial pneumonia. The link between ciliated cell function and bacterial resistance has been well established (Tilley et al., 2015), as ciliated cells are critical to the function of the mucociliary escalator. In order to determine if MIWI2 regulated ciliogenesis we obtained a novel mouse model from our collaborator, Dr. Dónal O'Caroll, in which he used CRISPR/Cas9 genome editing to introduce a loss-of-function tdTomato allele into the native locus for *Miwi2.* Hence, *Miwi2*$^{+/tdTomato}$ mice are functional heterozygotes, and *Miwi2*$^{tdTomato/tdTomato}$ mice are functionally MIWI2 deficient. In each genotype however, tdTomato expression should be a reporter of *Miwi2* mRNA expression, thus allowing us to simultaneously monitor MIWI2 expression and functionality in the specific subset of ciliated cells. Expression of the reporter was confirmed using immunohistochemistry on paraffin section prepared from uninfected *Miwi2*$^{+/tdTomato}$ and *Miwi2*$^{tdTomato/tdTomato}$ mice. Results confirm a similar expression pattern to that of *Miwi2*$^{HA/+}$ mice, with immunoreactive Tomato^{+} cells localized to large and intrapulmonary airways in both genotypes **(Figure 15A, B)**. To confirm that tdTomato^{+} cells are indeed staining ciliated cells in this model, we co-stained sections with several markers of lung cell type. In agreement with data from wildtype mice, tdTomato expression is restricted to a subset of FOXJ1 expressing cells in both *Miwi2*$^{+/tdTomato}$ and *Miwi2*$^{tdTomato/tdTomato}$ mice. These data

validate that the Tomato knock-in allele is a faithful reporter for MIWI2 activity **(Figure 16)**.

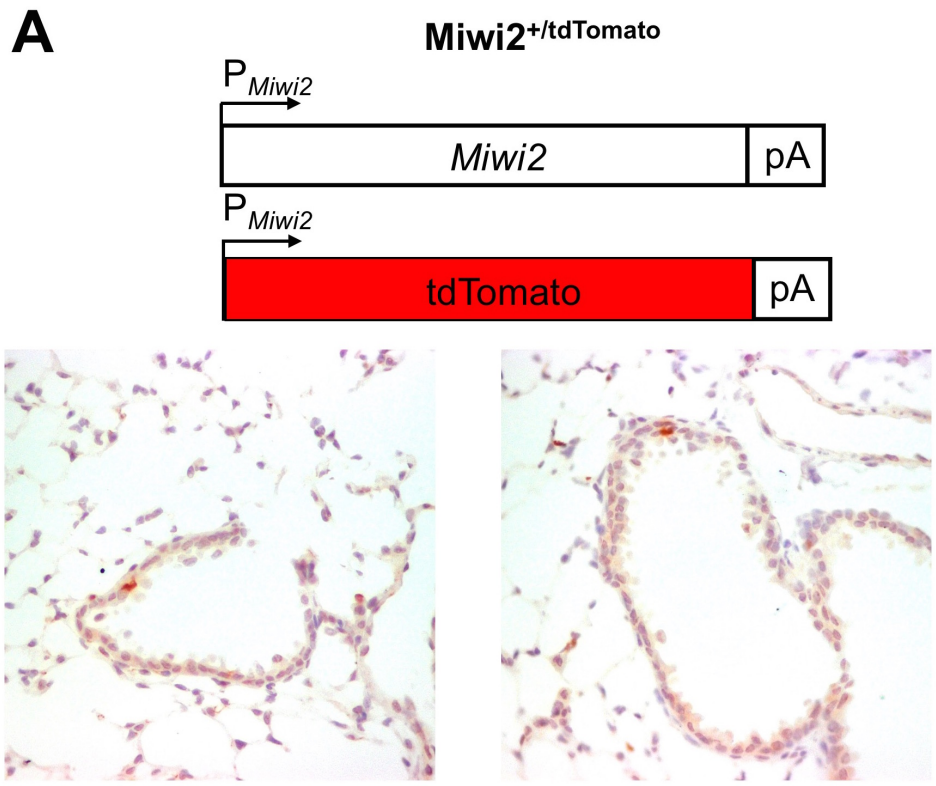
A
Miwi2+/tdTomato
P Miwi2
Miwi2
pA
P Miwi2
tdTomato
pA

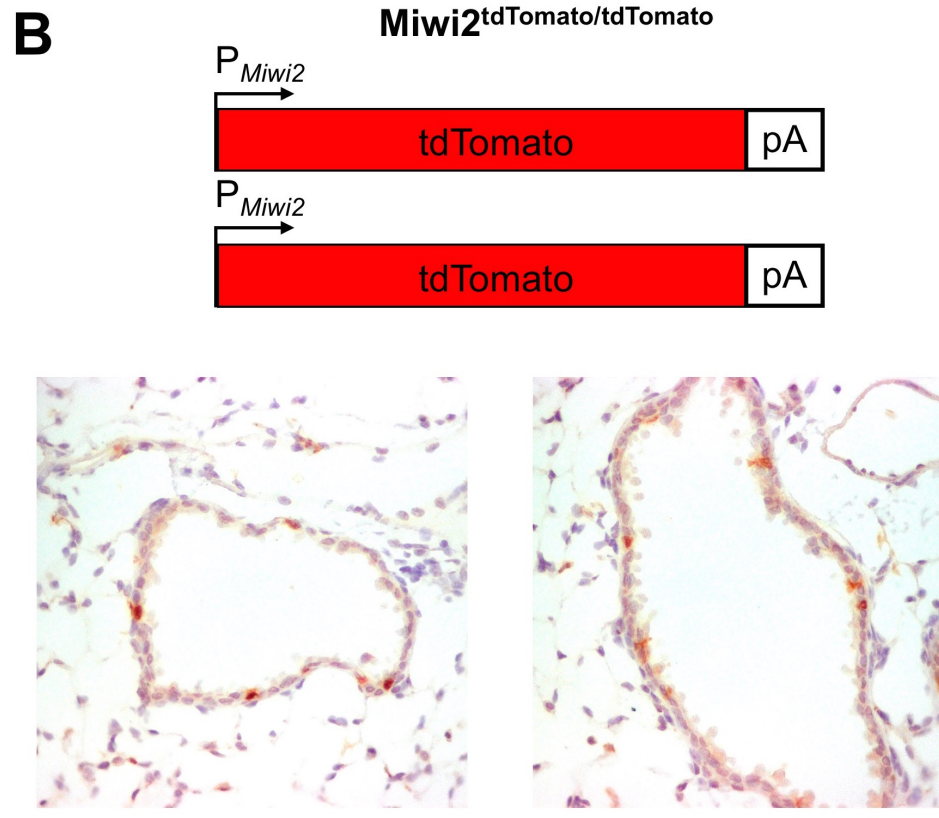
B
Miwi2tdTomato/tdTomato
P Miwi2
tdTomato
pA
P Miwi2
tdTomato
pA

Figure 15: MIWI2::tdTomato is expressed in airway epithelium

A loss of function tdTomato allele was engineered into the native locus for *Miwi2.* Schematic and immunohistochemical analysis of paraffin lung sections from **(A)** *Miwi2*$^{+/tdTomato}$ and **(B)** *Miwi2*$^{tdTomato/tdTomato}$ stained with an antibody against tdTomato. Representative results are shown from staining performed on at least 2 sections from 1 mouse of each genotype.

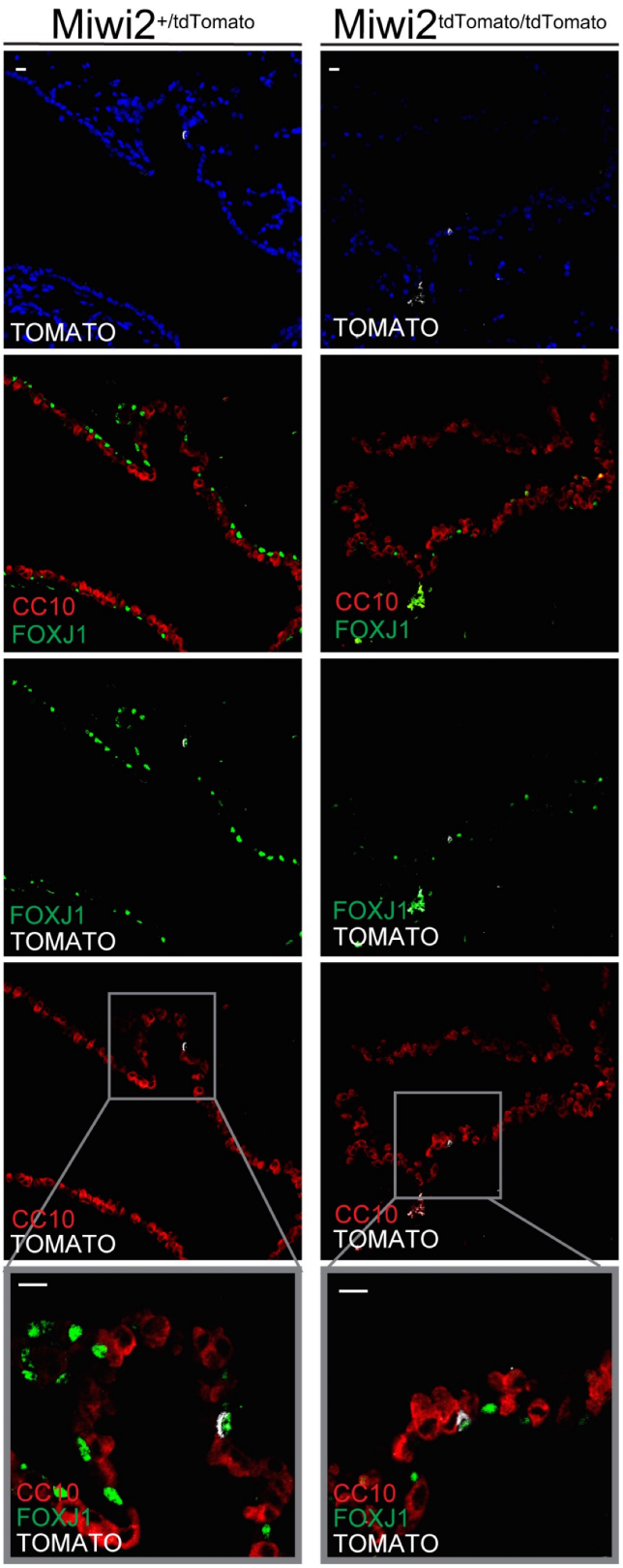
Miwi2+/tdTomato
Miwi2tdTomato/tdTomato
TOMATO
TOMATO
CC10
FOXJ1
CC10
FOXJ1
FOXJ1
TOMATO
FOXJ1
TOMATO
CC10
TOMATO
CC10
TOMATO
CC10
FOXJ1
TOMATO
CC10
FOXJ1
TOMATO

Figure 16: Miwi2 mRNA is induced by multiple inflammatory stimuli

Immunostaining for CC10 (red) tdTomato (white) FOXJ1 (green) or Hoechst (blue) on paraffin lung sections from uninfected *Miwi2*$^{+/tdTomato}$ or *Miwi2*$^{tdTomato/tdTomato}$ mice. Grey box indicates area enlarged in bottom panel. Representative results are shown from staining performed on at least 2 sections from 3 mice of each genotype. Scale bars, 10 μm.

In order to begin probing ciliated cell function we first designed a cell sorting strategy to isolate ciliated cells from distal airways by adapting a previously reported method (Pardo-Saganta et al., 2015). We performed lung digests on C57BL/6 mice on isolated potential ciliated cells by FACS based on relative expression of CD45, EpCAM, and the cell adhesion molecule CD24, which is expressed on a variety of different cell types (King et al., 2012; Overdevest et al., 2012; Naumov et al., 2014; Zhang et al., 2012; Thaxton et al., 2014; Ayre et al., 2015). After gating on live $CD45^{-}$ $EpCAM^{+}$ cells (total epithelial cells), 3 expression patterns of CD24 were identified. We sorted low, mid, and high expressing populations and performed cytospins followed by staining for mature cilia using immunofluorescence **(Figure 17A)**. Cells from the 'High' population were significantly enriched for cells expressing mature cilia whereas few to no ciliated cells were identified in the 'low' and 'mid' groups confirming the utility of $CD24^{Hi}$ as a reliable marker of the ciliated cell population **(Figure 17B,C)**.

The expression of FOXJ1, the master transcription factor for ciliated cells does not indicate the production of mature cilia, as several important factors are necessary for ciliagenesis (You et al., 2004). To determine if the $MIWI2^{+}$ ciliated cell subset produce mature cilia in the absence of MIWI2, we performed lung digests on uninfected *Miwi2*$^{+/tdTomato}$ and *Miwi2*$^{tdTomato/tdTomato}$ mice and sorted the ciliated cell population as described above. We stained cytospins prepared from these mice and analyzed for expression of tdTomato and acetylated alpha

tubulin, the major protein constituent of cilia. Indeed, we were able to identify numerous tdTomato expressing cells in both genotypes, all of which expressed mature cilia **(Figure 18)**. From this, we conclude that MIWI2 is not required for the production of mature cilia.

Finally, given that no difference was seen in the production of $MIWI2^{+}$ cell autonomous cilia, we sought to determine if MIWI2 deficient mice have defects in total ciliated cells. To test this, we produced lung sections for *Miwi2*$^{+/+}$ *or Miwi2*$^{-/-}$ mice and stained for markers of lung cell populations. These sections were then quantitated to determine if cellular composition of the airways were consistent. Surprisingly, we found that MIWI2 deficient mice had a statistically significant, 25% decrease in ciliated cells in the intrapulmonary airways as compared to MIWI2 competent mice (**Figure 19A)**. This decrease in ciliated cells was accompanied by an increase in CC10 expressing club cells **(Figure 19B)** This is despite no change in the total number of airway cells counted **(Figure 19C).** These data lead us to conclude that MIWI2 plays a role in regulating the normal development of cell fate and identity in the murine airways.

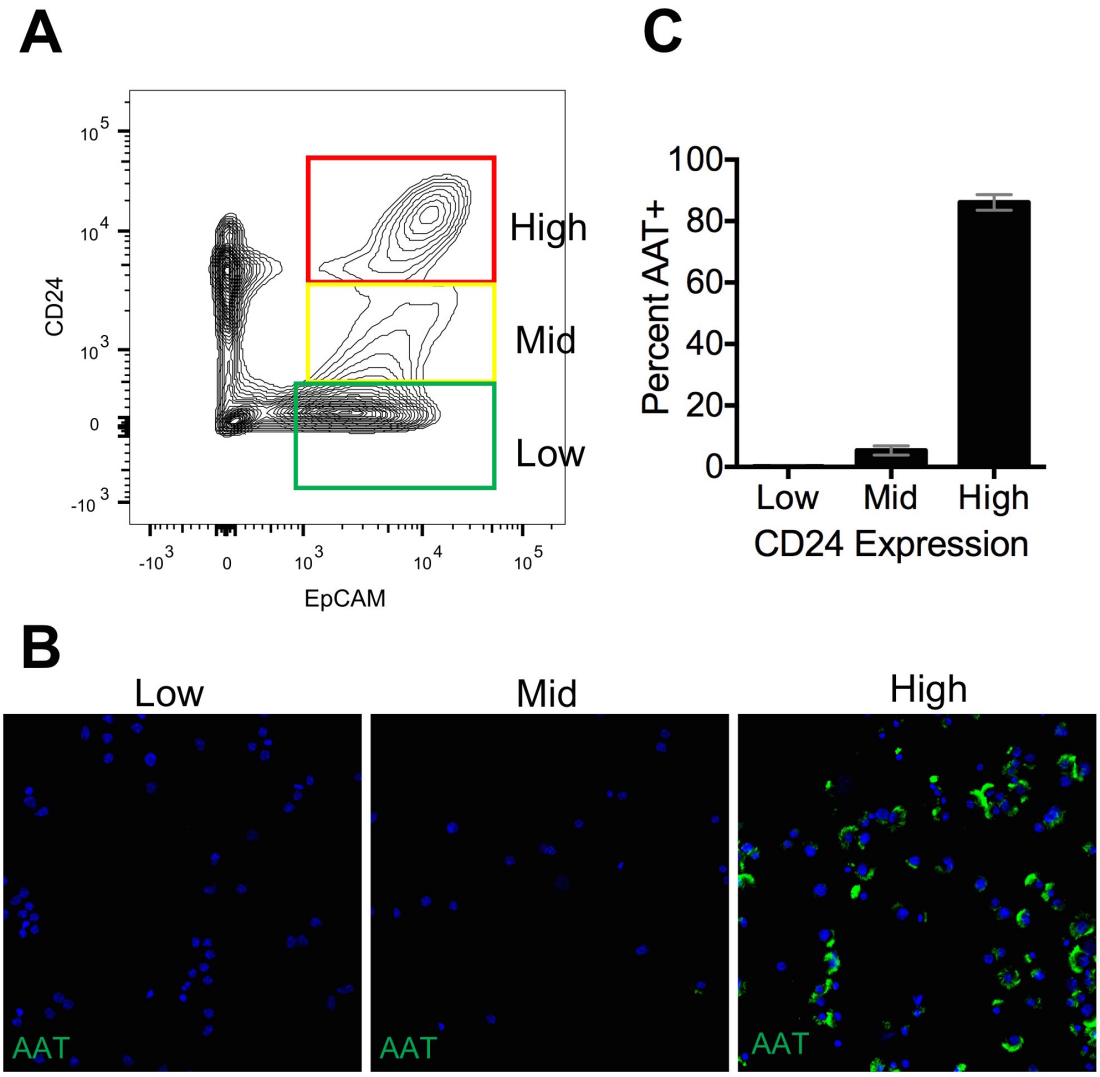
A
CD24
EpCAM
High
Mid
Low
C
Percent AAT+
CD24 Expression
Low
Mid
High
B
Low
Mid
High
AAT
AAT
AAT

Figure 17: EpCAM^{+} CD24^{Hi} cells are multiciliated

C57BL/6 lungs were harvested and digested to single cells by elastase. **(A)** Representative flow cytometry plot indicated sorting gates based on relative selection of CD24 and EpCAM. Plot already selected on Live CD45^{+} cells. **(B)** Sorted cells were cytocentrifugated and immunostained for acetylated alpha tubulin (AAT)(green) and DAPI (blue). **(B)** Quantification of all acetylated alpha tubulin positive cells on the cytospin (*n*= 3 mice per group, means ± s.e.m).

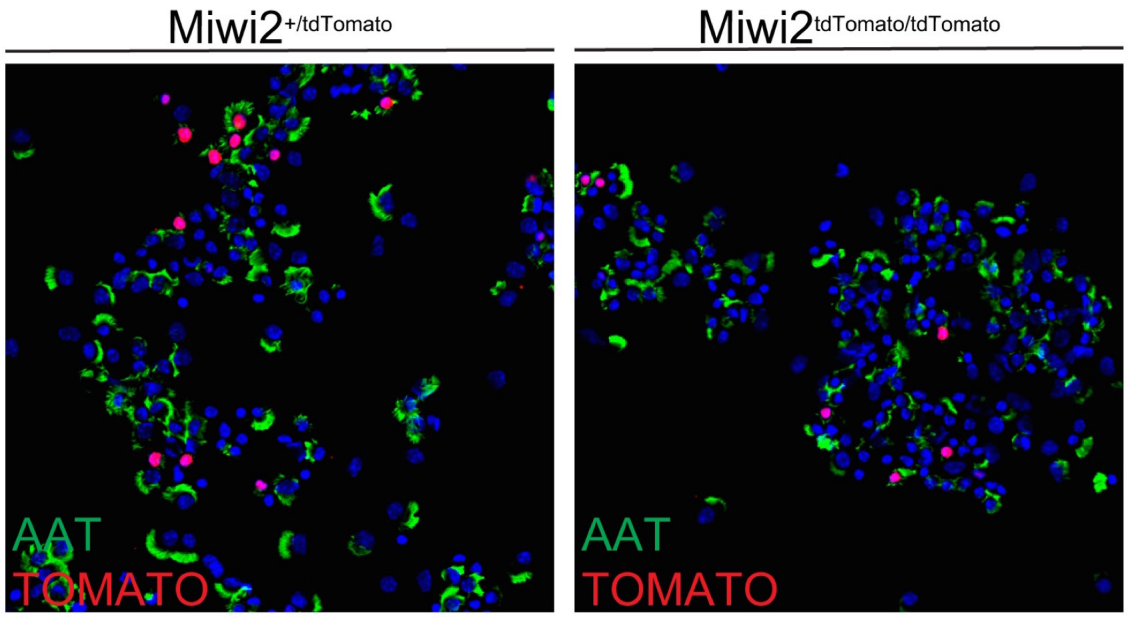
Miwi2+/tdTomato
Miwi2tdTomato/tdTomato
AAT
TOMATO
AAT
TOMATO

Figure 18: MIWI2::tdTomato knockout mice produce multicilia

Lungs were harvested from *Miwi2*$^{+/tdTomato}$ and *Miwi2*$^{tdTomato/tdTomato}$ mice and digested to single cells by elastase. Live CD45^{-} EpCAM^{+} CD24^{HI} cells were sorted cytocentrifugated and immunostained for acetylated alpha tubulin (AAT)(green) tdTomato (red) and DAPI (blue).

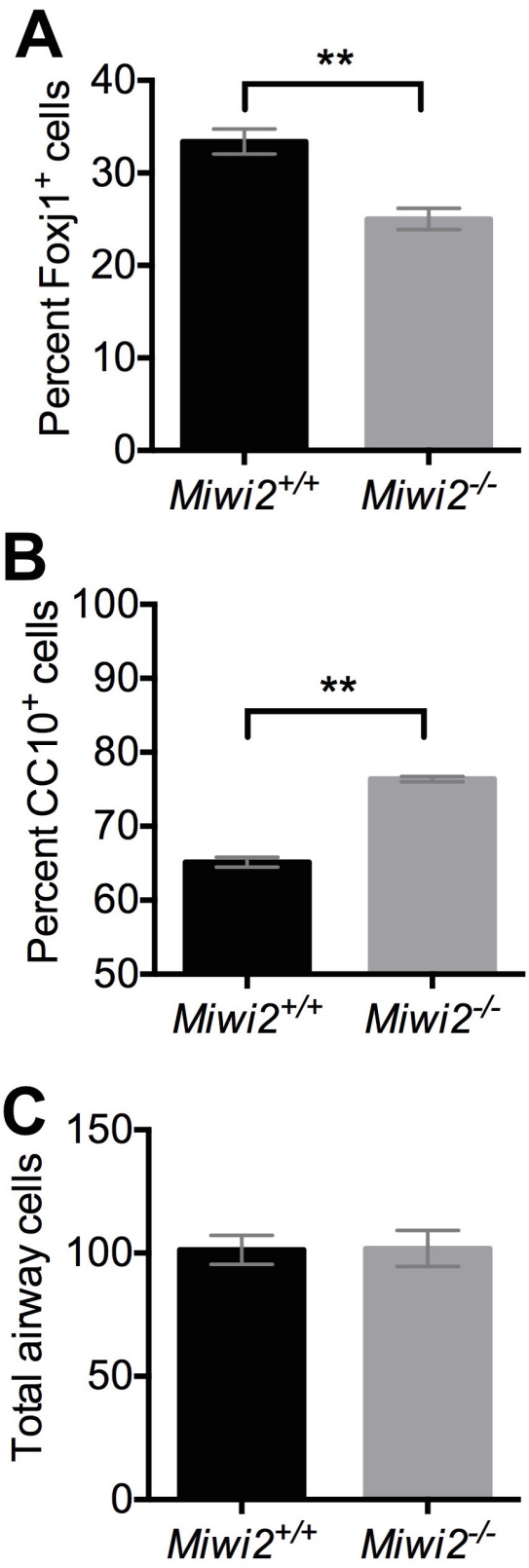
A
**
40
30
20
10
0
Percent Foxj1+ cells
Miwi2+/+
Miwi2-/-
B
**
100
90
80
70
60
50
Percent CC10+ cells
Miwi2+/+
Miwi2-/-
C
150
100
50
0
Total airway cells
Miwi2+/+
Miwi2-/-

Figure 19: MIWI2 deficient mice have a decrease in ciliated cells and an increase in club cells

Lungs sections from uninfected *Miwi2*$^{+/+}$ and *Miwi2*$^{-/-}$ mice were immunostained for CC10, FOXJ1, and DAPI and the total numbers of **(A)** Ciliated cells **(B)** Club Cells and **(C)** total airway cells were quantified (*n*= 4,3 mice per group, means ± s.e.m, $P<0.05$ as determined by unpaired t-test).

3.10 Miwi2 deficiency results in enhanced host defense to pneumonia

Previous studies aimed at identifying a somatic cell function of Miwi2 have focused on hematopoietic development (Nolde et al., 2013; Jacobs et al., 2013) and pluripotency (Cheng et al., 2014) but were unable to define a clear role. In addition, the function of piRNA binding proteins under cellular stress has yet to be elucidated. MIWI2 is induced during bacterial infection and is expressed in a cell type critical to pulmonary host defense. We also demonstrate that MIWI2 deficiency has an effect on the cellular composition of the airway, resulting in an increase in secretory cells. Hence, we sought to test if MIWI2 plays a role in the integrated host response to bacterial pneumonia. We infected *Miwi2*$^{+/+}$ and *Miwi2*$^{-/-}$ mice with a non-lethal strain of pneumococcus and assayed immune cell emigration by bronchoalveolar lavage. 4 hours post infection, *Miwi2*$^{-/-}$ mice demonstrated a statistically significant increase in BAL total cells **(Figure 20A)**. Cytospin and staining followed by quantification revealed an increase in both emigrated neutrophils and macrophages **(Figure 20B,C)**. To determine if the increase in cellularity is the cause of a basal increase in airspace cells, we performed BALs and cytospins on uninfected *Miwi2*$^{+/+}$ and *Miwi2*$^{-/-}$ mice. No difference was noted in the cell number, or cell type (>99% macrophages) in uninfected mice **(Figure 20D).** Neutrophil recruitment during pneumococcal pneumonia is primarily mediated by neutrophil chemotactic factors. The chemokines KC (CXCL1), MIP2 (CXCL2), and LIX(CXCL5) were measured by

ELISA in BAL fluid. We detected a trending increase in CXCL1 expression, and a statistically significant increase in CXCL2 expression **(Figure 20E, F)**.

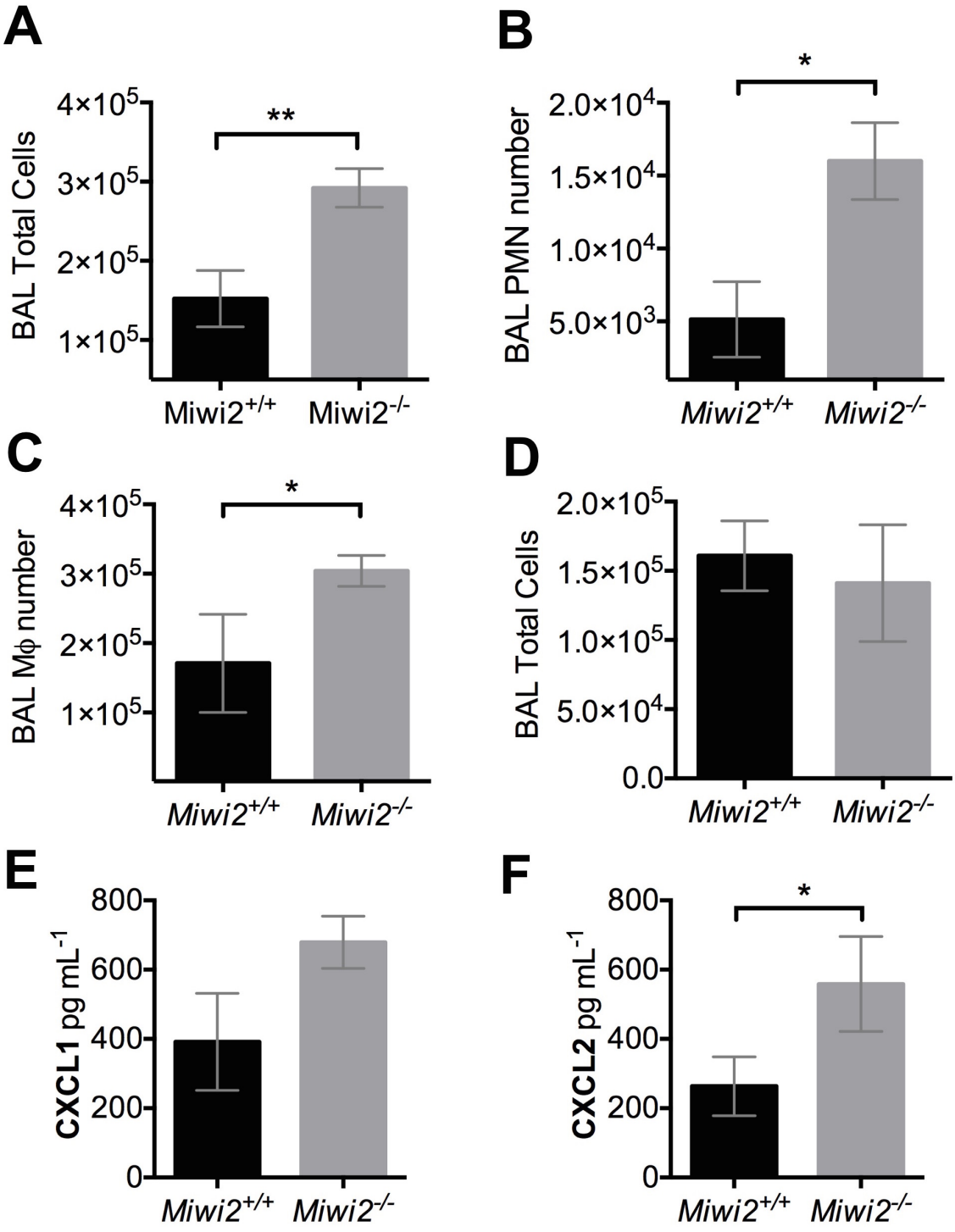
A
BAL Total Cells
4×10^5
3×10^5
2×10^5
1×10^5
**
Miwi2+/+
Miwi2-/-
B
BAL PMN number
2.0×10^4
1.5×10^4
1.0×10^4
5.0×10^3
*
Miwi2+/+
Miwi2-/-
C
BAL Mϕ number
4×10^5
3×10^5
2×10^5
1×10^5
*
Miwi2+/+
Miwi2-/-
D
BAL Total Cells
2.0×10^5
1.5×10^5
1.0×10^5
5.0×10^4
0.0
Miwi2+/+
Miwi2-/-
E
CXCL1 pg mL-1
800
600
400
200
0
Miwi2+/+
Miwi2-/-
F
CXCL2 pg mL-1
800
600
400
200
0
*
Miwi2+/+
Miwi2-/-

Figure 20: MIWI2 deficient mice have an enhanced early response to pneumococcal pneumonia

Miwi2$^{+/+}$ and *Miwi2*$^{-/-}$ mice were infected intratracheally with 5x10^{6} CFU of Sp19 for 4 hours and **(A)** total BAL cells **(B)** recruited neutrophils and **(C)** airspace macrophages were enumerated. (**D)** Total BAL cells in uninfected *Miwi2*$^{+/+}$ and *Miwi2*$^{-/-}$ (*n*= 3 mice per group, means ± s.e.m., NS by unpaired t-test). **(E)** CXCL1 and **(F)** CXCL2 cytokine expression as measured by ELISA in *Miwi2*$^{+/+}$ and *Miwi2*$^{-/-}$ mice infected as in (A). (*n*=6,7 mice per group, means ± s.e.m., *P<0.05 **P<0.01 by unpaired t-test).

To determine the effect of increased early cell recruitment on the global host response, we infected *Miwi2*$^{+/+}$ and *Miwi2*$^{-/-}$ mice with the same strain of pneumococcus and performed BALs 24 hours post infection. Total BAL cells were unchanged, as were differential cell counts as analyzed by cytospin **(Figure 21A,B,C)** Several cytokines were measured by ELISA, with a statistical decrease in IL-6, CXCL1, and CXCL2, all necessary for efficient defense against pneumococcus **(Figure 22)**(Cai et al., 2010; Greenberger et al., 1996; Jones et al., 2006). Several other cytokines tested had no significant difference. Given the statistically significant dysregulation of cytokine expression in MIWI2 depleted animals, we tested the hypothesis that early neutrophil recruitment would enhance bacterial clearance. We infected *Miwi2*$^{+/+}$ and *Miwi2*$^{-/-}$ mice with pneumococcus and harvested lung tissue 24 and 30 hours after instillation with Sp19 and enumerated bacterial counts. Miwi2 deficient mice show no difference in CFU at 24 hours post infection **(Figure 23A)**, however at 30 hours post infection they demonstrate a marked, statistically significant reduction in bacterial load **(Figure 23B)** indicating more efficient bacterial clearance. Collectively, these data suggest that MIWI2 is responsible for controlling exuberant inflammation. These data are the first to demonstrate a clear role for MIWI2 function in lung epithelial cells during pneumonia, and to our knowledge the first extra gonadal function of MIWI2 in mammals.

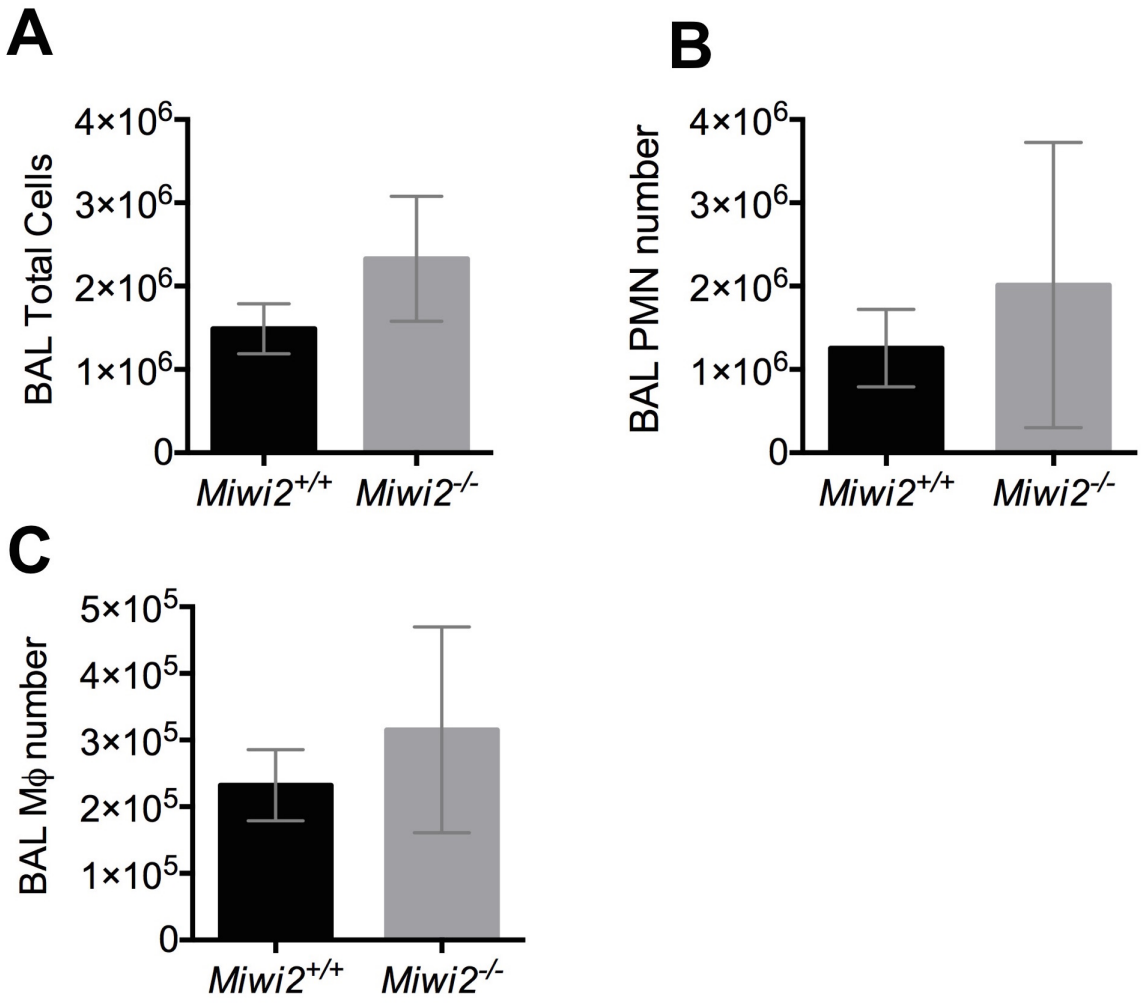
A
BAL Total Cells
4×10^6
3×10^6
2×10^6
1×10^6
0
Miwi2+/+
Miwi2-/-
B
BAL PMN number
4×10^6
3×10^6
2×10^6
1×10^6
0
Miwi2+/+
Miwi2-/-
C
BAL Mϕ number
5×10^5
4×10^5
3×10^5
2×10^5
1×10^5
0
Miwi2+/+
Miwi2-/-

Figure 21: Recruited cells are unchanged 24 hours after pneumococcal pneumonia in MIWI2 deficient mice

Miwi2$^{+/+}$ and *Miwi2*$^{-/-}$ mice were infected intratracheally with 5x10^{6} CFU of Sp19 for 24 hours and **(A)** total BAL cells **(B)** recruited neutrophils and **(C)** airspace macrophages were enumerated. (*n*= 3 mice per group, means ± s.e.m, NS by unpaired t-test).

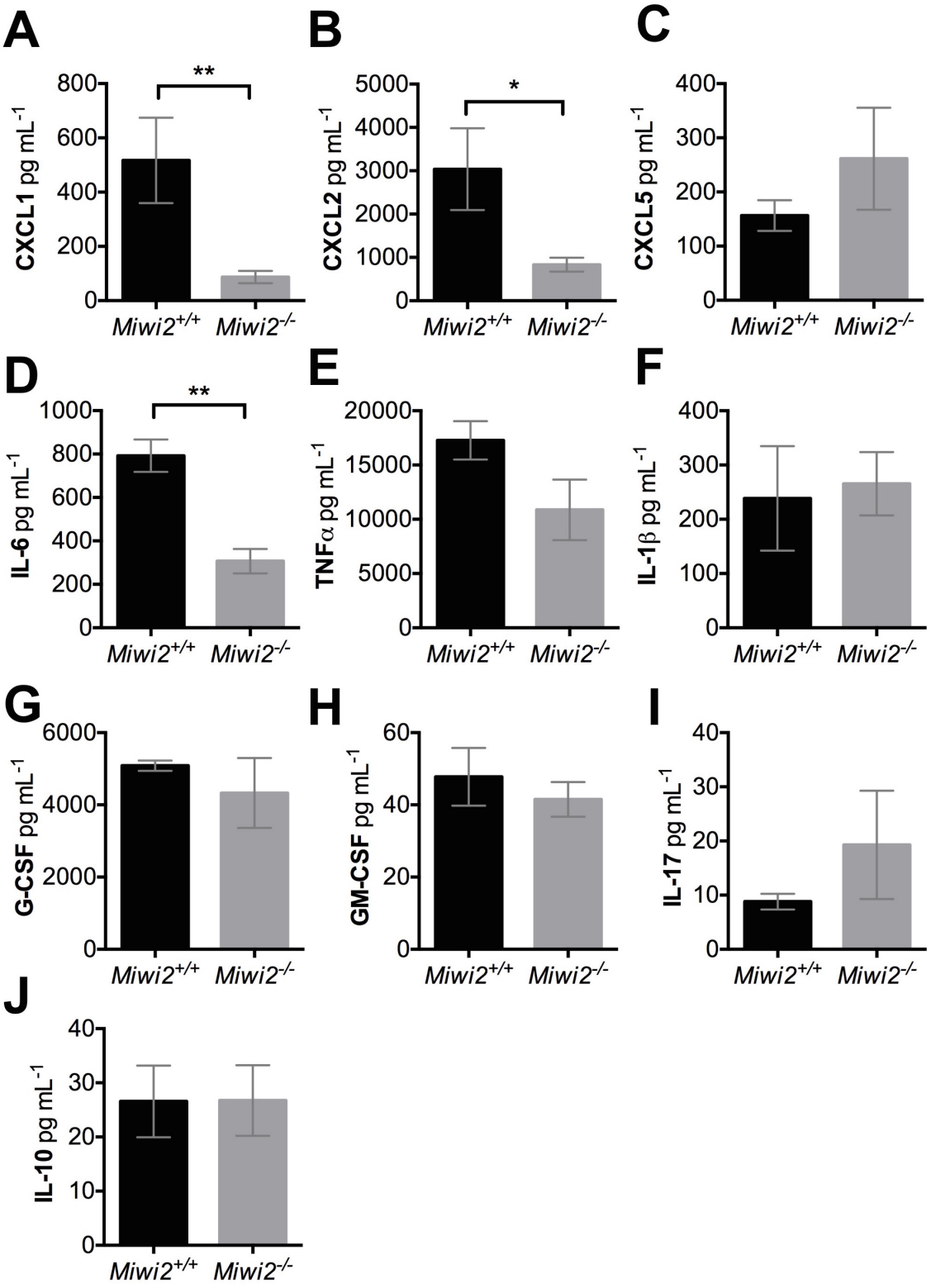
A
CXCL1 pg mL-1
800
600
400
200
0
**
Miwi2+/+
Miwi2-/-
B
CXCL2 pg mL-1
5000
4000
3000
2000
1000
0
*
Miwi2+/+
Miwi2-/-
C
CXCL5 pg mL-1
400
300
200
100
0
Miwi2+/+
Miwi2-/-
D
IL-6 pg mL-1
1000
800
600
400
200
0
**
Miwi2+/+
Miwi2-/-
E
TNFα pg mL-1
20000
15000
10000
5000
0
Miwi2+/+
Miwi2-/-
F
IL-1β pg mL-1
400
300
200
100
0
Miwi2+/+
Miwi2-/-
G
G-CSF pg mL-1
6000
4000
2000
0
Miwi2+/+
Miwi2-/-
H
GM-CSF pg mL-1
60
40
20
0
Miwi2+/+
Miwi2-/-
I
IL-17 pg mL-1
40
30
20
10
0
Miwi2+/+
Miwi2-/-
J
IL-10 pg mL-1
40
30
20
10
0
Miwi2+/+
Miwi2-/-

Figure 22: Dysregulated cytokine expression 24 hours post pneumococcal pneumonia in MIWI2 deficient mice

(A)-(J) *Miwi2*$^{+/+}$ and *Miwi2*$^{-/-}$ mice were infected intratracheally with 5x10^{6} CFU of Sp19 for 24 hours and BAL cytokine expression measured by multiplex bead array. (*n*= 3,6 mice per group, means ± s.e.m, *P<0.05 as determined by unpaired t-test).

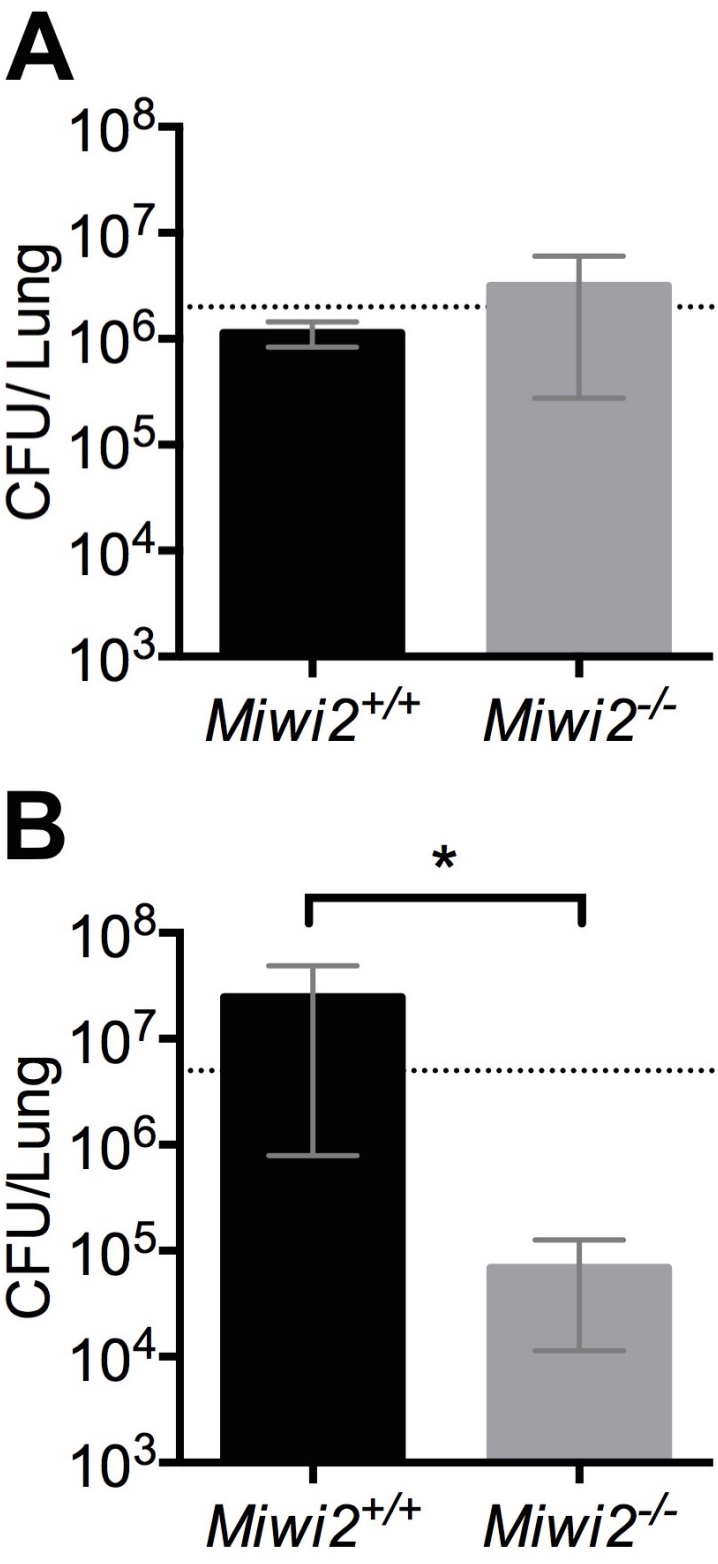
A
10^8
10^7
10^6
10^5
10^4
10^3
CFU/ Lung
Miwi2+/+
Miwi2-/-
B
*
10^8
10^7
10^6
10^5
10^4
10^3
CFU/Lung
Miwi2+/+
Miwi2-/-

Figure 23: MIWI2 depletion results in enhanced host defense to pneumococcus

Miwi2$^{+/+}$ and *Miwi2*$^{-/-}$ mice were infected intratracheally with Sp19 for **(A)** 24 hours or **(B)** 30 hours and lungs harvested for CFU quantification. (*n*= 7,5 and 6,9 mice per group, means ± s.e.m., *P<0.05 as determined by unpaired t-test). Dotted line indicates input CFU.

CHAPTER FOUR: DISCUSSION

4.1 Summary of Results

The results of this study provide to our knowledge, the first *in vivo* evidence for expression of the piRNA binding protein MIWI2 outside of the germline in mammals. It is also the first identification of a somatic cell function for MIWI2 that is independent of its role in retroelement silencing. We demonstrate that *Miwi2* mRNA is induced specifically in epithelial cells both *in vitro* in response to a variety of different inflammatory stimuli, as well as *in vivo* in response to *Streptococcus pneumoniae* infection. MIWI2 protein expression is restricted to the cytoplasm of only a subset of respiratory ciliated cells after post natal day 7, however its expression in airways precedes expression of the master transcription factor for ciliogenesis, *Foxj1.* Immunoprecipitation of MIWI2 indicates that full length MIWI2 is expressed outside of the germline, and is bound to an RNA species larger than a traditional piRNA. Using both an *in vitro* approach as well as an integrated genetic model of *Miwi2* deficiency, we identified that retroelement repression was not affected by loss of MIWI2 expression in somatic cells, collectively indicating that lung MIWI2 is independent of the piRNA silencing pathway. The localization in ciliated cells led us to test if MIWI2 function was required for cilia cell formation or function of the mucociliary escalator. We found that MIWI2 function was dispensible for the formation of multicilia, as we detected *Miwi2*$^{tdTomato/tdTomato}$ mice with normal cilia. Surprisingly, however we detected that loss of MIWI2 expression results in a decrease in total

ciliated cell number, and a concomitant increase in club cells in the intrapulmonary airways. This change was not due to the loss of the MIWI2^{+} expressing cells, as tomato expression was detected in FOXJ1 cells in *Miwi2*$^{tdTomato/tdTomato}$ mice. Given the alteration of airway cell type, we tested the hypothesis that MIWI2 mice would have an altered immune response to bacterial infection. Using a clinically relevant model of community acquired pneumonia, we demonstrate that MIWI2 deficiency results in enhanced host defense due to more rapid chemokine expression and neutrophil accumulation in the airspace

4.2 The demonstration that MIWI2 protein is expressed in the mammalian soma is novel

Despite the primary focus in the germline, substantial evidence prior to these studies suggested that Piwi-clade proteins may be expressed in somatic cells. Not long after the first identification of *Piwi* as a critical factor for stem cell renewal in germline stem cells, it was identified that it was also expressed in the supporting somatic cells of the *Drosophila* ovary (Ma et al., 2014), and in the testicular somatic cells (Gonzalez et al., 2015). Reports of Piwi-clade protein mRNA expression in mammals, however has been focused on stem cell and cancer populations, yet a clear functional role has not been identified, nor has definitive proof of protein expression been demonstrated. HIWI, the human homologue of *Drosophila Piwi* and mouse *Miwi,* is expressed in a CD34^{+} hematopoietic progenitor cells and is downregulated upon differentiation to mature myeloid cells (Sharma et al., 2001). This presented the hypothesis that

Piwi proteins may play a role in maintaining stem cell properties in somatic cells in mammals, similar to their role in the *Drosophila* ovary. However, work from several groups indicate that *Miwi2* is highly expressed in undifferentiated hematopoietic cells yet mice deficient in all three Piwi-clade proteins *Miwi, Mili, and Miwi2* have no differences in the generation of mature myeloid lineages, or dysregulation of progenitor cell gene expression (Nolde et al., 2013; Jacobs et al., 2013). Work from the same group has also demonstrated that iPS cells generated from *Miwi/Mili/Miwi2* triple knockout mice are able to differentiate into all three germ layers indicating that *Miwi, Mili, and Miwi2* are collectively dispensable for stem cell differentiation and maintenance in mice (Cheng et al., 2014). It should be stressed that even though *Miwi2* mRNA was detected in these cells, they did not evaluate protein expression (Nolde et al., 2013; Jacobs et al., 2013; Cheng et al., 2014).

Several studies to date have demonstrated that mRNA expression of HIWI2, the human homologue of *Miwi2,* is expressed in cancer cell lines, and surgical biopsies (Su et al., 2012; Keam et al., 2014; Tan et al., 2015; Suzuki et al., 2012) and may be a potential biomarker for disease progression (Wang et al., 2012). HIWI2 has been proposed as a potential “cancer testis antigen”, a group of proteins that are normally expressed only in the germline and are re-expressed in tumor cells, making them attractive treatment targets (Tan et al., 2015). The potential role of HIWI2 in cancer has yet to be identified, but several possible functions have been proposed including promoting cell proliferation (Su

et al., 2012) facilitating migration and invasion, and resisting apoptosis (Sugimoto et al., 2007) all of which have been attributed to epigenetic function that take place in the nucleus, and contributes to their stem cell properties.

4.3 The demonstration that lung MIWI2 is not expressed in a stem cell population is contrary to available evidence

Given the available evidence in mice and humans, that Piwi-clade proteins are expressed primarily in stem cell populations or cancer cells, which are known to express germline antigens, our finding that MIWI2 is expressed in the terminally differentiated ciliated cells of the lung is of great interest and contrary to the hypothesis that MIWI2 is necessary for maintaining multipotency in somatic cells. The lung is remarkably resistant organ to tissue injury, with robust mechanisms for repair and maintenance of the airway epithelium. The airways in human and in mice are comprised of several specialized cell types including basal cells, club cells, goblet cells, ciliated cells, neuroendocrine cells and alveolar epithelial cells, many of which are capable of differentiation into other mature epithelial lineages (Rock and Hogan, 2011a; Hogan et al., 2014). Multiple injury models such as toxic gas inhalation (SO_2) which kills all luminal cells, naphthalene administration which ablates club cells, or influenza infection have been used in conjunction with lineage tracing mice utilizing various Cre drivers to determine the origin and differentiation capacity of many of the mature airway epithelial cells. The consensus from these studies is that basal cells, which characteristically express cytokeratin 5 (*Krt5*) are the main stem cell population of

the lung, capable of differentiation into secretory and ciliated cells (Wansleeben et al., 2012). Additional studies have identified that in the distal airways, club cells differentiate into ciliated cells and type II pneumocytes which collectively contributes to tissue homeostasis after injury. Interesting, ciliated cells appear to be one of the only airway cells that are non- proliferating and terminally differentiated cells, and do not contribute to the repair of the epithelium after damage (Rock and Hogan, 2011a; Hogan et al., 2014; Rawlins et al., 2007). Evidence for this was generated using lineage tracing mice where Cre expression is driven by the major ciliated cell transcription factor *Foxj1,* and exposed to either sulfur dioxide or naphthalene. The authors found no evidence of labeled cells expressing non-ciliated cell lineage markers in either model (Rawlins et al., 2007). In addition, they could not identify any lineage labeled ciliated cells that incorporated BrdU, a marker of proliferation, in either injury model. This is in agreement with our data that ciliated cells of the airways are non-proliferating, and do not express the proliferation marker Ki67. These data have also been confirmed in additional models including ovalbumin exposure which leads to an asthma-like phenotype, as well as influenza infection (Pardo-Saganta et al., 2013). Collectively, our demonstration of MIWI2 expression in the terminally differentiated ciliated cells in the lungs, rather than in a stem cell population suggest perhaps an alternative function to those proposed for cancer cells. One of the many questions that arise from these data is what is the significance of MIWI2 expression in only a subset of the ciliated population.

4.4 The Identification of a subset of ciliated cells is novel

Several lung epithelial cells are heterogeneous in their gene expression profiles. In some cases, differences may reflect a transition state (Treutlein et al., 2014), but in other cases, heterogeneity is the result of phenotypic differences and distinct functions. One example is illustrated by the apparent resistance of a subset of club cells adjacent to neuroepithelial bodies (NEBs) to survive naphthalene administration. These so-called variant club cells, act as a progenitor population for club and ciliated cells after injury (Guha et al., 2012). An alternative example is the discovery of an $\alpha 6\beta 4^{+}$ integrin expressing alveolar epithelial progenitor cell which serves as a multipotent progenitor cell during injury repair (Chapman et al., 2011). In contrast to club cells and type II cells, variations of ciliated cells have not been identified. Our data suggest that approximately 30 percent of ciliated cells express MIWI2, however this is dynamic as the number of positive cells is increased during infection with pneumococcus. Staining in post natal day 7 and adult mice indicate that all MIWI2 positive cells are ciliated cells, however in embryonic lungs we were able to detect MIWI2 positive cells that were not expressing FOXJ1, indicating that they may be a discrete cell lineage. Assuming that the cells expressing MIWI2 in the embryos become the same $MIWI2^{+}$ ciliated cells seen during later time points, the questions that arise including whether MIWI2 functionality is necessary for the generation of this discrete lineage of cells? While additional tools are needed to comprehensively test the origin and fate of $MIWI2^{+}$ ciliated

cells both during embryogenesis and during injury and repair, we were able to gain insight using a novel mouse model engineered by our collaborator where expression of a loss-of-function tdTomato reporter allele was detectable in both heterozygous animals and homozygous animals, and was expressed in FOXJ1^{+} cells. Thus indicating that at least *Miwi2* promoter activity is restricted to a subset of ciliated cells in adult mice, even in the absence of functional MIWI2. Co-staining for tdTomato and acetylated alpha tubulin revealed that cells which are deficient in functional MIWI2 also contain cilia, indicating that MIWI2 functionality is not required for cilia formation. Importantly, it should not be concluded that MIWI2 deficient cells have normal ciliary function as this was not directly tested. In fact, complementary studies using *Miwi2* deficient mice revealed fewer ciliated cells, and an increase in mucus secreting club cells in the intrapulmonary airways. Interestingly, ciliated cells are reduced 25% in mice lacking *Miwi2,* which is the same fraction of ciliated cells that are MIWI2^{+}. Results generated from *Miwi2*$^{tdTomato/tdTomato}$ mice suggest that is it not the MIWI2^{+} lineage that is ablated, as RFP positive cells are present in the absence of functional MIWI2. This decrease in ciliated cells does not however alter the total number of cells in the airways but rather we detect an increase in the number of club cells in *Miwi2* deficient animals. Notch signaling is major regulator of airway cell identity in the human and murine lung (Lafkas et al., 2015). Overexpression of Notch drives secretory cell metaplasia and a loss of ciliated cells (Rock et al., 2011). We consider the possibility that MIWI2 regulates Notch in embryonic lungs which in

turn influences cell fate decisions in the developing airways. Soluble factors, such as IL-13, which is induced in human asthma, could also influence ciliated cell number through downregulation of the ciliated transcription factor *Foxj1.* While we have not tested if mucus production *per se* is altered in *MIwi2* deficient mice, the increase in clara cells would be consistent with an enhanced bacterial clearance and elaborated cytokine production. In one study, transgenic mice which are engineered to overexpress the mucin gene *Muc5b* in club cells, have an increase in inflammation and immune cell recruitment when infected with a gram-positive pathogen (Roy et al., 2013).

4.5 Lung MIWI2 function is independent of the piRNA pathway

MIWI2 protein expression in the male germline is dogmatically expressed during pre-pachytene, beginning at embryonic day 15.5 and absent at postnatal day 3. Aravin and colleagues, using an ectopically expressed transgenic GFP-MIWI2 fusion demonstrated that MIW2 expression in testis are primary localized in the nucleus, with some perinuclear staining evident (Aravin et al., 2008; 2009). The translocation to the nucleus was dependent on coexpression of MILI, another piRNA binding protein that has been shown to be necessary for piRNA generation. Together with work from additional investigators, the model that has emerged postulates that piRNAs are generated by several factors, including MILI in the cytoplasm, where they are loaded into MIWI2 which then translocates to the nucleus to execute transcriptional silencing of retroelement expression (Aravin et al., 2008). Our data indicate that in contrast to expression in the testis,

lung MIWI2 is expressed throughout the lifetime of the organism, detectable in embryonic lungs at E16.5 through at least week 30. In addition, lung MIWI2 is predominantly, if not exclusively restricted to the cytoplasm. We would thus hypothesize that based on the germ cell model, lung MIWI2 is not bound to an RNA species, however our data clearly refute this prediction. Lung MIWI2 is bound to an RNA species, larger than the 30 nt traditional piRNA (Fu and Wang, 2014). What is the identity of this RNA? The existence of somatic cell piRNAs in mammals is controversial. One recent study used high throughput RNA sequencing of RNA collected from various organs in *Rhesus macaque*, and mice and found that piRNA like RNAs were expressed (Yan et al., 2011). These studies however, did not show direct association with known piRNA binding proteins, a hallmark and defining feature of piRNAs. Additionally, as others have commented, the library size and lack of negative controls makes interpretation of these results difficult (Ross et al., 2014). One study, transduced a breast cancer cell line with a vector expressing an epitope tagged copy of HIWI2, the human variant of MIWI2, and found that localization was restricted to the cytoplasm (Keam et al., 2014). The authors also found that FLAG-HIWI2 was bound to fragments of tRNAs and the complex was associated with polysomes and translation machinery. As all Argonaute proteins will bind RNA with a 5' phosphate group, it is unclear whether overexpression of MIWI2, which has RNA slicing capability, alters the associated RNA substrate, and whether this overexpression also influences the protein binding partners. However the

restriction to the cytoplasm and association with translational machinery is more consistent with described characteristics of AGO clade Argonaute proteins, which associate with miRNAs and siRNAs. While 50 nt would also be substantially longer than a traditional piRNA, it is plausible that MIWI2 would bind RNA degradation products, derived from mRNA, pre-miRNA, or long non-coding RNAs.

Substantial evidence supports that retroelement expression is not restricted to the mammalian germline. In murine B cells for example, cross linking of the B cell receptor by T cell independent type II antigens, such as Pneumovax, the major vaccine against *Streptococcus pneumoniae* induces retroelement expression and influences the formation of plasma cells (Zeng et al., 2014). Given the known role of MIWI2 in the testis as a repressor of retroelement expression, we used a whole genome approach to identify if MIWI2 in lung cells participates in retroelement restriction. Our data, using whole genome microarray technology both *in vitro* and *in vivo* suggest that deficiency of MIWI2 does not result in alterations of retroelement expression. Limitations of our approach include the use of whole lung RNA rather than a pure MIWI2 expressing population, however our method was able to identify true gene expression differences. The fact that MIWI2 is not bound to piRNAs, coupled with its exclusion from the nucleus complement the retroelement expression data and suggest that lung MIWI2 is independent of the piRNA system. It has been

suggested that the restriction of retroelements in the soma may be carried out by various other mechanisms (Chambers, 2014).

4.6 Implications and Future Directions

Mortality from bacterial pneumonia and specifically, acute lung injury remains unacceptably high despite numerous advances in modern medicine. In this study we sought to identify and characterize novel mechanism that regulate lung inflammation with the hope that these pathways may serve as a foundation for future diagnostics or therapeutics. Our studies report the surprising finding that MIWI2, a piRNA binding protein and PIWI-clade Argonaute protein is expressed and induced in lung epithelial cells and regulates inflammation during bacterial pneumonia. A clear molecular link between MIWI2 and the enhancement of immunity and regulation of cell fate remains elusive.

One of the most pressing questions that remains is the identity of the RNA bound to MIWI2 in lung epithelial cells. Our results suggest that the associated RNA is larger than a traditional piRNA, however numerous attempts to prepare a library have failed. It is likely that the RNA is either not phosphorylated at the 5' end or contains additional modifications that prevent library preparation. Future experiments should include alternative methods of library preparation such as the one described recently (Jaskiewicz et al., 2012). Additionally, our RNA labeling experiments, while repeated several times, could be conducted with a more appropriate control, namely embryonic testis from an HA-MIWI2 mouse where piRNAs could be isolated, ensuring that our IP protocol does not interfere with

the preparation of a library. Immediate experiments should be focused on elucidating the associated RNA as this will provide necessary insight into potential molecular targets of regulation.

Our demonstration that MIWI2 is a marker of a discrete population of ciliated cells is of great interest. Ciliated cells play an important role in pulmonary host defense, and to date, no subsets with differing function have been identified. In order to gain insight into the complexity of the MIWI2^{+} lineage, a key experiment will be sorting and transcriptomic comparison of the MIWI2^{+} and MIWI2^{-} ciliated cells from infected and uninfected mice. This can be performed using the *Miwi2*$^{+/tdTomato}$ mice coupled with our identification of CD24 as a reliable marker of lung ciliated cells. Sorting of *Miwi2*$^{tdTomato/tdTomato}$ cells can also be included and compared to tdTomato^{+} cells from functional heterozygotes to reveal genes regulated by MIWI2. Results from these experiments will shed important light on the heterogeneity of ciliated cells and perhaps provide insight into how MIWI2 regulates airway cell fate and gene expression.

The regulation of airway cell fate was a surprising finding in MIWI2 deficient animals. Similarly, the expression of MIWI2 in embryonic lungs antecedent to the expression of mature lung lineage markers is puzzling, given that all adult MIWI2^{+} cells are committed to a single (ciliated) fate. A critical tool that is needed to expand on these findings is the generation of a Miwi2 lineage tracing mouse. The ideal construct would be a Tamoxifen inducible CreERT2::GFP allele knocked in to the native *Miwi2* locus. This mouse could

then be crossed to a mouse containing a CRE inducible expression allele (*loxP*-STOP-*loxP*:: tdTomato) at the Rosa locus. With this mouse, GFP would serve as a current reporter of Miwi2 transcription, while tdTomato expression could be used to identify the fate of MIWI2 cells during development or injury. The knock-in strategy here will also allow for the tracing of cell fate in cells which are functionally MIWI2 deficient.

We initially discovered MIWI2 using a clinically relevant model of bacterial pneumonia, however given the cell type of expression there may be additional models where MIWI2 function may be implicated. Ciliated cells directly, or defects in ciliated cell function contribute to the pathology of asthma, COPD, and cystic fibrosis. Elucidating possible MIWI2 functions in these diseases may open new areas of investigation. Similarly, we identified that *Miwi2* mRNA is highly responsive to type I interferon, and hence exploration of function in a lung viral infection such as influenza may be enlightening.

Our model, implies that MIWI2 regulates, through a currently not understood mechanism, the cell identity of the adult airway. Loss of MIWI2 expression results in an increase in club cells, and increased production of mucus, which enhances neutrophil emigration and inflammation. One question that arises is why then do MIWI2 deficient animals not show signs of chronic inflammation such as recurrent or spontaneous infection or basal differences in cell recruitment? One explanation is that our mice are housed in a specific pathogen free clean facility that is carefully monitored for pathogens. Future

studies may include housing of mice in a facility where opportunistic infections are more common. Additionally, in contrast to our model strain, studies with a strain of bacteria that is not easily cleared in wildtype mice may exacerbate differences in tissue injury.

A severe limitation to continued progress in the study of MIWI2 regulation is the restriction to a whole animal model. Establishing a cell system that can be used to study MIWI2 function is critical. We have attempted to use pre-established air-liquid interface cultures, however no $MIWI2^{+}$ cells were identified, likely indicating they do not arise from basal cells. Over the past several years, substantial progress has been made in the application of iPS cells for the study of lung developmental biology. Much of this work has been performed here at Boston University and in the Pulmonary Center. While it is not currently possible to generate in large quantity ciliated cells from induced lung progenitors, the role of MIWI2 in early cell differentiation could be assessed. This would also be an attractive model to determine the function of MIWI2 in human lung epithelium.

Collectively, this dissertation has expanded our current understanding of PIWI proteins, and their role in somatic cells. While many questions still remain unanswered, the work will serve as a foundation for future investigation and hypothesis generation about the functions of Piwi proteins, and ciliated cell biology.

BIBLIOGRAPHY

Aravin, A.A., G.W. van der Heijden, J. Castañeda, V.V. Vagin, G.J. Hannon, and A. Bortvin. 2009. Cytoplasmic compartmentalization of the fetal piRNA pathway in mice. *PLoS Genetics*. 5:e1000764. doi:10.1371/journal.pgen.1000764.

Aravin, A.A., M. Lagos-Quintana, A. Yalcin, M. Zavolan, D. Marks, B. Snyder, T. Gaasterland, J. Meyer, and T. Tuschl. 2003. The Small RNA Profile during Drosophila melanogaster Development. *Developmental Cell*. 5:337–350. doi:10.1016/S1534-5807(03)00228-4.

Aravin, A.A., N.M. Naumova, A.V. Tulin, V.V. Vagin, Y.M. Rozovsky, and V.A. Gvozdev. 2001. Double-stranded RNA-mediated silencing of genomic tandem repeats and transposable elements in the D. melanogaster germline. *Current Biology*. 11:1017–1027.

Aravin, A.A., R. Sachidanandam, A. Girard, K. Fejes-Toth, and G.J. Hannon. 2007. Developmentally Regulated piRNA Clusters Implicate MILI in Transposon Control. *Science*. 316:744–747. doi:10.1126/science.1142612.

Aravin, A.A., R. Sachidanandam, D. Bourc'his, C. Schaefer, D. Pezic, K.F. Toth, T. Bestor, and G.J. Hannon. 2008. A piRNA Pathway Primed by Individual Transposons Is Linked to De Novo DNA Methylation in Mice. *Molecular Cell*. 31:785–799. doi:10.1016/j.molcel.2008.09.003.

Aristotle. 2014. Complete Works of Aristotle, Volume 1. Princeton University Press. 1 pp.

Armstrong, G.L., L.A. Conn, and R.W. Pinner. 1999. Trends in infectious disease mortality in the United States during the 20th century. *JAMA: The Journal of the American Medical Association*. 281:61–66.

Austrian, R. 1981. Pneumococcus: the first one hundred years. *Review of Infectious Diseases.* 3(2):183–189.

Ayre, D.C., M. Elstner, N.C. Smith, E.S. Moores, A.M. Hogan, and S.L. Christian. 2015. Dynamic regulation of CD24 expression and release of CD24-containing microvesicles in immature B cells in response to CD24 engagement. *Immunology*. 146:217–233. doi:10.1111/imm.12493.

Bals, R., and P.S. Hiemstra. 2004. Innate immunity in the lung: how epithelial cells fight against respiratory pathogens. *European Respiratory Journal*. 23:327–333. doi:10.1183/09031936.03.00098803.

Baron, E.J., J.M. Miller, M.P. Weinstein, S.S. Richter, P.H. Gilligan, J. Richard B Thomson, P. Bourbeau, K.C. Carroll, S.C. Kehl, W.M. Dunne, B. Robinson-Dunn, J.D. Schwartzman, K.C. Chapin, J.W. Snyder, B.A. Forbes, R. Patel, J.E. Rosenblatt, and B.S. Pritt. 2013. A Guide to Utilization of the Microbiology Laboratory for Diagnosis of Infectious Diseases: 2013 Recommendations by the Infectious Diseases Society of America (IDSA) and the American Society for Microbiology (ASM). *Clinical Infectious Diseases*. 57:cit278–e121. doi:10.1093/cid/cit278.

Barrett-Connor, E. 1971. The nonvalue of sputum culture in the diagnosis of pneumococcal pneumonia. *American Review of Respiratory Disease*. 103:845–848. doi:10.1164/arrd.1971.103.6.845.

Bartel, D.P. 2004. MicroRNAs: genomics, biogenesis, mechanism, and function. *Cell*. 116:281–297.

Bartel, D.P. 2009. MicroRNAs: Target Recognition and Regulatory Functions. *Cell*. 136:215–233. doi:10.1016/j.cell.2009.01.002.

Bartlett, J.G. 2011. Diagnostic Tests for Agents of Community-Acquired Pneumonia. *Clinical Infectious Diseases*. 52:S296–S304. doi:10.1093/cid/cir045.

Bartlett, J.G., and L.M. Mundy. 1995. Community-acquired pneumonia. *New England Journal of Medicine*. 333:1618–1624. doi:10.1056/NEJM199512143332408.

Beck, J.M., V.B. Young, and G.B. Huffnagle. 2012. The microbiome of the lung. *Translational Research*. 160:258–266. doi:10.1016/j.trsl.2012.02.005.

Belancio, V.P., D.J. Hedges, and P. Deininger. 2008. Mammalian non-LTR retrotransposons: For better or worse, in sickness and in health. *Genome Research*. 18:343–358. doi:10.1101/gr.5558208.

Benjamini, Y., and Y. Hochberg. 1995. Controlling the false discovery rate: a practical and powerful approach to multiple testing. *Journal of the Royal Statistical Society*. 57(1):289–300. doi:10.2307/2346101.

Bernstein, E., S.Y. Kim, M.A. Carmell, E.P. Murchison, H. Alcorn, M.Z. Li, A.A. Mills, S.J. Elledge, K.V. Anderson, and G.J. Hannon. 2003. Dicer is essential for mouse development. *Nature Genetics*. 35:215–217. doi:10.1038/ng1253.

Blasi, F., S. Aliberti, M. Pappalettera, and P. Tarsia. 2007. 100 years of respiratory medicine: Pneumonia. *Respiratory Medicine*. 101:875–881. doi:10.1016/j.rmed.2007.02.016.

Bohmert, K., I. Camus, C. Bellini, D. Bouchez, M. Caboche, and C. Benning. 1998. AGO1 defines a novel locus of Arabidopsis controlling leaf development. *EMBO Journal*. 17:170–180. doi:10.1093/emboj/17.1.170.

Brettschneider, J., F. Collin, B.M. Bolstad, and T.P. Speed. 2008. Quality Assessment for Short Oligonucleotide Microarray Data. *Technometrics*. 50:241–264. doi:10.1198/004017008000000334.

Brinkmann, V., U. Reichard, C. Goosmann, B. Fauler, Y. Uhlemann, D.S. Weiss, Y. Weinrauch, and A. Zychlinsky. 2004. Neutrophil extracellular traps kill bacteria. *Science*. 303:1532–1535. doi:10.1126/science.1092385.

Burgess, A., S. Vigneron, E. Brioudes, J.-C. Labbé, T. Lorca, and A. Castro. 2010. Loss of human Greatwall results in G2 arrest and multiple mitotic defects due to deregulation of the cyclin B-Cdc2/PP2A balance. *Proceedings of the National Academy of Sciences*. 107:12564–12569. doi:10.1073/pnas.0914191107.

Burri, P.H. 1984. Fetal and postnatal development of the lung. *Annual Review of Physiology*. 46:617–628. doi:10.1152/ajplung.00105.2015.

Cai, S., S. Batra, S.A. Lira, J.K. Kolls, and S. Jeyaseelan. 2010. CXCL1 Regulates Pulmonary Host Defense to Klebsiella Infection via CXCL2, CXCL5, NF-kB, and MAPKs. *Journal of immunology*. 185:6214–6225. doi:10.4049/jimmunol.0903843.

Cardoso, W.V. 2004. Lung Morphogenesis, Role of Growth Factors and Transcription Factors. *In* The Lung. Elsevier. 3–11.

Carmell, M.A., A. Girard, H.J.G. van de Kant, D. Bourc'his, T.H. Bestor, D.G. de Rooij, and G.J. Hannon. 2007. MIWI2 Is Essential for Spermatogenesis and Repression of Transposons in the Mouse Male Germline. *Developmental Cell*. 12:503–514. doi:10.1016/j.devcel.2007.03.001.

Carmell, M.A., Z. Xuan, M.Q. Zhang, and G.J. Hannon. 2002. The Argonaute family: tentacles that reach into RNAi, developmental control, stem cell maintenance, and tumorigenesis. *Genes & Development*. 16:2733–2742. doi:10.1101/gad.1026102.

Chambers, S.A. 2014. Stability at the surface. *Science*. 346:1186–1187. doi:10.1126/science.aaa1543.

Chapman, H.A., X. Li, J.P. Alexander, A. Brumwell, W. Lorizio, K. Tan, A. Sonnenberg, Y. Wei, and T.H. Vu. 2011. Integrin α6β4 identifies an adult distal lung epithelial population with regenerative potential in mice. *The*

Journal of Clinical Investigation. 121:2855–2862. doi:10.1172/JCI57673.

Cheng, E.-C., D. Kang, Z. Wang, and H. Lin. 2014. PIWI Proteins Are Dispensable for Mouse Somatic Development and Reprogramming of Fibroblasts into Pluripotent Stem Cells. *PLoS One*. 9:e97821. doi:10.1371/journal.pone.0097821.s001.

Cordaux, R., and M.A. Batzer. 2009. The impact of retrotransposons on human genome evolution. *Nature Reviews. Genetics*. 10:691–703. doi:10.1038/nrg2640.

Cox, D.N., A. Chao, and H. Lin. 2000. piwi encodes a nucleoplasmic factor whose activity modulates the number and division rate of germline stem cells. *Development*. 127:503–514.

Dai, M., P. Wang, A.D. Boyd, G. Kostov, B. Athey, E.G. Jones, W.E. Bunney, R.M. Myers, T.P. Speed, H. Akil, S.J. Watson, and F. Meng. 2005. Evolving gene/transcript definitions significantly alter the interpretation of GeneChip data. *Nucleic Acids Research*. 33:e175–e175. doi:10.1093/nar/gni179.

De Fazio, S., N. Bartonicek, M. Di Giacomo, C. Abreu-Goodger, A. Sankar, C. Funaya, C. Antony, P.N. Moreira, A.J. Enright, and D. O'Carroll. 2011. The endonuclease activity of Mili fuels piRNA amplification that silences LINE1 elements. *Nature*. 480:259–263. doi:10.1038/nature10547.

de Roux, A., M. Cavalcanti, M.A. Marcos, E. Garcia, S. EWIG, J. Mensa, and A. TORRES. 2006. Impact of alcohol abuse in the etiology and severity of community-acquired pneumonia. *Chest*. 129:1219–1225. doi:10.1378/chest.129.5.1219.

Deng, W., and H. Lin. 2002. miwi, a murine homolog of piwi, encodes a cytoplasmic protein essential for spermatogenesis. *Developmental Cell*. 2:819–830.

Dockrell, D.H., P.J. Collini, and H.M. Marriott. 2013. Alveolar Macrophages. In A. Prince (ed.) *Mucosal Immunology of Acute Bacterial Pneumonia* (pp. 1–48). New York: Springer Science+Business Media.

Drijkoningen, J.J.C., and G.G.U. Rohde. 2014. Pneumococcal infection in adults burden of disease. *Clinical Microbiology and Infection*. 20:45–51. doi:10.1111/1469-0691.12461.

Elkayam, E., C.-D. Kuhn, A. Tocilj, A.D. Haase, E.M. Greene, G.J. Hannon, and L. Joshua-Tor. 2012. The structure of human argonaute-2 in complex with miR-20a. *Cell*. 150:100–110. doi:10.1016/j.cell.2012.05.017.

File, T.M., Jr, and T.J. Marrie. 2010. Burden of Community-Acquired Pneumonia in North American Adults. *Postgraduate Medicine*. 122:130–141. doi:10.3810/pgm.2010.03.2130.

Fink, M.P. 2002. Role of reactive oxygen and nitrogen species in acute respiratory distress syndrome. *Current Opinion in Critical Care*. 8:6.

Finnegan, D.J. 1997. Transposable elements: how non-LTR retrotransposons do it. *Current Biology*. 7:R245–8.

Fire, A., S. Xu, M.K. Montgomery, S.A. Kostas, S.E. Driver, and C.C. Mello. 1998. Potent and specific genetic interference by double-stranded RNA in Caenorhabditis elegans. *Nature*. 391:806–811. doi:10.1038/35888.

Fu, Q., and P.J. Wang. 2014. Mammalian piRNAs. *Spermatogenesis*. 4:e27889. doi:10.4161/spmg.27889.

Gautier, L., L. Cope, B.M. Bolstad, and R.A. Irizarry. 2004. affy--analysis of Affymetrix GeneChip data at the probe level. *Bioinformatics*. 20:307–315. doi:10.1093/bioinformatics/btg405.

Gavet, O., and J. Pines. 2010. Progressive Activation of CyclinB1-Cdk1 Coordinates Entry to Mitosis. *Developmental Cell*. 18:533–543. doi:10.1016/j.devcel.2010.02.013.

GBD 2013 Mortality and Causes of Death Collaborators. 2015. Global, regional, and national age-sex specific all-cause and cause-specific mortality for 240 causes of death, 1990–2013: a systematic analysis for the Global Burden of Disease Study 2013. *Lancet*. 385(9963):117–171. doi: http://dx.doi.org/10.1016/S0140-6736(14)61682-2

Gentleman, R.C., V.J. Carey, D.M. Bates, B. Bolstad, M. Dettling, S. Dudoit, B. Ellis, L. Gautier, Y. Ge, J. Gentry, K. Hornik, T. Hothorn, W. Huber, S. Iacus, R. Irizarry, F. Leisch, C. Li, M. Maechler, A.J. Rossini, G. Sawitzki, C. Smith, G. Smyth, L. Tierney, J.Y.H. Yang, and J. Zhang. 2004. Bioconductor: open software development for computational biology and bioinformatics. *Genome Biology*. 5:R80. doi:10.1186/gb-2004-5-10-r80.

Ghildiyal, M., and P.D. Zamore. 2009. Small silencing RNAs: an expanding universe. *Nature Reviews. Genetics*. 10:94–108. doi:10.1038/nrg2504.

Girard, A., R. Sachidanandam, G.J. Hannon, and M.A. Carmell. 2006. A germline-specific class of small RNAs binds mammalian Piwi proteins. *Nature*. 442(7099):199–202. doi:10.1038/nature04917.

Gonzalez, J., H. Qi, N. Liu, and H. Lin. 2015. Piwi Is a Key Regulator of Both Somatic and Germline Stem Cells in the Drosophila Testis. *Cell Reports*. 12:150–161. doi:10.1016/j.celrep.2015.06.004.

Goodier, J.L., and H.H. Kazazian Jr. 2008. Retrotransposons Revisited: The Restraint and Rehabilitation of Parasites. *Cell*. 135:23–35. doi:10.1016/j.cell.2008.09.022.

Green, G.M., G.J. Jakab, and R.B. Low. 1977. Defense Mechanisms of the Respiratory Membrane. *American Review of Respiratory Disease*. 115(3): 479–514. doi:10.1164/arrd.1977.115.3.479.

Greenberger, M.J., R.M. Strieter, S.L. Kunkel, J.M. Danforth, L.L. Laichalk, D.C. McGillicuddy, and T.J. Standiford. 1996. Neutralization of macrophage inflammatory protein-2 attenuates neutrophil recruitment and bacterial clearance in murine Klebsiella pneumonia. *Journal of Infectious Diseases*. 173:159–165.

Greither, T., F. Koser, M. Kappler, M. Bache, C. Lautenschläger, S. Göbel, H.-J. Holzhausen, S. Wach, P. Würl, and H. Taubert. 2012. Expression of human Piwi-like genes is associated with prognosis for soft tissue sarcoma patients. *BMC Cancer*. 12:272. doi:10.1186/1471-2407-12-272.

Griffin, M.R., Y. Zhu, M.R. Moore, C.G. Whitney, and C.G. Grijalva. 2013. U.S. Hospitalizations for Pneumonia after a Decade of Pneumococcal Vaccination. *New England Journal of Medicine*. 369:155–163. doi:10.1056/NEJMoa1209165.

Guha, A., M. Vasconcelos, Y. Cai, M. Yoneda, A. Hinds, J. Qian, G. Li, L. Dickel, J.E. Johnson, S. Kimura, J. Guo, J. McMahon, A.P. McMahon, and W.V. Cardoso. 2012. Neuroepithelial body microenvironment is a niche for a distinct subset of Clara-like precursors in the developing airways. *Proceedings of the National Academy of Sciences*. 109:12592–12597. doi:10.1073/pnas.1204710109.

Herriges, M., and E.E. Morrisey. 2014. Lung development: orchestrating the generation and regeneration of a complex organ. *Development*. 141:502–513. doi:10.1242/dev.098186.

Hogan, B.L.M., C.E. Barkauskas, H.A. Chapman, J.A. Epstein, R. Jain, C.C.W. Hsia, L. Niklason, E. Calle, A. Le, S.H. Randell, J. Rock, M. Snitow, M. Krummel, B.R. Stripp, T. Vu, E.S. White, J.A. Whitsett, and E.E. Morrisey. 2014. Repair and Regeneration of the Respiratory System: Complexity, Plasticity, and Mechanisms of Lung Stem Cell Function. *Cell Stem Cell*. 15:123–138. doi:10.1016/j.stem.2014.07.012.

Holt, P.G., D.H. Strickland, M.E. Wikström, and F.L. Jahnsen. 2008. Regulation of immunological homeostasis in the respiratory tract. *Nature Reviews. Immunology*. 8:142–152. doi:10.1038/nri2236.

Horwich, M.D., C. Li, C. Matranga, V. Vagin, G. Farley, P. Wang, and P.D. Zamore. 2007. The Drosophila RNA methyltransferase, DmHen1, modifies germline piRNAs and single-stranded siRNAs in RISC. *Current Biology*. 17:1265–1272. doi:10.1016/j.cub.2007.06.030.

Howard, L.S.G.E., M. Sillis, M.C. Pasteur, A.V. Kamath, and B.D.W. Harrison. 2005. Microbiological profile of community-acquired pneumonia in adults over the last 20 years. *Journal of Infection*. 50:107–113. doi:10.1016/j.jinf.2004.05.003.

Hussell, T., and T.J. Bell. 2014. Alveolar macrophages: plasticity in a tissue-specific context. *Nature Reviews. Immunology*. 14:81–93. doi:10.1038/nri3600.

Hutvagner, G., and M.J. Simard. 2008. Argonaute proteins: key players in RNA silencing. *Nature Reviews. Molecular Cell Biology*. 9:22–32. doi:10.1038/nrm2321.

Hyatt, L.D., G.A. Wasserman, Y.J. Rah, K.Y. Matsuura, F.T. Coleman, K.L. Hilliard, Z.A. Pepper-Cunningham, M. Ieong, D.J. Stumpo, P.J. Blackshear, L.J. Quinton, J.P. Mizgerd, and M.R. Jones. 2014. Myeloid ZFP36L1 Does Not Regulate Inflammation or Host Defense in Mouse Models of Acute Bacterial Infection. *PLoS One*. 9:e109072. doi:10.1371/journal.pone.0109072.

Ipsaro, J.J., A.D. Haase, S.R. Knott, L. Joshua-Tor, and G.J. Hannon. 2012. The structural biochemistry of Zucchini implicates it as a nuclease in piRNA biogenesis. *Nature*. 491:279–283. doi:10.1038/nature11502.

Irizarry, R.A., B. Hobbs, F. Collin, Y.D. Beazer-Barclay, K.J. Antonellis, U. Scherf, and T.P. Speed. 2003. Exploration, normalization, and summaries of high density oligonucleotide array probe level data. *Biostatistics*. 4:249–264. doi:10.1093/biostatistics/4.2.249.

Iwasaki, Y.W., M.C. Siomi, and H. Siomi. 2014. PIWI-Interacting RNA: Its Biogenesis and Functions. *Annual Review of Biochemistry*. 84:150306093657004. doi:10.1146/annurev-biochem-060614-034258.

Jacobs, J.E., M. Wagner, J. Dhahbi, D. Boffelli, and D.I.K. Martin. 2013. Deficiency of MIWI2 (Piwil4) induces mouse erythroleukemia cell differentiation, but has no effect on hematopoiesis in vivo. *PLoS One*

8:e82573. doi:10.1371/journal.pone.0082573.

Jain, S., W.H. Self, R.G. Wunderink, S. Fakhran, R. Balk, A.M. Bramley, C. Reed, C.G. Grijalva, E.J. Anderson, D.M. Courtney, J.D. Chappell, C. Qi, E.M. Hart, F. Carroll, C. Trabue, H.K. Donnelly, D.J. Williams, Y. Zhu, S.R. Arnold, K. Ampofo, G.W. Waterer, M. Levine, S. Lindstrom, J.M. Winchell, J.M. Katz, D. Erdman, E. Schneider, L.A. Hicks, J.A. McCullers, A.T. Pavia, K.M. Edwards, and L. Finelli. 2015. Community-Acquired Pneumonia Requiring Hospitalization among U.S. Adults. *New England Journal of Medicine*. 373:415–427. doi:10.1056/NEJMoa1500245.

Jaskiewicz, L., B. Bilen, J. Hausser, and M. Zavolan. 2012. Argonaute CLIP- A method to identify in vivo targets of miRNAs. *Methods* 58(2):106–112. doi:10.1016/j.ymeth.2012.09.006.

Johnson, D.E., and M.K. Georgieff. 1989. Pulmonary Neuroendocrine Cells: Their Secretory Products and Their Potential Roles in Health and Chronic Lung Disease in Infancy. *American Review of Respiratory Disease*. 140:1807–1812. doi:10.1164/ajrccm/140.6.1807.

Jones, M.R., L.J. Quinton, B.T. Simms, M.M. Lupa, M.S. Kogan, and J.P. Mizgerd. 2006. Roles of interleukin-6 in activation of STAT proteins and recruitment of neutrophils during Escherichia coli pneumonia. *Journal of Infectious Diseases*. 193:360–369. doi:10.1086/499312.

Kadioglu, A., J.N. Weiser, J.C. Paton, and P.W. Andrew. 2008. The role of Streptococcus pneumoniae virulence factors in host respiratory colonization and disease. *Nature Reviews. Microbiology*. 6:288–301. doi:10.1038/nrmicro1871.

Kathuria, H. 2004. Transcription of the Caveolin-1 Gene Is Differentially Regulated in Lung Type I Epithelial and Endothelial Cell Lines: A role for ETS proteins in epithelial cell expression. *Journal of Biological Chemistry*. 279:30028–30036. doi:10.1074/jbc.M402236200.

Kay, G.F., S.C. Barton, M.A. Surani, and S. Rastan. 1994. Imprinting and X chromosome counting mechanisms determine Xist expression in early mouse development. *Cell*. 77:639–650.

Keam, S.P., P.E. Young, A.L. McCorkindale, T.H.Y. Dang, J.L. Clancy, D.T. Humphreys, T. Preiss, G. Hutvagner, D.I.K. Martin, J.E. Cropley, and C.M. Suter. 2014. The human Piwi protein Hiwi2 associates with tRNA-derived piRNAs in somatic cells. *Nucleic Acids Research*. 42:8984–8995. doi:10.1093/nar/gku620.

King, J.B., R.J. von Furstenberg, B.J. Smith, K.K. McNaughton, J.A. Galanko, and S.J. Henning. 2012. CD24 can be used to isolate Lgr5+ putative colonic epithelial stem cells in mice. *American Journal of Physiology. Gastrointestinal and Liver Physiology*. 303:G443–452. doi:10.1152/ajpgi.00087.2012.

Kobayashi, S., A. Isotani, N. Mise, M. Yamamoto, Y. Fujihara, K. Kaseda, T. Nakanishi, M. Ikawa, H. Hamada, K. Abe, and M. Okabe. 2006. Comparison of Gene Expression in Male and Female Mouse Blastocysts Revealed Imprinting of the X-Linked Gene, Rhox5/Pem, at Preimplantation Stages. *Current Biology*. 16:166–172. doi:10.1016/j.cub.2005.11.071.

Kuramochi-Miyagawa, S. 2004. Mili, a mammalian member of piwi family gene, is essential for spermatogenesis. *Development*. 131:839–849. doi:10.1242/dev.00973.

Lafkas, D., A. Shelton, C. Chiu, G. de Leon Boenig, Y. Chen, S.S. Stawicki, C. Siltanen, M. Reichelt, M. Zhou, X. Wu, J. Eastham-Anderson, H. Moore, M. Roose-Girma, Y. Chinn, J.Q. Hang, S. Warming, J. Egen, W.P. Lee, C. Austin, Y. Wu, J. Payandeh, J.B. Lowe, and C.W. Siebel. 2015. Therapeutic antibodies reveal Notch control of transdifferentiation in the adult lung. *Nature*. 528(7580):127–131. doi:10.1038/nature15715.

Lander, E.S., L.M. Linton, B. Birren, C. Nusbaum, M.C. Zody, J. Baldwin, K. Devon, K. Dewar, M. Doyle, W. FitzHugh, R. Funke, D. Gage, K. Harris, A. Heaford, J. Howland, L. Kann, J. Lehoczky, R. LeVine, P. McEwan, K. McKernan, J. Meldrim, J.P. Mesirov, C. Miranda, W. Morris, J. Naylor, C. Raymond, M. Rosetti, R. Santos, A. Sheridan, C. Sougnez, Y. Stange-Thomann, N. Stojanovic, A. Subramanian, D. Wyman, J. Rogers, J. Sulston, R. Ainscough, S. Beck, D. Bentley, J. Burton, C. Clee, N. Carter, A. Coulson, R. Deadman, P. Deloukas, A. Dunham, I. Dunham, R. Durbin, L. French, D. Grafham, S. Gregory, T. Hubbard, S. Humphray, A. Hunt, M. Jones, C. Lloyd, A. McMurray, L. Matthews, S. Mercer, S. Milne, J.C. Mullikin, A. Mungall, R. Plumb, M. Ross, R. Shownkeen, S. Sims, R.H. Waterston, R.K. Wilson, L.W. Hillier, J.D. McPherson, M.A. Marra, E.R. Mardis, L.A. Fulton, A.T. Chinwalla, K.H. Pepin, W.R. Gish, S.L. Chissoe, M.C. Wendl, K.D. Delehaunty, T.L. Miner, A. Delehaunty, J.B. Kramer, L.L. Cook, R.S. Fulton, D.L. Johnson, P.J. Minx, S.W. Clifton, T. Hawkins, E. Branscomb, P. Predki, P. Richardson, S. Wenning, T. Slezak, N. Doggett, J.F. Cheng, A. Olsen, S. Lucas, C. Elkin, et al. 2001. Initial sequencing and analysis of the human genome. *Nature*. 409:860–921. doi:10.1038/35057062.

Lee, T.A., F.M. Weaver, and K.B. Weiss. 2007. Impact of pneumococcal vaccination on pneumonia rates in patients with COPD and asthma. *Journal of General Internal Medicine*. 22:62–67. doi:10.1007/s11606-007-0118-3.

Leopold, P.L., M.J. O'Mahony, X.J. Lian, A.E. Tilley, B.-G. Harvey, and R.G. Crystal. 2009. Smoking Is Associated with Shortened Airway Cilia. *PLoS One*. 4:e8157. doi:10.1371/journal.pone.0008157.

Levin, H.L., and J.V. Moran. 2011. Dynamic interactions between transposable elements and their hosts. *Nature Reviews. Genetics*. 12:615–627. doi:10.1038/nrg3030.

Levitzky, M.G. 2013. Nonrespiratory Functions of the Lung. *In* Pulmonary Physiology 8/E. M.G. Levitzky, editor. McGraw Hill Professional, New York.

Li, X.Z., C.K. Roy, X. Dong, E. Bolcun-Filas, J. Wang, B.W. Han, J. Xu, M.J. Moore, J.C. Schimenti, Z. Weng, and P.D. Zamore. 2013. An Ancient Transcription Factor Initiates the Burst of piRNA Production during Early Meiosis in Mouse Testes. *Molecular Cell*. 50:67–81. doi:10.1016/j.molcel.2013.02.016.

Livak, K.J., and T.D. Schmittgen. 2001. Analysis of Relative Gene Expression Data Using Real-Time Quantitative PCR and the 2−ΔΔCT Method. *Methods*. 25:402–408. doi:10.1006/meth.2001.1262.

Ma, X., S. Wang, T. Do, X. Song, M. Inaba, Y. Nishimoto, L.-P. Liu, Y. Gao, Y. Mao, H. Li, W. McDowell, J. Park, K. Malanowski, A. Peak, A. Perera, H. Li, K. Gaudenz, J. Haug, Y. Yamashita, H. Lin, J.-Q. Ni, and T. Xie. 2014. Piwi Is Required in Multiple Cell Types to Control Germline Stem Cell Lineage Development in the Drosophila Ovary. *PLoS One*. 9:e90267. doi:10.1371/journal.pone.0090267.

MacCallum, N.S., and T.W. Evans. 2005. Epidemiology of acute lung injury. *Current Opinion in Critical Care*. 11:43–49.

Mandell, L.A., R.G. Wunderink, A. Anzueto, J.G. Bartlett, G.D. Campbell, N.C. Dean, S.F. Dowell, T.M. File, D.M. Musher, M.S. Niederman, A. Torres, C.G. Whitney, Infectious Diseases Society of America, American Thoracic Society. 2007. Infectious Diseases Society of America/American Thoracic Society consensus guidelines on the management of community-acquired pneumonia in adults. *Clinical Infectious Diseases*. 44(Suppl. 2):S27–72.

Matthay, M.A., and G.A. Zimmerman. 2005. Acute lung injury and the acute respiratory distress syndrome: four decades of inquiry into pathogenesis and rational management. *American Journal of Respiratory Cell and Molecular Biology*. 33:319–327. doi:10.1165/rcmb.F305.

Matthay, M.A., L.B. Ware, and G.A. Zimmerman. 2012. The acute respiratory distress syndrome. *Journal of Clinical Investigation*. 122:2731–2740.

doi:10.1172/JCI60331.

McClintock, B. 1956. Controlling Elements and the Gene. *Cold Spring Harbor Symposia on Quantitative Biology.* 21:197–216. doi:10.1101/SQB.1956.021.01.017.

McCullers, J.A. 2006. Insights into the interaction between influenza virus and pneumococcus. *Clinical Microbiology Reviews*. 19:571–582. doi:10.1128/CMR.00058-05.

Metlay, J.P., R. Schulz, Y.-H. Li, D.E. Singer, T.J. Marrie, C.M. Coley, L.J. Hough, D.S. Obrosky, W.N. Kapoor, and M.J. Fine. 1997. Influence of Age on Symptoms at Presentation in Patients With Community-Acquired Pneumonia. *Archives of Internal Medicine*. 157:1453–1459. doi:10.1001/archinte.1997.00440340089009.

Mikkelsen, M.E., J.D. Christie, P.N. Lanken, R.C. Biester, B.T. Thompson, S.L. Bellamy, A.R. Localio, E. Demissie, R.O. Hopkins, and D.C. Angus. 2012. The adult respiratory distress syndrome cognitive outcomes study: long-term neuropsychological function in survivors of acute lung injury. *American Journal of Respiratory and Critical Care Medicine*. 185:1307–1315. doi:10.1164/rccm.201111-2025OC.

Mizgerd, J.P. 2006. Lung Infection—A Public Health Priority. *PLoS Medicine*. 3:e76. doi:10.1371/journal.pmed.0030076.

Mizgerd, J.P. 2008. Acute lower respiratory tract infection. *New England Journal of Medicine*. 358:716–727. doi:10.1056/NEJMra074111.

Mizgerd, J.P. 2012. Respiratory infection and the impact of pulmonary immunity on lung health and disease. *American Journal of Respiratory and Critical Care Medicine*. 186:824–829. doi:10.1164/rccm.201206-1063PP.

Mouse Genome Sequencing Consortium, R.H. Waterston, K. Lindblad-Toh, E. Birney, J. Rogers, J.F. Abril, P. Agarwal, R. Agarwala, R. Ainscough, M. Alexandersson, P. An, S.E. Antonarakis, J. Attwood, R. Baertsch, J. Bailey, K. Barlow, S. Beck, E. Berry, B. Birren, T. Bloom, P. Bork, M. Botcherby, N. Bray, M.R. Brent, D.G. Brown, S.D. Brown, C. Bult, J. Burton, J. Butler, R.D. Campbell, P. Carninci, S. Cawley, F. Chiaromonte, A.T. Chinwalla, D.M. Church, M. Clamp, C. Clee, F.S. Collins, L.L. Cook, R.R. Copley, A. Coulson, O. Couronne, J. Cuff, V. Curwen, T. Cutts, M. Daly, R. David, J. Davies, K.D. Delehaunty, J. Deri, E.T. Dermitzakis, C. Dewey, N.J. Dickens, M. Diekhans, S. Dodge, I. Dubchak, D.M. Dunn, S.R. Eddy, L. Elnitski, R.D. Emes, P. Eswara, E. Eyras, A. Felsenfeld, G.A. Fewell, P. Flicek, K. Foley, W.N. Frankel, L.A. Fulton, R.S. Fulton, T.S. Furey, D. Gage, R.A. Gibbs, G.

Glusman, S. Gnerre, N. Goldman, L. Goodstadt, D. Grafham, T.A. Graves, E.D. Green, S. Gregory, R. Guigó, M. Guyer, R.C. Hardison, D. Haussler, Y. Hayashizaki, L.W. Hillier, A. Hinrichs, W. Hlavina, T. Holzer, F. Hsu, A. Hua, T. Hubbard, A. Hunt, I. Jackson, D.B. Jaffe, L.S. Johnson, M. Jones, T.A. Jones, et al. 2002. Initial sequencing and comparative analysis of the mouse genome. *Nature*. 420:520–562. doi:10.1038/nature01262.

Musher, D.M., and A.R. Thorner. 2014. Community-Acquired Pneumonia. *New England Journal of Medicine*. 371:1619–1628. doi:10.1056/NEJMra1312885.

Nakanishi, K., D.E. Weinberg, D.P. Bartel, and D.J. Patel. 2012. Structure of yeast Argonaute with guide RNA. *Nature*. 486:368–374. doi:10.1038/nature11211.

Naumov, I., A. Zilberberg, S. Shapira, D. Avivi, D. Kazanov, R. Rosin-Arbesfeld, N. Arber, and S. Kraus. 2014. CD24 knockout prevents colorectal cancer in chemically induced colon carcinogenesis and in APC(Min)/CD24 double knockout transgenic mice. *International Journal of Cancer*. 135:1048–1059. doi:10.1002/ijc.28762.

NCBI Resource Coordinators. 2016. Database resources of the National Center for Biotechnology Information. *Nucleic Acids Research*. 44(D1):D7–19. doi: 10.1093/nar/gkv1290

Nogee, L.M., D.E. deMello, and L.P. Dehner. 1993. Deficiency of pulmonary surfactant protein B in congenital alveolar proteinosis. *New England Journal of Medicine*. 328:406–410. doi:10.1056/NEJM199302113280606.

Nolde, M.J., E. Cheng, S. Guo, and H. Lin. 2013. Piwi Genes Are Dispensable for Normal Hematopoiesis in Mice. *PLoS One.* 8(8):e71950 doi:10.1371/journal.pone.0071950.g001.

Ohara, T., Y. Sakaguchi, T. Suzuki, H. Ueda, K. Miyauchi, and T. Suzuki. 2007. The 3“ termini of mouse Piwi-interacting RNAs are 2-”O-methylated. *Nature Structural & Molecular Biology*. 14:349–350. doi:10.1038/nsmb1220.

Orme, J., J.S. Romney, R.O. Hopkins, D. Pope, K.J. Chan, G. Thomsen, R.O. Crapo, and L.K. Weaver. 2003. Pulmonary function and health-related quality of life in survivors of acute respiratory distress syndrome. *American Journal of Respiratory and Critical Care Medicine*. 167:690–694. doi:10.1164/rccm.200206-542OC.

Overdevest, J.B., K.H. Knubel, J.E. Duex, S. Thomas, M.D. Nitz, M.A. Harding, S.C. Smith, H.F. Frierson, M. Conaway, and D. Theodorescu. 2012. CD24 expression is important in male urothelial tumorigenesis and metastasis in

mice and is androgen regulated. *Proceedings of the National Academy of Sciences*. 109:E3588–96. doi:10.1073/pnas.1113960109.

Pardo-Saganta, A., B.M. Law, M. Gonzalez-Celeiro, V. Vinarsky, and J. Rajagopal. 2013. Ciliated Cells of Pseudostratified Airway Epithelium Do Not Become Mucous Cells after Ovalbumin Challenge. *American Journal of Respiratory Cell and Molecular Biology*. 48:364–373. doi:10.1165/rcmb.2012-0146OC.

Pardo-Saganta, A., P.R. Tata, B.M. Law, B. Saez, R.D.-W. Chow, M. Prabhu, T. Gridley, and J. Rajagopal. 2015. Parent stem cells can serve as niches for their daughter cells. *Nature*. 523:597–601. doi:10.1038/nature14553.

Parker, D., and A. Prince. 2011. Innate Immunity in the Respiratory Epithelium. *American Journal of Respiratory Cell and Molecular Biology*. 45:189–201. doi:10.1165/rcmb.2011-0011RT.

Pavlidis, P., and W.S. Noble. 2003. Matrix2png: a utility for visualizing matrix data. *Bioinformatics*. 19:295–296.

Peleg, A.Y., and D.C. Hooper. 2010. Hospital-Acquired Infections Due to Gram-Negative Bacteria. *New England Journal of Medicine*. 362:1804–1813.

Pinkerton, K.E., and C.G. Plopper. 2004. The Lung. Academic Press. 1 pp.

Pittet, L.A., L.J. Quinton, K. Yamamoto, B.E. Robson, J.D. Ferrari, H. Algul, R.M. Schmid, and J.P. Mizgerd. 2011. Earliest Innate Immune Responses Require Macrophage RelA during Pneumococcal Pneumonia. *American Journal of Respiratory Cell and Molecular Biology*. 45:573–581. doi:10.1165/rcmb.2010-0210OC.

Plopper, C.G., and M.V. Fanucchi. 2004. Development of Airway Epithelium. *In* The Lung. Academic Press. 1–20.

Prina, E., O.T. Ranzani, and A. Torres. 2015. Community-acquired pneumonia. *Lancet*. 386(9998):1097–1108.

Prince, A. (ed.) 2013. Mucosal Immunology of Acute Bacterial Pneumonia. New York: Springer Science+Business Media.

Quinton, L.J., M.R. Jones, B.T. Simms, M.S. Kogan, B.E. Robson, S.J. Skerrett, and J.P. Mizgerd. 2007. Functions and regulation of NF-kappaB RelA during pneumococcal pneumonia. *Journal of immunology*. 178:1896–1903.

Rackley, C.R., and B.R. Stripp. 2012. Building and maintaining the epithelium of the lung. *Journal of Clinical Investigation*. 122:2724–2730. doi:10.1172/JCI60519.

Rawlins, E.L., and B.L.M. Hogan. 2008. Ciliated epithelial cell lifespan in the mouse trachea and lung. *American Journal of Physiology. Lung Cellular and Molecular Physiology*. 295:L231–L234. doi:10.1152/ajplung.90209.2008.

Rawlins, E.L., L.E. Ostrowski, S.H. Randell, and B.L.M. Hogan. 2007. Lung development and repair: contribution of the ciliated lineage. *Proceedings of the National Academy of Sciences*. 104:410–417. doi:10.1073/pnas.0610770104.

Ricciardolo, F.L.M., A. Di Stefano, F. Sabatini, and G. Folkerts. 2006. Reactive nitrogen species in the respiratory tract. *European Journal of Pharmacology*. 533:240–252. doi:10.1016/j.ejphar.2005.12.057.

Rock, J.R., and B.L.M. Hogan. 2011a. Epithelial Progenitor Cells in Lung Development, Maintenance, Repair, and Disease. *Annual Review of Cell and Developmental Biology*. 27:493–512. doi:10.1146/annurev-cellbio-100109-104040.

Rock, J.R., and B.L.M. Hogan. 2011b. Epithelial Progenitor Cells in Lung Development, Maintenance, Repair, and Disease. *Annual Review of Cell and Developmental Biology*. 27:493–512. doi:10.1146/annurev-cellbio-100109-104040.

Rock, J.R., X. Gao, Y. Xue, S.H. Randell, Y.-Y. Kong, and B.L.M. Hogan. 2011. Notch-dependent differentiation of adult airway basal stem cells. *Cell Stem Cell*. 8:639–648. doi:10.1016/j.stem.2011.04.003.

Ross, R.J., M.M. Weiner, and H. Lin. 2014. PIWI proteins and PIWI-interacting RNAs in the soma. *Nature*. 505:353–359. doi:10.1038/nature12987.

Roy, M.G., A. Livraghi-Butrico, A.A. Fletcher, M.M. McElwee, S.E. Evans, R.M. Boerner, S.N. Alexander, L.K. Bellinghausen, A.S. Song, Y.M. Petrova, M.J. Tuvim, R. Adachi, I. Romo, A.S. Bordt, M.G. Bowden, J.H. Sisson, P.G. Woodruff, D.J. Thornton, K. Rousseau, M.M. De la Garza, S.J. Moghaddam, H. Karmouty-Quintana, M.R. Blackburn, S.M. Drouin, C.W. Davis, K.A. Terrell, B.R. Grubb, W.K. O'Neal, S.C. Flores, A. Cota-Gomez, C.A. Lozupone, J.M. Donnelly, A.M. Watson, C.E. Hennessy, R.C. Keith, I.V. Yang, L. Barthel, P.M. Henson, W.J. Janssen, D.A. Schwartz, R.C. Boucher, B.F. Dickey, and C.M. Evans. 2013. Muc5b is required for airway defence. *Nature*. 505:412–416. doi:10.1038/nature12807.

Saito, K., K.M. Nishida, T. Mori, and Y. Kawamura. 2006. Specific association of Piwi with rasiRNAs derived from retrotransposon and heterochromatic regions in the Drosophila genome. *Genes & Development.* 20(16): 2214–2222doi:10.1101/gad.1454806.

Sasaki, T., A. Shiohama, S. Minoshima, and N. Shimizu. 2003. Identification of eight members of the Argonaute family in the human genome small star, filled. *Genomics*. 82:323–330. doi:10.1016/S0888-7543(03)00129-0.

Saxe, J.P., M. Chen, H. Zhao, and H. Lin. 2013. Tdrkh is essential for spermatogenesis and participates in primary piRNA biogenesis in the germline. *EMBO Journal*. 32:1869–1885. doi:10.1038/emboj.2013.121.

Schirle, N.T., and I.J. MacRae. 2012. The Crystal Structure of Human Argonaute2. *Science*. 336:1037–1040. doi:10.1126/science.1221551.

Schuchat, A., C.V. Broome, A. Hightower, S.J. Costa, and W. Parkin. 1991. Use of surveillance for invasive pneumococcal disease to estimate the size of the immunosuppressed HIV-infected population. *JAMA: The Journal of the American Medical Association*. 265:3275–3279.

Sedivy, J.M., J.A. Kreiling, N. Neretti, M.D. Cecco, S.W. Criscione, J.W. Hofmann, X. Zhao, T. Ito, and A.L. Peterson. 2013. Death by transposition - the enemy within? *BioEssays*. 35(12):1035–1043. doi:10.1002/bies.201300097.

Sharma, A.K., M.C. Nelson, J.E. Brandt, and M. Wessman. 2001. Human CD34+ stem cells express the hiwigene, a human homologue of the Drosophila genepiwi. *Blood*. 97(2):426–434.

Siomi, M.C., K. Sato, D. Pezic, and A.A. Aravin. 2011. PIWI-interacting small RNAs: the vanguard of genome defence. *Nature Reviews Molecular Cell Biology*. 12:246–258. doi:10.1038/nrm3089.

Slotkin, R.K., and R. Martienssen. 2007. Transposable elements and the epigenetic regulation of the genome. *Nature Reviews Genetics*. 8:272–285. doi:10.1038/nrg2072.

Su, C., Z.-J. Ren, F. Wang, M. Liu, X. Li, and H. Tang. 2012. PIWIL4 regulates cervical cancer cell line growth and is involved in down-regulating the expression of p14ARF and p53. *FEBS Letters*. 586:1356–1362. doi:10.1016/j.febslet.2012.03.053.

Sugimoto, K., H. Kage, N. Aki, A. Sano, H. Kitagawa, T. Nagase, Y. Yatomi, N. Ohishi, and D. Takai. 2007. The induction of H3K9 methylation by PIWIL4 at

the p16Ink4a locus. *Biochemical and Biophysical Research Communications*. 359:497–502. doi:10.1016/j.bbrc.2007.05.136.

Suzuki, R., S. Honda, and Y. Kirino. 2012. PIWI Expression and Function in Cancer. *Frontiers in Genetics*. 3:1–8. doi:10.3389/fgene.2012.00204.

Swarts, D.C., K. Makarova, Y. Wang, K. Nakanishi, R.F. Ketting, E.V. Koonin, D.J. Patel, and J. van der Oost. 2014. The evolutionary journey of Argonaute proteins. *Nature Structural & Molecular Biology*. 21:743–753. doi:10.1038/nsmb.2879.

Tan, Y., L. Liu, M. Liao, C. Zhang, S. Hu, M. Zou, M. Gu, and X. Li. 2015. Emerging roles for PIWI proteins in cancer. *Acta Biochimica et Biophysica Sinica*. 47:315–324. doi:10.1093/abbs/gmv018.

Tellier, R. 2006. Review of aerosol transmission of influenza A virus. *Emerging Infectious Diseases*. 12:1657–1662. doi:10.3201/eid1211.060426.

Thaxton, J.E., B. Liu, P. Zheng, Y. Liu, and Z. Li. 2014. Deletion of CD24 impairs development of heat shock protein gp96-driven autoimmune disease through expansion of myeloid-derived suppressor cells. *Journal of Immunology*. 192:5679–5686. doi:10.4049/jimmunol.1302755.

Thomson, T., and H. Lin. 2009. The Biogenesis and Function of PIWI Proteins and piRNAs: Progress and Prospect. *Annual Review of Cell and Developmental Biology*. 25:355–376. doi:10.1146/annurev.cellbio.24.110707.175327.

Tilley, A.E., M.S. Walters, R. Shaykhiev, and R.G. Crystal. 2015. Cilia Dysfunction in Lung Disease. *Annual Review of Physiology*. 77:379–406. doi:10.1146/annurev-physiol-021014-071931.

Treutlein, B., D.G. Brownfield, A.R. Wu, N.F. Neff, G.L. Mantalas, F.H. Espinoza, T.J. Desai, M.A. Krasnow, and S.R. Quake. 2014. Reconstructing lineage hierarchies of the distal lung epithelium using single-cell RNA-seq. *Nature*. 509:371–375. doi:10.1038/nature13173.

Vagin, V.V., A. Sigova, C. Li, H. Seitz, V. Gvozdev, and P.D. Zamore. 2006. A distinct small RNA pathway silences selfish genetic elements in the germline. *Science*. 313:320–324. doi:10.1126/science.1129333.

Wang, C.Y., C.S. Calfee, D.W. Paul, D.R. Janz, A.K. May, H. Zhuo, G.R. Bernard, M.A. Matthay, L.B. Ware, and K.N. Kangelaris. 2014. One-year mortality and predictors of death among hospital survivors of acute respiratory distress syndrome. *Intensive Care Medicine*. 40:388–396.

doi:10.1007/s00134-013-3186-3.

Wang, Y., Y. Liu, X. Shen, X. Zhang, X. Chen, C. Yang, and H. Gao. 2012. The PIWI protein acts as a predictive marker for human gastric cancer. *International Journal of Clinical and Experimental Pathology*. 5:315–325.

Wansleeben, C., C.E. Barkauskas, J.R. Rock, and B.L.M. Hogan. 2012. Stem cells of the adult lung: their development and role in homeostasis, regeneration, and disease. *Wiley Interdisciplinary Reviews. Developmental Biology*. 2:131–148. doi:10.1002/wdev.58.

Wara, D.W. 1981. Host defense against Streptococcus pneumoniae: the role of the spleen. *Reviews of Infectious Diseases.* 3:299–309.

Ware, L.B., and M.A. Matthay. 2000. The acute respiratory distress syndrome. *New England Journal of Medicine*. 342:1334–1349.

Watanabe, T., S. Chuma, Y. Yamamoto, S. Kuramochi-Miyagawa, Y. Totoki, A. Toyoda, Y. Hoki, A. Fujiyama, T. Shibata, T. Sado, T. Noce, T. Nakano, N. Nakatsuji, H. Lin, and H. Sasaki. 2011. MITOPLD is a mitochondrial protein essential for nuage formation and piRNA biogenesis in the mouse germline. *Developmental Cell*. 20:364–375. doi:10.1016/j.devcel.2011.01.005.

Welte, T., A. Torres, and D. Nathwani. 2012. Clinical and economic burden of community-acquired pneumonia among adults in Europe. *Thorax*. 67:71–79. doi:10.1136/thx.2009.129502.

Whitsett, J.A., and T. Alenghat. 2014. Respiratory epithelial cells orchestrate pulmonary innate immunity. *Nature Immunology*. 16:27–35. doi:10.1038/ni.3045.

Wicker, T., F. Sabot, A. Hua-Van, J.L. Bennetzen, P. Capy, B. Chalhoub, A. Flavell, P. Leroy, M. Morgante, O. Panaud, E. Paux, P. SanMiguel, and A.H. Schulman. 2007. A unified classification system for eukaryotic transposable elements. *Nature Reviews Genetics*. 8:973–982. doi:10.1038/nrg2165.

Xing, J., D.J. Witherspoon, D.A. Ray, M.A. Batzer, and L.B. Jorde. 2007. Mobile DNA elements in primate and human evolution. *American Journal of Physical Anthropology.* 134:2–19. doi:10.1002/ajpa.20722.

Xu, F., D. Droemann, J. Rupp, H. Shen, X. Wu, T. Goldmann, S. Hippenstiel, P. Zabel, and K. Dalhoff. 2008. Modulation of the Inflammatory Response to Streptococcus pneumoniaein a Model of Acute Lung Tissue Infection. *American Journal of Respiratory Cell and Molecular Biology*. 39:522–529. doi:10.1165/rcmb.2007-0328OC.

Yamamoto, K., A.-N.N. Ahyi, Z.A. Pepper-Cunningham, J.D. Ferrari, A.A. Wilson, M.R. Jones, L.J. Quinton, and J.P. Mizgerd. 2013. Roles of Lung Epithelium in Neutrophil Recruitment During Pneumococcal Pneumonia. *American Journal of Respiratory Cell and Molecular Biology*. 130906140418002. doi:10.1165/rcmb.2013-0114OC.

Yamamoto, K., J.D. Ferrari, Y. Cao, M.I. Ramirez, M.R. Jones, L.J. Quinton, and J.P. Mizgerd. 2012. Type I alveolar epithelial cells mount innate immune responses during pneumococcal pneumonia. *Journal of Immunology*. 189:2450–2459. doi:10.4049/jimmunol.1200634.

Yan, Z., H.Y. Hu, X. Jiang, V. Maierhofer, E. Neb, L. He, Y. Hu, H. Hu, N. Li, W. Chen, and P. Khaitovich. 2011. Widespread expression of piRNA-like molecules in somatic tissues. *Nucleic Acids Research*. 39:6596–6607. doi:10.1093/nar/gkr298.

You, Y., T. Huang, E.J. Richer, J.-E.H. Schmidt, J. Zabner, Z. Borok, and S.L. Brody. 2004. Role of f-box factor foxj1 in differentiation of ciliated airway epithelial cells. *American Journal of Physiology. Lung Cellular and Molecular Physiology*. 286:L650–L657. doi:10.1152/ajplung.00170.2003.

Young, G.R., B. Mavrommatis, and G. Kassiotis. 2014. Microarray analysis reveals global modulation of endogenous retroelement transcription by microbes. *Retrovirology*. 11:59. doi:10.1186/1742-4690-11-59.

Young, G.R., U. Eksmond, R. Salcedo, L. Alexopoulou, J.P. Stoye, and G. Kassiotis. 2012. Resurrection of endogenous retroviruses in antibody-deficient mice. *Nature*. 491(7426):774–778. doi:10.1038/nature11599.

Zeng, M., Z. Hu, X. Shi, X. Li, X. Zhan, X.-D. Li, J. Wang, J.H. Choi, K.-W. Wang, T. Purrington, M. Tang, M. Fina, R.J. DeBerardinis, E.M.Y. Moresco, G. Pedersen, G.M. McInerney, G.B. Karlsson Hedestam, Z.J. Chen, and B. Beutler. 2014. MAVS, cGAS, and endogenous retroviruses in T-independent B cell responses. *Science*. 346:1486–1492. doi:10.1126/science.346.6216.1486.

Zhang, X., J.-Q. Liu, Y. Shi, H.H. Reid, R.L. Boyd, M. Khattabi, H.Y. El-Omrani, P. Zheng, Y. Liu, and X.-F. Bai. 2012. CD24 on thymic APCs regulates negative selection of myelin antigen-specific T lymphocytes. *European Journal of Immunology*. 42:924–935. doi:10.1002/eji.201142024.

CURRICULUM VITAE

GREGORY ALEXANDER WASSERMAN
Born: 1987
255 Massachusetts Avenue
Apartment #219
Boston, MA 02115
gaw@bu.edu

EDUCATION

2005-2009 UNIVERSITY OF VERMONT, Burlington, VT
Bachelor of Science, Microbiology and Molecular Genetics

2009-2011 LONG ISLAND UNIVERSITY, CW POST CAMPUS, Brookville, NY
Master of Science, Medical Microbiology
Advisor: Bo Shopsin, M.D., Ph.D., & Richard P. Novick, M.D., NYU School of Medicine, Department of Medicine, Division of Infectious Diseases.
Thesis: "Studies on selective loss of *agr* function in *Staphylococcus aureus*"

2011-Present BOSTON UNIVERSITY SCHOOL OF MEDICINE, Boston, MA
Doctor of Philosophy, Microbiology
Advisor: Matthew R. Jones, Ph.D., Assistant Professor, Department of Medicine & The Pulmonary Center

RESEARCH EXPERIENCE

2005 NYU SCHOOL OF MEDICINE, New York, NY
Summer Research Student
Topic: **"**Nitric oxygen species and *Campylobacter jejuni infection"*
Advisor: Nicole Iovine, MD, Ph.D.

2007 NYU SCHOOL OF MEDICINE, New York, NY
Summer Research Student
Topic: **"**Autophagy during *Campylobacter jejuni* infection"
Advisor: Nicole Iovine, MD, Ph.D.

2009-2011 NYU SCHOOL OF MEDICINE, New York, NY
Masters Degree Student
Topic: "Gene regulation in *Staphylococcus aureus"*
Advisor: Bo Shopsin, MD, Ph.D. & Richard Novick, M.D.

2011-Pres BOSTON UNIVERSITY SCHOOL OF MEDICINE, Boston, MA
Doctoral Dissertation Research
Topic: "small RNA regulation of innate immunity during bacterial pneumonia"
Advisor: Matthew R. Jones, Ph.D.

PUBLICATIONS

1. Iovine NM, Pursnani S, Voldman A, **Wasserman GA**, Blaser MJ, Weinrauch Y. Reactive nitrogen species contribute to innate host defense against Campylobacter jejuni. Infect. Immun. 2008 Mar;76(3):986–93. PMCID: PMC2258852

2. Shopsin B, Eaton C, **Wasserman GA**, Mathema B, Adhikari RP, Agolory S, Altman DR, Holzman RS, Kreiswirth BN, Novick RP. Mutations in agr do not persist in natural populations of methicillin-resistant Staphylococcus aureus. J. Infect. Dis. 2010 Nov 15;202(10):1593–9.

3. Benson MA, Lilo S, **Wasserman GA**, Thoendel M, Smith A, Horswill AR, Fraser J, Novick RP, Shopsin B, Torres VJ. Staphylococcus aureus regulates the expression and production of the staphylococcal superantigen-like secreted proteins in a Rot-dependent manner. Mol Microbiol. 2011 Aug;81(3):659–75. PMCID: PMC3217042

4. Chen L, Shopsin B, Zhao Y, Smyth D, **Wasserman GA**, Fang C, Liu L, Kreiswirth BN. A real-time nucleic acid sequence-based amplification (NASBA) assay for rapid detection and quantification of agr functionality in clinical Staphylococcus aureus isolates. J Clin Microbiol. 2012 Jan 4. PMCID: PMC3295125

5. Smyth DS, Kafer JM, **Wasserman GA**, Velickovic L, Mathema B, Holzman RS, Knipe TA, Becker K, Eiff von C, Peters G, Chen L, Kreiswirth BN, Novick RP, Shopsin B. Nasal Carriage as a Source of agr-defective Staphylococcus aureus Bacteremia. J. Infect. Dis. 2012 Aug 2. PMCID: PMC3448967

6. Natarajan M, Schiralli Lester GM, Lee C, Missra A, **Wasserman GA**, Steffen M, Gilmour DS, Henderson AJ. NELF coordinates RNA polymerase II pausing, premature termination and chromatin remodeling to regulate HIV transcription. Journal of Biological Chemistry. 2013 Jul 24. PMCID: PMC3764804

7. Rose HR, Holzman RS, Altman DR, Smyth DS, **Wasserman GA**, Kafer JM, Wible M, Mendes RE, Torres VJ, Shopsin B. Cytotoxic virulence predicts mortality in nosocomial pneumonia due to methicillin-resistant Staphylococcus aureus. J. Infect. Dis. 2014 Oct 7.

8. Hyatt LD, **Wasserman GA**, Rah YJ, Matsuura KY, Coleman FT, Hilliard KL, Pepper-Cunningham ZA, Ieong M, Stumpo DJ, Blackshear PJ, Quinton LJ, Mizgerd JP, Jones MR. Myeloid ZFP36L1 Does Not Regulate Inflammation or Host Defense in Mouse Models of Acute Bacterial Infection. PLoS ONE. 2014;9(10):e109072. PMCID: PMC4192124

9. Hilliard KL, Allen E, Traber KE, Yamamoto K, Stauffer NM, **Wasserman GA**, Jones MR, Mizgerd JP, Quinton LJ. The Lung-Liver Axis Facilitates Pulmonary Innate Immunity and Hepatoprotection during Pneumonia. American Journal of Respiratory Cell and Molecular Biology. 2015 Jan 21.

10. Traber KE, Hilliard KL, Allen E, **Wasserman GA**, Yamamoto K, Jones MR, Mizgerd JP, Quinton LJ. Oncostatin M Induces STAT3-dependent CXCL5 Expression and Neutrophil Recruitment During Pneumonia. American Journal of Respiratory Cell and Molecular Biology. 2015 Feb 18.

11. Hilliard KL, Allen E, Traber KE, Kim Y, **Wasserman GA**, Jones MR, Mizgerd JP, Quinton LJ. Activation of Hepatic STAT3 Maintains Pulmonary Defense during Endotoxemia. Infect. Immun. 2015 Jul 27.

12. Wilde AD, Snyder DJ, Putnam NE, Valentino MD, Hammer ND, Lonergan ZR, Hinger SA, Aysanoa EE, Blanchard C, Dunman PM, **Wasserman GA**, Chen J, Shopsin B, Gilmore MS, Skaar EP, Cassat JE. Bacterial Hypoxic Responses Revealed as Critical Determinants of the Host-Pathogen Outcome by TnSeq Analysis of Staphylococcus aureus Invasive Infection. PLoS Pathog. 2015 Dec;11(12):e1005341. PMCID: PMC4684308

<u>In submission or revision</u>

Christine M. Willinger*, Jian Rong*, Kahraman Tanriverdi*, Paul Courchesne, Tianxiao Huan, **Gregory A. Wasserman**, Honghuang Lin, Josée Dupuis, Roby Joehanes, Matthew R. Jones, Emelia Benjamin, George O'Connor, Joseph P. Mizgerd, Jane Freedman, Martin Larson, and Daniel Levy. A Whole Blood-Derived MicroRNA Signature of Cigarette Smoking. In revision, Circulation.

Hirofumi Kamata, Kazuko Yamamoto, **Gregory A. Wasserman**, Mary C. Zabinski, Constance K. Yuen, Wing Yi. Lung, Adam C. Gower, Maria I. Ramirez, Jane C. Deng, Lee J. Quinton, Matthew R. Jones, and Joseph P. Mizgerd. Secreted and Transmembrane 1a (Sectm1a) is an Epithelial Cell-derived

Activator of Neutrophils During Pneumonia. In revision, American Journal of Respiratory Cell and Molecular Biology

Deena R. Altman, Hannah Rose, Robert S. Holzman, Davida S. Smyth, **Gregory A. Wasserman**, Jared M. Kafer, Michelle Wible, Rodrigo E. Mendes, Anne-Catrin Uhlemann, and Bo Shopsin. Involvement of glycopeptide resistance in persistence of agr-defective mutants. In submission

Elyse Kozlowski, **Gregory A. Wasserman**, Marcos Morgan, Dónal O'Caroll, Nora-Guadalupe P. Ramirez, Suryaram Gummuluru, Jasmine Y. Rah, Michael Ieong, Lee J. Quinton, Joseph P. Mizgerd and Matthew R. Jones. The RNA Uridyltransferase Zcchc6 Regulates Macrophage Cytokines and Innate Immunity. In Submission

PRESENTATIONS

Abstract Presentations:

1. Haq, I.U., Wasserman, H.C., Wasserman, R., Berman, S., **Wasserman, G.A**., Haq, N. Use of Tumescent Local Anesthesia for Repair of Abdominal Wall Hernias. Poster presented at: International Hernia Society, 2006.

2. Shopsin B, Eaton C, **Wasserman GA,** Mathema B, Adhikari RP, Agolory S, Altman DR, Holzman RS, Kreiswirth BN, and Novick RP. Mutations in *agr* do not persist in natural populations of methicillin-resistant *Staphylococcus aureus* . Poster presented at: Gordon Conference on Staphylococcal Diseases, Waterville Valley, NH, 2009

3. **Wasserman GA**, Chen J, Liese J, Kafer JM, Novick RP, and Shopsin B. Selective Loss of *agr* function in *Staphylococcus aureus.* Poster presented at: Skirball Institute of Biomedical Sciences at NYU School of Medicine annual retreat. Lenox, MA, October 19-21, 2010

4. Lilo S*, Benson MA*, **Wasserman GA**, Smith A, McDonald H, Horswill AR, Fraser J, Novick RP, Shopsin B, and Torres VJ. *Staphylococcus aureus* compensates for *agr* dysfunction by coordinating an anti- immunomodulatory response. Poster presented at: NYU School of Medicine Department of Microbiology annual retreat. Cold Spring, NY, November 8-9, 2010

5. **Wasserman GA**, Chen J, Liese J, Geisinger E, Kafer JM, Novick RP, and Shopsin B. Selective Loss of *agr* function is independent of RNAIII in *Staphylococcus aureus.* Poster presented at: NYU School of Medicine Department of Medicine 10th annual research day. May 11, 2011.

6. **Wasserman GA**, Chen J, Kafer JM, Liese J, Geisinger E, , Novick RP, and Shopsin B. Selective Loss of agr function in vitro and in vivo. Poster presented at: Gordon Conference on Staphylococcal Diseases. Lucca, Italy, July 24–29th, 2011.

7. Ivelisse Rodriguez-Pagan, John Chen, **Gregory A. Wasserman**, Richard P. Novick, and Michael Engelbert. agr, a global regulator of virulence is a determinant of pathogenesis in experimental endophthalmitis caused by community acquired epidemic S. aureus Strain USA300. Poster presented at: Association for Research in Vision and Ophthalmology. Ft. Lauderdale, FL, May 6–10, 2012.

8. **Wasserman GA**, Kozlowski E, Yamamoto K, Quinton LJ, Mizgerd JP, and Jones MR. The piRNA binding protein PIWIL4 promotes cytokine expression during bacterial pneumonia. Poster presented at: BUSM Evan's Day. October 17, 2013.

9. **Wasserman GA**, Kozlowski E, Yamamoto K, Quinton LJ, Mizgerd JP, and Jones MR. The piRNA binding protein MIWI2, promotes cytokine expression during bacterial pneumonia. Poster presented at: Keystone Symposia on RNA Silencing. Seattle, WA, January 2014.

10. Kozlowski E, **Wasserman GA,** Quinton LJ, Mizgerd JP, and Jones MR. The Zcchc6 TUTase is upregulated in macrophages to drive inflammatory cytokine expression. Poster presented at: Keystone Symposia on RNA Silencing. Seattle, WA, January 2014.

11. Kamata H, Yamamoto K, **Wasserman GA**, Zabinski MC, Quinton LJ, Jones MR, and Mizgerd JP. Epithelial specific Immune Responses During Pneumonia. Poster presented at: American Thoracic Society. May 2014

12. Kristie L. Hilliard, Eri Allen, Katrina E. Traber, Kazuko Yamamoto, Nicole M. Stauffer, **Gregory A. Wasserman**, Matthew R. Jones, Joseph P. Mizgerd and Lee J. Quinton. The Lung-Liver Axis Facilitates Innate Immunity and Survival during Pneumonia. Poster presented at: American Thoracic Society. May 2014

Oral Presentations:

Selective loss of *agr* function. NYU School of Medicine, Skirball Institute of Biomolecular Medicine, Molecular Pathogenesis Seminar Series. New York, NY

Does Alternative microRNA Utilization Regulate Cytokine Expression During Acute Bacterial Infection? Boston University School of Medicine, Department of Microbiology, Molecular Pathogenesis and Host Defense Seminar Series. February 4, 2013. Boston, MA

The piRNA binding protein MIWI2 is induced during infection to promote cytokine expression. Boston University School of Medicine, Department of Microbiology, Molecular Pathogenesis and Host Defense Seminar Series. February 24, 2014. Boston, MA

Role of the piRNA binding protein MIWI2 during bacterial pneumonia. Boston University School of Medicine, Department of Microbiology, Molecular Pathogenesis and Host Defense Seminar Series. November 3, 2014. Boston, MA

MIWI2 exerts piRNA independent regulation of innate immunity during bacterial pneumonia. Boston University School of Medicine, Department of Microbiology, Molecular Pathogenesis and Host Defense Seminar Series. November 16, 2015. Boston, MA

TEACHING EXPERIENCE

2013- 2015	BUSM Foundations in Biomedical Sci.- Struc. and Function of the Genome- Teaching Fellow
2013- 2015	BUSM- Disease and Therapy Course (DRx)- Infectious Diseases module discussion facilitator
2014	BUGSDM- Tutor for Dental Microbiology and Immunology course
2014	BUSM Foundations in Biomedical Sci.- Translational Genetics and Genomics - Teaching Fellow
2014	BUSM- Tutor for 1st year Medical Immunology course

SERVICE TO THE UNIVERSITY

2012	Coordinator, Department of Microbiology Journal Club
2013	Round Table discussion facilitator, Career Choices in Science, BUSM Evans Day Retreat
2013- 2014	Panel Member, “How to choose a mentor” PiBS Retreat
2013- 2015	BUSM Graduate Student Recruitment Day Ambassador
2013- 2015	Program in Biomedical Sciences (PiBS) peer mentor
2014- 2016	Peer elected- student representative to the Microbiology Faculty Council
2015	Member, Pulmonary Center Committee on Data Management and Research Records

AWARDS and HONORS

2011	NYU School of Medicine, Department of Medicine Dorathea Zucker Best Poster Award
2012	Selected participant, Gordon Conference on Post Transcriptional Gene Regulation, Newport, RI
2013	BUSM Division of Graduate Medical Sciences Travel Award
2014	Department of Microbiology Travel Award, Second Prize
2014	BUMC Department of Medicine Evans Research Day- 4th Prize- Basic Science
2014	Competitive appointment to NIH T32- Program in Inflammatory Disorders
2015	Ruth L. Kirschstein National Research Service Award (NRSA) Individual Predoctoral Fellowship
2015	BUSM Henry I Russek Student Achievement Award- 2nd Prize
2015	Department of Microbiology Lawrence W. Corwin Award

SOCIETY MEMBERSHIP

2013- Pres	American Thoracic Society
2013- Pres	American Academy for the Advancement of Science (AAAS)

RESEARCH SUPPORT

Current

F31 HL127978 Wasserman (PI) 9/1/15-8/31/17
NIH/NHLBI
The piRNA binding protein Miwi2 promotes cytokine expression during bacterial pneumonia.
The goal of this study is to determine the function of the piRNA binding protein Miwi2 in the host response to bacterial pneumonia.
Role: Principal Investigator
Sponsor: Matthew R. Jones, Ph.D.
Co-Sponsor: Joseph P. Mizgerd, Sc.D.

Completed

T32 AI089673 Genco (PI) 9/1/14- 8/31/15
NIH/NIAID
Boston University Inflammatory Disorders Training Grant.
The goal of the training program is to provide predoctoral and postdoctoral trainees with a solid academic background in immunology with emphasis on multi disciplinary approaches to study common mechanisms of inflammation.
Role: Pre-doctoral Trainee